Reprinted from:
ADVANCES IN APPLIED MECHANICS, VOL. 14

ACADEMIC PRESS, INC.
New York San Francisco London

Plastic Buckling

JOHN W. HUTCHINSON

Division of Engineering and Applied Physics,
Harvard University, Cambridge, Massachusetts

I. Introduction

Plastic buckling has received a great deal of attention in the past and progress in the subject has been slow but steady. The column under axial compression has been studied more than any other single structure and its history is well known. The turning points in this history are marked by the work of Considère (1891) and von Kármán (1910) to obtain the load at

which the straight column becomes unstable. Then almost 40 years later, Shanley (1947) explained, by way of a simple model and careful experimentation, the significance of the tangent-modulus load of Engesser (1889) at which the straight column would start to deflect laterally under increasing load. It was recognized that the tangent-modulus load is the lowest possible bifurcation load; the straight configuration loses its uniqueness at this load but not its stability (von Kármán, 1947). Shortly thereafter Duberg and Wilder (1952) studied the post-buckling behavior of a column model. They showed that the inclusion of imperfections and realistic stress–strain behavior gave rise to a maximum support load that was closely approximated by the tangent-modulus load, as Shanley had conjectured and in accord with existing experimental data.

Extensive testing of plates and to some extent shells was carried out in the late 1940's and early 1950's and solutions for the lowest bifurcation load, analogous to the tangent-modulus load for columns, were obtained for many cases of interest [see, for example, Bijlaard (1949) and Gerard and Becker (1957)]. A major obstacle to further progress surfaced in this period. It was discovered that bifurcation loads calculated using the simplest incremental, or flow, theories of plasticity consistently overestimated buckling loads of plates and shells obtained in tests. Calculations based on the less respectable deformation theories of plasticity gave reasonably good agreement with test results. It was found that the difficulty could be largely overcome if the smooth yield surface of the simplest flow theories was discarded. In fact, the bifurcation load predictions of a deformation theory could be justified rigorously in nearly all cases by establishing the connection between the deformation theory and a more sophisticated incremental theory which develops a sharp corner on its yield surface (Batdorf, 1949). Yet basic experiments on the multiaxial stress–strain behavior of typical metals failed to show conclusively that corners on yield surfaces do actually develop. Almost 20 years later this state of affairs remains at essentially the same impasse.

On the theoretical side, Hill (1956, 1958, 1959, 1961) placed the bifurcation criterion for elastic-plastic solids on a firm mathematical foundation which embraces solids characterized by smooth or cornered yield surfaces. His formulation applies not only to bifurcation under compressive loading—that is, problems which are loosely categorized under the heading of plastic buckling—but also to less thoroughly explored problems such as necking which can involve bifurcation in tension.

Thus, except for the difficulty in identifying an adequate plasticity theory, bifurcation theory for compressive loadings is reasonably well understood. A recent survey by Sewell (1972) includes an organized bibliography of much of the enormous amount of work on plastic buckling. Relatively less is known about post-bifurcation behavior and imperfection sensitivity in the

plastic range. What is known comes largely from tests and a relatively few model studies such as that of Duberg and Wilder (1952). This can be contrasted with the situation which now prevails for elastic buckling where a great deal is known about these matters and where a general theory of initial post-buckling behavior and imperfection sensitivity is available (Koiter, 1945, 1963a).

The importance of post-bifurcation considerations in the plastic range can immediately be appreciated in noting that in almost all cases of compressive loading the lowest bifurcation occurs under increasing load in the sense of Shanley, even for a structure which bifurcates unstably in the elastic range. Furthermore, this occurs even though material nonlinearity in the form of decreasing stiffness with increasing deformation contributes an additional destabilizing influence to the geometric nonlinearity already present. By itself, the fact that the initial slope of the load-deflection relation is positive can be highly misleading since recent work has shown that the magnitude of the initial curvature of the load-deflection curve is usually infinite (Hutchinson, 1973a), and the maximum support load of the perfect structure may be only very slightly above the lowest bifurcation load. It is also significant that even the column under axial compression, which has a fully stable post-buckling behavior in the elastic range, is appreciably affected by small imperfections in the plastic range.

The main accent in this article is placed on post-bifurcation and imperfection-sensitivity aspects of plastic buckling. A combination of model studies and analytical and numerical work has been drawn on to illustrate as wide a range of behaviors as possible.

In Section II a simple two degree of freedom model is used to introduce post-bifurcation behavior and a second model brings out some of the features peculiar to the behavior of continuous solids and structures. Hill's bifurcation criterion for a class of three-dimensional solids is given in the first part of Section III and is then applied to a widely used theory for plates and shells, the Donnell–Mushtari–Vlasov (DMV) theory. Following specification of the bifurcation criterion, a detailed commentary is given on the extent to which bifurcation predictions for plates and shells depend on the plasticity theory used with particular focus on the differences between predictions based on the simplest deformation and incremental theories. Much of what will be said was common knowledge in the 1950's but seems to be less widely appreciated now.

A general treatment of the initial post-bifurcation behavior of plates and shells is given in Section IV within the context of the DMV theory. The theory is illustrated by applications to several column and plate problems. A discussion of some of the effects of imperfections is also given. The article ends with a selection of numerical results for columns, plates, and shells.

II. Simple Models

A. Discrete Shanley-Type Model

The first model to be examined is similar in all respects to Shanley's (1947) model of plastic column buckling except that it also is capable of illustrating the behavior of a highly imperfection-sensitive structure. In this respect it is similar to the model of von Kármán *et al.* (1940) for the elastic buckling of imperfection-sensitive structures. The model succumbs to an elementary analysis yet still retains many of the essentials of plastic buckling. The results given in this section are taken from Hutchinson (1972).

As shown in Fig. 1, the rigid-rod model has two degrees of freedom: the

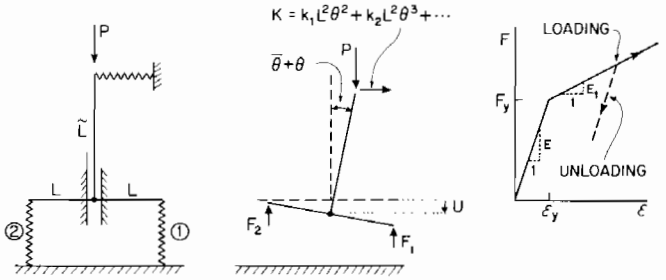

FIG. 1. Rigid-rod model with two degrees of freedom.

downward vertical displacement u and the rotation θ. An initial rotation from the vertical in the unloaded state is identified as the imperfection and is denoted by $\bar{\theta}$ so that the total rotation from the vertical is $\theta + \bar{\theta}$. An increment in the compressive force in either of the two support springs depends on whether plastic loading or elastic unloading occurs according to

$$\dot{F} = E_t \dot{\varepsilon} \quad \text{for} \quad F = F^{\max} \quad \text{and} \quad \dot{F} > 0,$$

$$\dot{F} = E\dot{\varepsilon} \quad \text{for} \quad F < F^{\max} \quad \text{or} \quad F = F^{\max} \quad \text{and} \quad \dot{F} < 0, \tag{2.1}$$

where ε is the contraction of the spring. Initial yield occurs for $F = F_y$ and $F^{\max}$ is set to be F_y at the start. The tangent modulus E_t is taken to be constant. Geometric nonlinearity is incorporated into the model only through the nonlinear elastic spring which develops a force $K(\theta) = k_1 L^2\theta^2 + k_2 L^2\theta^3 + \cdots$ under rotation with the sign convention shown in Fig. 1. Equations of equilibrium and strain displacement are

$$F_1 + F_2 = P, \tag{2.2}$$

$$(F_2 - F_1)L + P\tilde{L}(\theta + \bar{\theta}) + \tilde{L}K(\theta) = 0, \tag{2.3}$$

$$\varepsilon_1 = u + L\theta \quad \text{and} \quad \varepsilon_2 = u - L\theta, \tag{2.4}$$

where the subscripts denote springs Nos. 1 and 2.

When the parameters of the model are such that buckling takes place in the elastic range the load-rotation behavior of the model is found to be

$$(P_c - P)\theta - K(\theta) = P\bar{\theta}, \tag{2.5}$$

where $P_c = 2EI^2/\tilde{L}$ is the bifurcation load of the perfect model. If $k_1 \neq 0$ the bifurcation point is asymmetric and for $k_1\bar{\theta} > 0$ the maximum support load of the slightly imperfect model is given by the asymptotic formula

$$P^{\max}/P_c = 1 - (2\tilde{L}k_1\bar{\theta}/E)^{1/2} + \cdots. \tag{2.6}$$

If the load-rotation behavior is symmetric in θ then $k_1 = 0$. If $k_2 > 0$, then

$$P^{\max}/P_c = 1 - (\tfrac{3}{2})(\tilde{L}k_2\bar{\theta}^2/E)^{1/3} + \cdots. \tag{2.7}$$

These two cases, depicted in Fig. 2, illustrate the two most common occur-

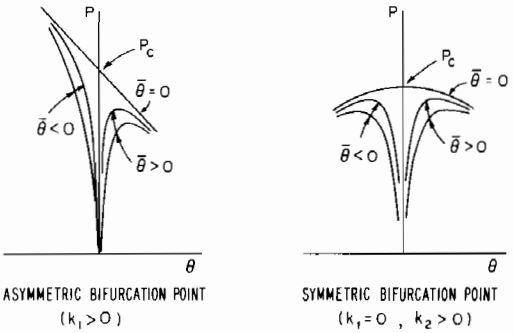

FIG. 2. Elastic post-bifurcation behavior and imperfection sensitivity of the models.

rences of imperfection sensitivity in elastic structures. When $K = 0$ (the Shanley model) the maximum support load of the model is always P_c and in this sense approximates the small deflection behavior of an axially compressed column.

1. *Behavior of the Perfect Model*

Throughout this article a subscript or superscript c will be reserved to denote quantities associated with the lowest possible bifurcation point. The lowest bifurcation load of the model in the plastic range is given by the tangent-modulus formula $P_c = 2E_t L^2/\tilde{L}$. Bifurcation occurs at P_c under increasing load as discussed by Shanley. When the model has an asymmetric

bifurcation point with, say, $k_1 < 0$, then the load increases linearly with positive values of θ in the neighborhood of the bifurcation point even in the elastic range. In the plastic range, one can readily show that both springs will continue to deform plastically in some finite range following bifurcation if

$$\pm k_1 L/(2E_t) > 1 \quad \text{and} \quad \dot{\theta} \lesseqgtr 0. \tag{2.8}$$

Thus, for example, if $k_1 L/(2E_t) > 1$ the geometric nonlinearity itself is sufficient to ensure that P increases with negative θ sufficiently rapidly to ensure that neither support spring unloads. Of the two bifurcation branches emanating from such a nonsymmetric bifurcation point, the above-mentioned branch is of inherently less interest than the opposite-signed deflection. On this latter branch the geometric nonlinearity has a destabilizing effect. We limit consideration to $k_1 \geq 0$ and $\dot{\theta} > 0$.

For this case spring No. 1 continues to load and No. 2 undergoes elastic unloading or neutral loading (i.e., $\dot{\varepsilon} = 0$) following bifurcation. With the bifurcation load denoted by P_{bif}, Eqs. (2.1) to (2.4) give

$$P = \left[P_{\text{bif}} + \frac{\tilde{L}}{L}\left(\frac{E + E_t}{E - E_t}\right)[P_{\text{rm}}\theta - K(\theta)]\right]\left[1 + \frac{\tilde{L}}{L}\left(\frac{E + E_t}{E - E_t}\right)\theta\right]^{-1} \tag{2.9}$$

$$= P_{\text{bif}} + 0\left[\frac{\tilde{L}}{L}\left(\frac{E + E_t}{E - E_t}\right)(P_{\text{rm}} - P_{\text{bif}})\right]$$

$$-\theta^2\left[\left(\frac{\tilde{L}}{L}\right)^2\left(\frac{E + E_t}{E - E_t}\right)^2(P_{\text{rm}} - P_{\text{bif}}) + k_1 L\tilde{L}\left(\frac{E + E_t}{E - E_t}\right)\right] + O(\theta^3). \tag{2.10}$$

In this formula P_{rm} is the reduced-modulus load of von Kármán (1910) where bifurcation takes place with no first-order change in load which is given by

$$P_{\text{rm}} = \frac{4E_t I^2}{(1 + E_t/E)\tilde{L}^2} = \frac{2P_c}{(1 + E_t/E)}. \tag{2.11}$$

Bifurcation can take place at every load in the range $P_c \leq P_{\text{bif}} \leq P_{\text{rm}}$ and for $P_{\text{bif}} < P_{\text{rm}}$ it occurs under increasing load as can clearly be seen from (2.10). A simple formula for the maximum support load cannot be obtained for a general function $K(\theta)$. However when $K = k_1 L^2\theta^2$ the maximum support load $P_0^{\max}$ associated with bifurcation at the tangent-modulus load P_c is given by the equation

$$(P_{\text{rm}} - P_0^{\max})^2 - 4k_1 L\tilde{L}\left(\frac{E - E_t}{E + E_t}\right)(P_0^{\max} - P_c) = 0. \tag{2.12}$$

If the geometric nonlinearity is strong in the sense that $k_1 L/E_t \gg 1$ then

$$P_0^{\max} = P_c\left[1 + \left(\frac{E_t}{2k_1 L}\right)\left(\frac{E - E_t}{E + E_t}\right) + O\left(\frac{E_t}{k_1 L}\right)^2\right]. \tag{2.13}$$

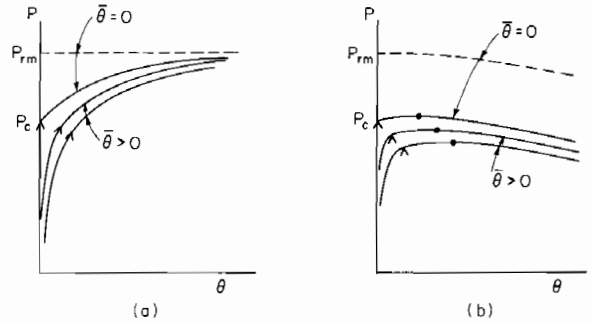

FIG. 3. Behavior of the model in the plastic range. (a) Shanley model, $k_1 = k_2 = 0$; (b) Model with a destabilizing geometric nonlinearity, $k_1 > 0$. Dashed-line curve corresponds to bifurcation at the reduced-modulus load P_{rm}. ($\hat{}$) ~ onset of elastic unloading; ($\cdot$) ~ maximum load. The lowest bifurcation load is P_c.

When $K = 0$, $P \to P_{rm}$ for large θ as can be seen from (2.9) and Fig. 3a. This is also similar to the behavior of the model of Duberg and Wilder for their constant tangent-modulus calculations. Even when the tangent modulus is constant, the present model has a maximum load which falls below the reduced-modulus load if the geometric nonlinearity has a destabilizing effect. A similar effect is also observed in the model studies of Sewell (1965), Augusti (1968), and Batterman (1971). A strong geometric nonlinearity results in a maximum load which is only slightly above P_c as can be seen from (2.13) and Fig. 3b.

2. *Effect of Initial Imperfections*

In the presence of an initial imperfection $\bar{\theta} > 0$ the load-rotation behavior of the model is more complicated; however a complete analysis can still be carried out for the case of the simplest geometric nonlinearity, $K = k_1 L^2\theta^2$. There are three distinct sequences of loading and unloading which can take place depending on the magnitude of $\bar{\theta}$. We will first consider the case for which $\bar{\theta}$ is sufficiently small such that the resulting formula will be valid in the limit as $\bar{\theta}$ vanishes.

In this case it is found that there are four steps to the loading history which must be treated separately in the analysis. With the first application of load both springs are elastic. Next, spring No. 1 starts to deform plastically and is followed by No. 2 at a slightly higher load. With the load still rising spring No. 2 starts to unload at a value of P and θ denoted by $\hat{P}$ and $\hat{\theta}$. From this point on spring No. 1 continues to load while No. 2 responds elastically. The maximum load is attained at a point (P^{max}, θ^*) following the onset of

elastic unloading at $(\hat{P}, \hat{\theta})$. The expressions for $\hat{\theta}$ and $\hat{P}$ are given by

$$\hat{\theta} = -\bar{\theta} + \left(\bar{\theta}^2 + \frac{L\bar{\theta}/\tilde{L} - \bar{\theta}^2}{1 + (k_1 L/2E_t)}\right)^{1/2} \tag{2.14}$$

$$= \left(\frac{L\bar{\theta}/\tilde{L}}{1 + (k_1 L/2E_t)}\right)^{1/2} + O(\bar{\theta}) \tag{2.15}$$

and

$$\hat{P}/P_c = 1 - \bar{\theta} - [1 + (k_1 L/E_t)](\hat{\theta} + \bar{\theta}) \tag{2.16}$$

$$= 1 - [1 + (k_1 L/E_t)]\left(\frac{L\bar{\theta}/\tilde{L}}{1 + (k_1 L/2E_t)}\right)^{1/2} + O(\bar{\theta}); \tag{2.17}$$

also,

$$\theta^* = \hat{\theta} + \left(\hat{\theta} + \bar{\theta} + \frac{E - E_t}{E + E_t}\right)\{[1 + (2E_t/k_1 L)]^{1/2} - 1\} \tag{2.18}$$

and

$$P^{\max} = P_0^{\max} - 2k_1 L^2[\hat{\theta} + (\hat{\theta} + \bar{\theta})([1 + (2E_t/k_1 L)]^{1/2} - 1)], \tag{2.19}$$

where $P_0^{\max}$ is the maximum load of the perfect model given by (2.12) for bifurcation from P_c.

If $k_1 = 0$ then $P \to P_{\mathrm{rm}}$ for all values of $\bar{\theta}$ as shown in Fig. 3a. If $k_1 > 0$ then we can show that (2.19) reduces to

$$P^{\max}/P_c = P_0^{\max}/P_c - (2k_1 \tilde{L}\bar{\theta}/E_t)^{1/2} + O(\bar{\theta}). \tag{2.20}$$

A small imperfection results in a reduction in the maximum support load which is proportional to the square root of its amplitude. The limit in which $\bar{\theta} \to 0$ is the bifurcation response of the perfect model for bifurcation from P_c. Asymptotically the reduction in the buckling load according to (2.20) is precisely of the same form as is the analogous formula (2.6) for the elastic model, except that the effect of a small imperfection is *magnified* by an amount E/E_t compared with the elastic case.

For larger imperfections the maximum load can be reduced to a sufficiently low level such that the force spring No. 2 does not reach F_y, and (2.19) ceases to be valid. In this sequence of loading spring No. 1 yields at a value of P just under $2F_y$ and the model deflects readily under a slight increase in load, helped along by the geometric nonlinearity, until the maximum support load is reached. The maximum load is not too different from the initial yield load of the perfect model, i.e.,

$$P^{\max} \cong 2F_y\,. \tag{2.21}$$

Load-rotation curves showing the effect of initial imperfections are shown in Fig. 3b.

For even larger values of the imperfection a third possibility may arise. Suppose the bifurcation load $P_c = 2E_t L^2/\tilde{L}$ is only slightly below the associated elastic load $2EI^2/\tilde{L}$. Then if $\bar{\theta}$ is large enough neither spring becomes plastic before the maximum load occurs and the elastic result holds. For $K = k_1 L^2 0^2$ the elastic result is given exactly by the equation

$$(1 - P^{\max}/P_c)^2 = (2k_1 \tilde{L}\bar{\theta}/E_t)P^{\max}/P_c\,. \tag{2.22}$$

Figure 4 shows the relation between $P^{\max}$ and $\bar{\theta}$ for such a case. On the portion of the curve A–B the strong imperfection sensitivity associated with (2.20) is seen; on B–C (2.21) holds; and on C–D the elastic result (2.22) pertains.

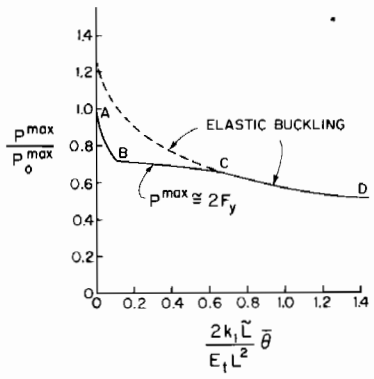

FIG. 4. Ratio of maximum support load to maximum support load of perfect model as a function of the imperfection amplitude. This case is an illustration of the effect of an imperfection in reducing the maximum load to the point where the structure no longer deforms plastically prior to buckling. $E_t/E = \frac{3}{4}$, $k_1 L/E_t = 10$, $\varepsilon_y \tilde{L}/L^2 = 0.525$. From Hutchinson (1972) *J. Appl. Mech.* **39**, 155–162, with permission.

The implication of the model is that if a structure is highly imperfection sensitive in the elastic range then an imperfect realization of the structure may buckle elastically even though a perfect version would buckle in the plastic range. The converse situation is also of interest. Namely, what is the effect of initial imperfections on the maximum support load of a structure designed such that a perfect realization bifurcates at a load which is slightly below initial plastic yielding? We will look at this question in connection with the next model which incorporates a more realistic stress–strain relation.

B. Continuous Model

According to the Shanley concept, bifurcation occurs at the lowest possible load under increasing load in such a way that no elastic unloading takes place at bifurcation. This is manifest in the simple model of Section-II,A in that one spring continues to load plastically and the other undergoes neutral loading ($\dot{\varepsilon} = 0$) at bifurcation and then unloads elastically immediately following bifurcation. Mathematically this is expressed by the fact that the contraction rate of the unloading spring is given by $\dot{\varepsilon} \sim -\dot{\theta}$ for small θ. It is clear that elastic unloading must *start* at the lowest bifurcation point in this sense. To see this, suppose that no elastic unloading occurred in some finite neighborhood of the bifurcation point. Within this neighborhood the response of the model would be identical to an *elastic* model with moduli E_t. But this leads to a contradiction since a reversal in sign of the contraction rate will occur in the elastic model at bifurcation, except when $\pm k_1 L/(2E_t) > 1$ and $\dot{\theta} \lesseqgtr 0$ as already discussed.

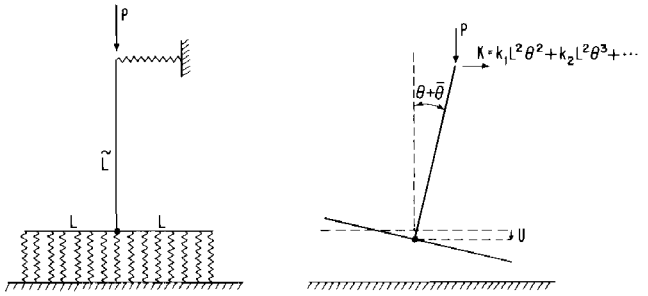

Fig. 5. Continuous model.

In a *continuous* elastic-plastic structure it is also generally true that elastic unloading must start at bifurcation at at least one point in the structure, as will be shown. As the bifurcation deflection increases the region of elastic unloading expands in a continuous fashion in most problems. It is this feature which makes an analytic treatment of the initial post-bifurcation behavior of a continuous elastic–plastic structure considerably more difficult to carry out than for an elastic structure. The model discussed in this section is perhaps the simplest meaningful model which is capable of illustrating some aspects of the analytical character of initial post-bifurcation behavior. It is the continuum version of the model of the previous section and is shown in Fig. 5.

This model is already sufficiently complicated that closed-form formulas analogous to those for the discrete model cannot be obtained. A representation of the behavior is obtained in the form of a perturbation expansion about the lowest bifurcation point. In this study the variation of the tangent modulus with increasing plastic deformation will also be taken into account. Most of the results for this model were previously given by Hutchinson (1973a,b). Here we will indicate an alternative method of analysis of the model which is very similar to the general method applied to columns, plates, and shells later in the article.

The model of Fig. 5 differs from the previous model only in that it is supported by a continuous distribution of springs. The contraction of a spring attached at a point x along the base is given by

$$\varepsilon = u + x\theta. \tag{2.23}$$

The rate of change of the compressive force per unit length $\dot{s}$ is related to the contraction rate at any point by

$$\begin{aligned} \dot{s} &= E_t \dot{\varepsilon} \qquad \text{for} \quad s = s^{\max} \quad \text{and} \quad \dot{s} \geq 0, \\ \dot{s} &= E\dot{\varepsilon} \qquad \text{for} \quad s < s^{\max} \qquad \text{or} \qquad s = s^{\max} \quad \text{and} \quad \dot{s} < 0, \end{aligned} \tag{2.24}$$

where E_t is taken to be a smooth function of ε or s. (Note that E_t and E have dimensions force per length^2 in the continuous model while in the discrete model they have the dimensions force per length.) Equations of vertical and moment equilibrium are

$$\dot{P} = \int_{-L}^{L} \dot{s}\, dx \qquad \text{and} \qquad [P\tilde{L}(\theta + \bar{\theta})]^{\cdot} + \dot{K}\tilde{L} = \int_{-L}^{L} \dot{s}x\, dx. \tag{2.25a,b}$$

These may be replaced by the single variational principle of virtual work

$$\dot{P}\delta u + [P\tilde{L}(\theta + \bar{\theta}) + K\tilde{L}]^{\cdot}\delta\theta = \int_{-L}^{L} \dot{s}\delta\varepsilon\, dx, \tag{2.26}$$

where $\delta\varepsilon = \delta u + x\delta\theta$.

The elastic bifurcation load is $P_c = 2EL^3/(3\tilde{L})$ and (2.5) continues to apply. Asymptotic formulas for the elastic buckling load are still given by (2.6) and (2.7) if k_1 is replaced by $3k_1/L$ in (2.6) and k_2 by $3k_2/L$ in (2.7).

1. *Behavior of Perfect Model*

The lowest bifurcation load in the plastic range is given by the tangent-modulus formula $P_c = 2E_t^c L^3/(3\tilde{L})$, where E_t^c is the value of the tangent modulus at P_c. Just as in the case of the discrete model no elastic unloading occurs in some range of positive or negative θ if the magnitude of k_1 is sufficiently large, but otherwise elastic unloading starts at bifurcation with the occurrence of neutral loading at one point.

First entertain the possibility that no elastic unloading occurs so that the model behaves as a nonlinear elastic model with variable moduli E_t, i.e., the unloading branch of (2.24) is suppressed. The behavior of this *comparison model* is readily analyzed. Its initial post-bifurcation expansion is found to be

$$P/P_c = 1 + a_1^e\theta + a_2^e\theta^2 + \cdots, \tag{2.27}$$

where

$$a_1^e = -\frac{3k_1\tilde{L}}{2E_t^cL}\left[1 - \frac{L^2}{3\tilde{L}}\left(\frac{dE_t}{ds}\right)_c\right]^{-1}, \tag{2.28}$$

and we have expanded E_t about the bifurcation point according to

$$E_t = E_t^c + (s - s_c)(dE_t/ds)_c + \tfrac{1}{2}(s - s_c)^2(d^2E_t/ds^2)_c + \cdots. \tag{2.29}$$

The superscript e is used to distinguish the initial slope of the elastic comparison model from that of the elastic-plastic model given below; a_1^e figures prominently in formulas for the elastic-plastic model.

The contraction rate in the comparison model just following bifurcation is given by

$$\dot{\varepsilon} = \frac{L^2}{3\tilde{L}}\left[a_1^e + \frac{3\tilde{L}}{L}\left(\frac{x}{L}\right)\right]\dot{\theta} + O(\theta\dot{\theta}). \tag{2.30}$$

For example, if k_1 is sufficiently large such that $a_1^e < -3\tilde{L}/L$ and $\dot{\theta} < 0$, then no reversal in sign of the contraction rate will occur in some finite range of negative θ. Over this range the behaviors of the comparison model and elastic-plastic model coincide. As already mentioned, the more interesting bifurcation branch has the opposite-signed rotation. From here on we will take $k_1 \geq 0$ so that $a_1^e \leq 0$ and consider bifurcation under monotonically increasing θ. In this case the comparison model does not pertain.

For the elastic-plastic model the Shanley loading condition requires $\dot{\varepsilon} \geq 0$ on $|x| \leq L$ which in turn implies

$$\frac{1}{P_c}\frac{dP}{d\theta}\bigg|_c \geq \frac{3\tilde{L}}{L}. \tag{2.31}$$

If the *inequality* holds in (2.31) then $\dot{\varepsilon} > 0$ everywhere at bifurcation and by continuity implies that no elastic unloading will occur in some finite range of positive θ. By the same argument made for the discrete model, this would imply that the comparison model pertains with its initial slope a_1^e. But since $a_1^e \leq 0$, (2.31) is contradicted and we must conclude that the *equality* in (2.31) must hold for bifurcation at the load P_c. Elastic unloading starts at bifurcation in the sense that $\dot{\varepsilon} = 0$ at $x = -L$. It follows then that

$$P/P_c = 1 + a_1\theta + \cdots \qquad \text{and} \qquad u/L = u_c/L + b_1\theta + \cdots, \tag{2.32}$$

where

$$a_1 = 3\tilde{L}/L \qquad \text{and} \qquad b_1 = 1. \tag{2.33}$$

The instantaneous position d of the boundary between the regions of elastic unloading and plastic loading occurs where $\dot{\varepsilon} = 0$ so that from (2.23)

$$d = -du/d\theta. \tag{2.34}$$

To obtain additional terms in the expansion (2.32) write

$$\begin{aligned} P/P_c &= 1 + a_1\theta + a_2\theta^{1+\beta} + \tilde{P}(\theta), \\ u/L &= u_c/L + b_1\theta + b_2\theta^{1+\beta} + \tilde{u}(\theta), \end{aligned} \tag{2.35}$$

where we anticipate that $0 < \beta \leq 1$, and require that $\theta^{-1-\beta}(\tilde{P}, \tilde{u}) = 0$, as $\theta \to 0$. Now make the identification

$$(\dot{\ }) \equiv d(\quad)/d\theta, \tag{2.36}$$

so that

$$\begin{aligned} \dot{P}/P_c &= a_1 + (1+\beta)a_2\theta^{\beta} + \dot{\tilde{P}}, \\ d/L &= -\dot{u}/L = -b_1 - (1+\beta)b_2\theta^{\beta} - \dot{\tilde{u}}. \end{aligned} \tag{2.37}$$

Substitute these expansions into the principle of virtual work (2.26) noting that one can write

$$\int_{-L}^{L} \dot{s}\delta\varepsilon \, dx = \int_{-L}^{L} E_t\dot{\varepsilon}\delta\varepsilon \, dx + \int_{-L}^{d} (E - E_t)\dot{\varepsilon}\delta\varepsilon \, dx, \tag{2.38}$$

and from (2.29) and (2.32)

$$E_t = E_t^c + \theta(L + x)E_t^c(dE_t/ds)_c + \cdots. \tag{2.39}$$

Using (2.31) and (2.32) to eliminate the lowest-order terms in the principle of virtual work (2.26) one obtains

$$\begin{aligned} &P_c[(1+\beta)a_2\theta^{\beta} + \dot{\tilde{P}}]\,\delta u + [2P_c\tilde{L}a_1\theta + 2k_1L^2\tilde{L}\theta + \cdots]\,\delta\theta \\ &\quad = \int_{-L}^{L} \left((1+\beta)E_t^cLb_2\theta^{\beta} + E_t^cL\dot{\tilde{u}} + \theta(L+x)^2E_t^c\left.\frac{dE_t}{ds}\right|_c + \cdots \right) \delta\varepsilon \, dx \\ &\qquad + \int_{-L}^{d} (E - E_t^c)\dot{\varepsilon}\delta\varepsilon \, dx + \cdots. \end{aligned} \tag{2.40}$$

The last term in the above equation arises from elastic unloading and must be examined closely. From (2.33) and (2.37)

$$\dot{\varepsilon}/L = 1 + (x/L) + (1+\beta)b_2\theta^{\beta} + \dot{\tilde{u}}, \tag{2.41}$$

and $\dot{\varepsilon} = 0$ at $x = -L$ at bifurcation as already noted. The last term in (2.40) vanishes as $\theta \to 0$ since $d \to -L$. To evaluate the lowest-order contribution of this integral, introduce a stretched coordinate $\overset{*}{x}$ chosen such that the position of the elastic-plastic boundary d is independent of θ to lowest order in this new coordinate system. With the choice

$$\overset{*}{x} = \theta^{-\beta}(1 + x/L)/[-(1 + \beta)b_2], \tag{2.42}$$

the limits of integration on the integral run from $\overset{*}{x} = 0$ to $\overset{*}{x} = 1 + O(\theta^{\alpha})$ where $\alpha > 0$. In terms of $\overset{*}{x}$,

$$\dot{\varepsilon}/L = \theta^{\beta}(1 + \beta)b_2(1 - \overset{*}{x}) + \dot{\tilde{u}}. \tag{2.43}$$

To lowest order,

$$\int_{-L}^{d} (E - E_t^c)\dot{\varepsilon}\,\delta\varepsilon\,dx = \theta^{2\beta}(1 + \beta)^2 b_2^2 (E - E_t^c)L^2 \int_0^1 (1 - \overset{*}{x})(\delta u - L\delta\theta)\,d\overset{*}{x}$$

$$= -\tfrac{1}{2}\theta^{2\beta}(1 + \beta)^2 b_2^2 (E - E_t^c)L^2(\delta u - L\delta\theta). \tag{2.44}$$

Requiring terms of order θ^{β} in (2.40) to vanish implies that $P_c a_2 = 2L^2 E_t^c b_2$. Next, take $\delta u = 0$ and $\delta\theta \neq 0$ and collect terms to get

$$\theta[P_c \tilde{L} a_1 + k_1 L^2 \tilde{L} - \tfrac{2}{3}L^4 E_t^c (dE_t/ds)_c]$$
$$- \theta^{2\beta} L^3 (1 + \beta)^2 b_2^2 (E - E_t^c)/4 + \cdots = 0. \tag{2.45}$$

If $\beta > \frac{1}{2}$, (2.45) cannot be satisfied since the terms of order θ will not vanish. Similarly, if $\beta < \frac{1}{2}$, (2.45) cannot be satisfied except with $b_2 = 0$, which implies that the assumed expansion is not possible. Suppose however that $\beta = \frac{1}{2}$. Then there is a balance of terms in (2.45) and the following expressions for b_2 and a_2 are obtained:

$$a_2 = \frac{3\tilde{L}}{L} b_2 = -\frac{4\tilde{L}}{L}\left\{2E_t^c L(a_1 - a_1^e)\left(1 - \frac{L^2}{3\tilde{L}}\frac{dE_t}{ds}\bigg|_c\right)\right\}^{1/2}$$

$$\equiv -\frac{4\tilde{L}}{L}\left\{\frac{2E_t^c[3\tilde{L} - (dE_t/ds)_c L^2] + 3k_1\tilde{L}}{3(E - E_t^c)L}\right\}^{1/2}, \tag{2.46}$$

where the negative root of b_2^2 was chosen consistent with (2.37) and (2.43).

The expansion can be continued by the above approach or by a direct method given by Hutchinson (1973a). One finds

$$P/P_c = 1 + a_1\theta + a_2\theta^{3/2} + a_3\theta^2 + a_4\theta^{5/2} + \cdots,$$
$$d/L = -1 - \tfrac{3}{2}b_2\theta^{1/2} - 2b_3\theta - \tfrac{5}{2}b_4\theta^{3/2} + \cdots, \tag{2.47}$$

where

$$b_3 = \frac{E_t^c[3\tilde{L} - (dE_t/ds)_c L^2] - k_1\tilde{L}}{3(E - E_t^c)L},$$

$$a_3 = \frac{3\tilde{L}}{L} b_3 - \frac{3\tilde{L}^2}{L^2} + 3\tilde{L}\left.\frac{dE_t}{ds}\right|_c - \frac{3k_1\tilde{L}^2}{2E_t^c L^2}. \tag{2.48}$$

The fractional powers which appear in the expansion (2.47) are absent from the initial post-bifurcation expansions for elastic systems (Koiter, 1945, 1963a) as well as from expansions for discrete element elastic-plastic systems—see (2.10) and the studies of Sewell (1965) and Augusti (1968). Terms involving fractional powers of the bifurcation amplitude arise in connection with the continuous growth of the region of elastic unloading. The significance of the term $a_2\theta^{3/2}$ in (2.47) is that it is negative and may become numerically significant compared to the lead positive term $a_1\theta$ at relatively small values of θ. For example, if the series is truncated after the term $a_2\theta^{3/2}$ and is then used to find an approximate estimate of the maximum support load of the perfect model, one finds

$$P_0^{\max}/P_c = 1 + 4a_1^3/(27a_2^2). \tag{2.49}$$

If the magnitude of a_2 is sufficiently large the maximum load will only slightly exceed P_c. Note that a_2, given by (2.46), depends on the geometric nonlinearity through k_1 as well as on the material nonlinearity through $(dE_t/ds)_c$.

Figures 6 and 7 show comparisons between predictions based on the expansion (2.47), up to and including the $a_2\theta^{3/2}$ term, and accurate numerical calculations carried out for the simple model. Nonlinear material behavior was introduced by using a Ramberg–Osgood-type stress–strain relation

$$\varepsilon/\varepsilon_y = s/s_y + \alpha(s/s_y)^n, \tag{2.50}$$

where ε_y and $s_y = E\varepsilon_y$ are effective initial yield values. In Fig. 6 the model has a strong geometric nonlinearity with $k_1\tilde{L}/(EL) = 1$ and $k_2 = 0$. The model of Fig. 7 has no geometric nonlinearity (i.e., $k_1 = k_2 = 0$). In both examples $\alpha = \frac{1}{5}$, $n = 3$, $\tilde{L}/L = 1$, and $(s_y/EL) = 0.1094$ (corresponding to the values $E_t^c/E = 0.46$ and $s_c/s_y = 1.4$, where s_c is the value of s at bifurcation).

The combination of strong material and geometrical nonlinearity of the model of Fig. 6 results in a maximum load which is only slightly greater than P_c and which occurs at a relatively small value of θ. In this case the first few terms in the expansion (2.47) provides an excellent approximation to the

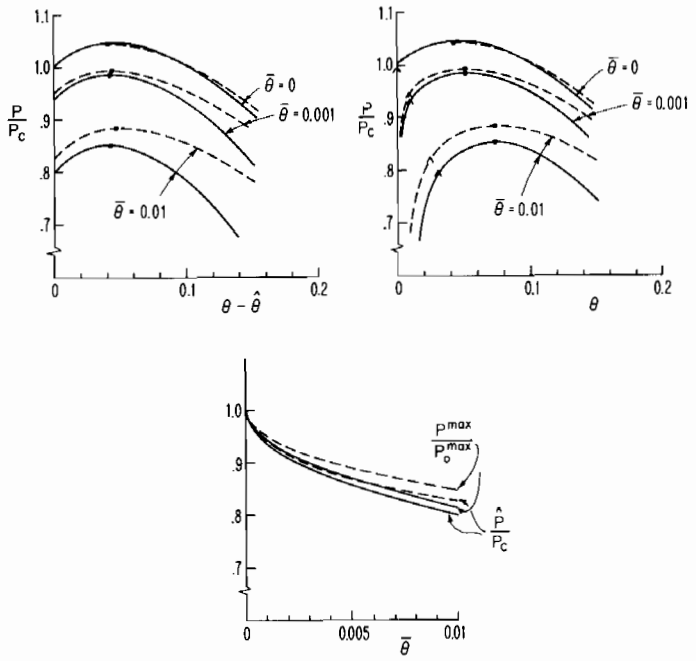

FIG. 6. Post-bifurcation behavior and imperfection sensitivity of continuous model for the case of a strong geometrical nonlinearity $[(k_1 \tilde{L}/EL) = 1$ and $k_2 = 0]$. Solid-line curves from asymptotic formulas and dashed-line curves from numerical analysis. From Hutchinson (1973b). *J. Mech. Phys. Solids* **21**, 191–204 with permission.

behavior in the range of interest. In the second example with only the material nonlinearity, the maximum support load is attained further from the bifurcation point and the expansion is not accurate over the full range of interest. Nevertheless, the maximum load prediction involves rather small error.

2. *Effect of Initial Imperfections*

Prior to the occurrence of any elastic unloading the behavior of the elastic-plastic model is identical to that of the nonlinear comparison model introduced in the preceding subsection. However, once strain-rate reversal starts elastic unloading must be accounted for in the analysis. Thus the analysis of the slightly imperfect model separates into two parts as discussed by Hutchinson (1973b) and the results presented here are condensed from this reference.

A Koiter-type initial post-buckling analysis can be used to obtain the behavior of the model prior to elastic unloading. The result of this analysis is

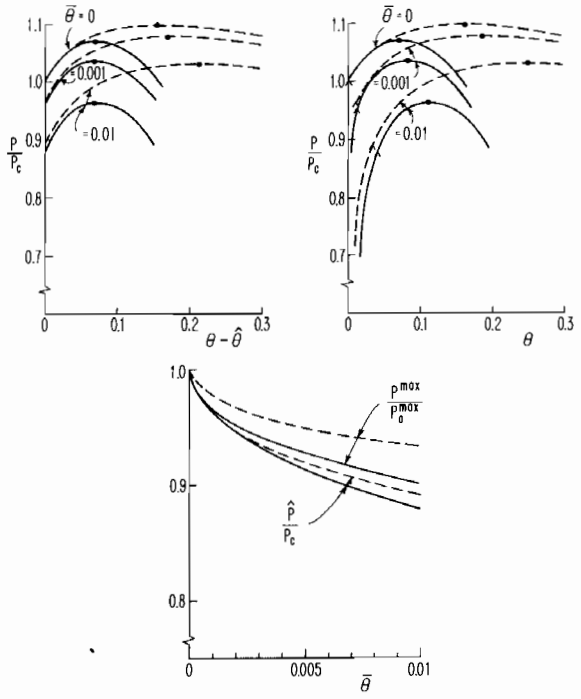

FIG. 7. Post-bifurcation behavior and imperfection sensitivity of continuous model with no geometrical nonlinearity $[k_1 = k_2 = 0]$. Solid-line curves from asymptotic formulas and dashed-line curves from numerical analysis. From Hutchinson (1973b). *J. Mech. Phys. Solids* **21**, 191–204, with permission.

an exact asymptotic equation relating the load, rotation, and initial imperfection $\bar{\theta}$ at load levels in the neighborhood of P_c:

$$(1 - P/P_c)\theta + a_1^e \theta^2 + \cdots = \rho\bar{\theta}, \tag{2.51}$$

where a_1^e is the initial slope of the perfect model (2.28) and

$$\rho = \left[1 - \frac{L^2}{3\tilde{L}}\frac{dE_t}{ds}\bigg|_c\right]^{-1}. \tag{2.52}$$

The first reversal in sign of the strain rate in the slightly imperfect model occurs when the slope of the load-rotation curve is reduced to the initial slope of the elastic-plastic model. With values marking the onset of elastic unloading topped by a wedge,

$$(P_c)^{-1}\, d\hat{P}/d\theta = a_1 + O(\hat{\theta}, \hat{P} - P_c, \bar{\theta}). \tag{2.53}$$

Condition (2.53) together with (2.51) gives

$$\hat{\theta} = [\rho\bar{\theta}/(a_1 - a_1^e)]^{1/2} + O(\bar{\theta}) \tag{2.54}$$

and

$$\hat{P}/P_c = 1 - (a_1 - 2a_1^e)[\rho\bar{\theta}/(a_1 - a_1^e)]^{1/2} + O(\bar{\theta}). \tag{2.55}$$

To obtain a uniformly valid expansion for the response following the onset of elastic unloading, which holds for small $\bar{\theta}$ and reduces to (2.47) for $\bar{\theta} \to 0$, it is necessary to introduce a new expansion parameter $\zeta \geq 0$ defined for $\theta \geq \hat{\theta}$ by

$$\theta - \hat{\theta} = \gamma\zeta\bar{\theta}^{1/2} + \zeta^2, \tag{2.56}$$

where γ is a constant parameter determined in the expansion process. The expansion has the form

$$\begin{aligned} P/P_c &= \hat{P}/P_c + p_1\zeta + p_2\zeta^2 + p_3\zeta^3 + \cdots, \\ d/L &= -1 + d_1\zeta + d_2\zeta^2 + \cdots, \end{aligned} \tag{2.57}$$

where the coefficients of the expansion are given in the above-mentioned reference.

Load-rotation curves showing the effect of initial imperfections are also shown in Figs. 6 and 7. Here again the solid line curves are based on the truncated expansion and the dashed line curves are based on an accurate numerical calculation and can be regarded as essentially exact for purposes of this comparison. A wedge marks the onset of elastic unloading in these figures and a dot the maximum load. Plots of $P^{\max}/P_0^{\max}$ (where $P_0^{\max}$ is the maximum load of the perfect model) and $\hat{P}/P_c$ as a function of $\bar{\theta}$ are also given in Figs. 6 and 7.

For model of Fig. 6 we see that

$$P^{\max}/P_0^{\max} \cong \hat{P}/P_c = 1 - (a_1 - 2a_1^e)[\rho\bar{\theta}/(a_1 - a_1^e)]^{1/2} + O(\bar{\theta}). \tag{2.58}$$

The pivotal role of $\hat{P}$ stems from the fact that in the presence of strongly destabilizing material and geometrical nonlinearities the maximum load is attained shortly after elastic unloading starts in both the perfect and imperfect model. The significant point is that the reduction in the maximum load appears to be proportional to the square root of the imperfection amplitude for small imperfections, similar to what was established conclusively for the discrete model with $k_1 \neq 0$ in (2.20). For the model with no destabilizing geometrical nonlinearity in Fig. 7, (2.58) is seen to be less accurate although it appears to be qualitatively correct. It should be possible to establish whether or not the reduction in cases in which $k_1 = 0$ is proportional to $\bar{\theta}^{1/2}$ or to some other power of $\bar{\theta}$. This has not been done. Nor for that matter has an analysis of the discrete model with $k_1 = 0$ and $k_2 > 0$ been carried out even though this would be considerably simpler and also very revealing in

this regard. Recall that in the elastic range the reduction is proportional to $\bar{\theta}^{2/3}$ when $k_1 = 0$ and $k_2 > 0$.

All the examples we have considered thus far have dealt with behavior when the parameters of the perfect model were chosen such that bifurcation occurred well into the plastic range. Equally of interest is the effect of initial imperfections on a structure whose perfect realization bifurcates in the elastic range or at least before appreciable plastic deformation occurs. Numerical calculations of the maximum support load have been made to illustrate the effect of initial imperfections under such circumstances for the continuous model with the Ramberg–Osgood stress–strain relation (2.50). In Fig. 8 we have followed Duberg (1962) and have plotted the maximum

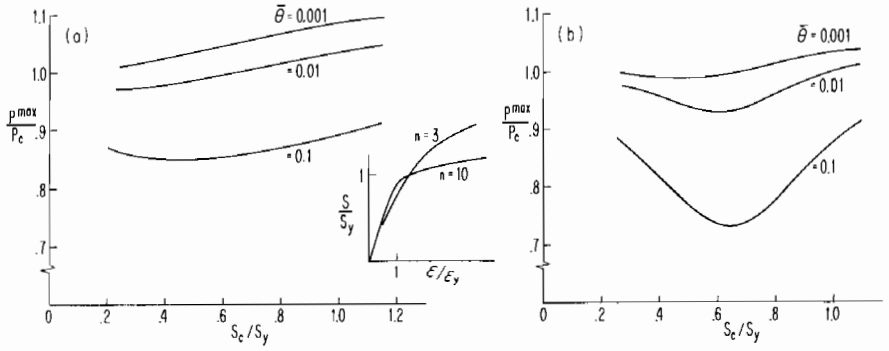

FIG. 8. Effect of imperfections on the maximum support load when the bifurcation stress of the perfect model s_c falls below the effective yield stress s_y. The model was taken to have no geometrical nonlinearity. (a) High-strain hardening: $n = 3$; (b) low-strain hardening: $n = 10$. ($k_1 = k_2 = 0$, $\bar{L}/L = 1$.)

support load normalized by the tangent-modulus load of the perfect model, P^{max}/P_c, as a function of the bifurcation stress of the perfect model over the effective yield stress, s_c/s_y, for several levels of imperfection. One set of curves pertains to a high strain-hardening material ($n = 3$) and the other to a low strain-hardening material ($n = 10$). In both cases $\alpha = \frac{3}{7}$ corresponding to the original suggestion of Ramberg and Osgood and the choice of Duberg. We defer a detailed discussion of these curves until Section V where they will be compared with analogous curves for columns and plates. Here we simply note that the curves of Fig. 8 are very similar to Duberg's results for a two-flanged column model and that they emphasize the possibility of strong interaction between imperfections and plastic deformation when the effective yield stress is not considerably in excess of the bifurcation stress of the perfect structure.

III. Bifurcation Criterion

A. Criterion for Three-Dimensional Solids

The theory given below is a specialized version of Hill's (1958, 1959, 1961) general theory of uniqueness and bifurcation in elastic-plastic solids which was given in somewhat less detail by Hutchinson (1973a). Sewell's (1972) survey article on plastic buckling deals at some length with Hill's theory. Here we are principally interested in presenting a suitable background for the bifurcation criterion to be presented in Section III,B for the most widely used theory of columns, plates, and shells. Most of the usable nonlinear theories of structures employ Lagrangian strain quantities where the undeformed configuration is usually chosen for reference, as has been discussed by Budiansky (1969). The three-dimensional approach given below is developed from the same point of view.

Let material points in the body be identified by a set of convected coordinates x^i and let g_{ij} and g^{ij} be the metric tensor and its inverse, respectively, in the undeformed body. Denote contravariant components of a tensor by superscripts and covariant components by subscripts in the usual way. With u_i and u^i as the components of the displacement vector referred to the undeformed base vectors, the Lagrangian strain tensor is

$$\eta_{ij} = \tfrac{1}{2}(u_{i,j} + u_{j,i}) + \tfrac{1}{2}u^k_{,i}\, u_{k,j}\,, \tag{3.1}$$

where the comma denotes covariant differentiation with respect to the metric of the undeformed body. Let $\mathbf{T}$ be the surface traction vector per unit original area and let T^i be its contravariant components referred to the undeformed base vectors. With dV and dS denoting volume and surface elements in the undeformed body the principle of virtual work is

$$\int_V \tau^{ij}\,\delta\eta_{ij}\,dV = \int_S T^i\,\delta u_i\,dS, \tag{3.2}$$

for all admissible variations δu_i where

$$\delta\eta_{ij} = \tfrac{1}{2}(\delta u_{i,j} + \delta u_{j,i}) + \tfrac{1}{2}(u^k_{,i}\delta u_{k,j} + u^k_{,j}\delta u_{k,i}). \tag{3.3}$$

Body forces will be omitted for simplicity.

The stress quantities τ^{ij} which enter into this exact statement of the principle of virtual work are the contravariant components of the symmetric Kirchhoff stress referred to base vectors in the deformed body. [See, for

example, Green and Zerna (1968), Bolotin (1963), or Budiansky (1969).] Application of the divergence theorem in the usual way to (3.2) yields the connection between the stress tensor and the nominal surface traction vector

$$T^i = (\tau^{ij} + \tau^{kj}u^i_{,k})n_j\,, \tag{3.4}$$

where n_j are the covariant components of the unit outward normal to the surface of the undeformed body referred to the undeformed base vectors. Similarly, the equilibrium equations are found to be

$$\tau^{ij}_{,j} + (\tau^{kj}u^i_{,k})_{,j} = 0. \tag{3.5}$$

With rates of change denoted by a dot, the incremental form of the principle of virtual work is

$$\int_V \{\dot{\tau}^{ij}\delta\eta_{ij} + \tau^{ij}\dot{u}^k_{,i}\delta u_{k,j}\}\,dV = \int_S \dot{T}^i\delta u_i\,dS. \tag{3.6}$$

First we consider the general rate-constitutive relation discussed by Hill (1967a) for the isothermal, finite deformation of elastic-plastic solids characterized by a smooth yield surface. At any stage of the deformation process denote the current elastic moduli based on the Kirchhoff stress-rates $\dot{\tau}^{ij}$ by $\mathscr{L}$. If the current stress is on the yield surface, denote the components of the unit tensor normal to the elastic domain in strain-rate space by m^{ij} where the strain rate is given by

$$\dot{\eta}_{ij} = \tfrac{1}{2}(\dot{u}_{i,j} + \dot{u}_{j,i}) + \tfrac{1}{2}(u^k_{,j}\dot{u}_{k,i} + u^k_{,i}\dot{u}_{k,j}). \tag{3.7}$$

The rate-constitutive relation is

$$\dot{\tau}^{ij} = L^{ijkl}\dot{\eta}_{kl} \qquad \text{for} \quad m^{kl}\dot{\eta}_{kl} \geq 0, \tag{3.8}$$

$$= \mathscr{L}^{ijkl}\dot{\eta}_{kl} \qquad \text{for} \quad m^{kl}\dot{\eta}_{kl} \leq 0, \tag{3.9}$$

where

$$L^{ijkl} = \mathscr{L}^{ijkl} - g^{-1}m^{ij}m^{kl}. \tag{3.10}$$

The constant g depends on the deformation history (as well as on the current point on the yield surface) and determines the current level of strain hardening. It is assumed that a pure dilatation rate gives rise to an elastic response independent of the sign of $m^{kl}\dot{\eta}_{kl}$ and this requires that $\mathbf{m}$ satisfy $G_{ij}m^{ij} = 0$, where G_{ij} is the metric tensor of the deformed body. When the stress lies within the yield surface (3.9) holds for all strain rates.

Hill (1967a) has discussed the transformation of this constitutive relation in going from one choice of objective stress rate to another. For the purposes of this article it need only be noted that the rate-constitutive relation for any elastic-plastic solid with a smooth yield surface can be cast into the present

form (3.8) to (3.10).† In particular, the simple J_2 flow theory of strain-hardening plasticity is a special case of this relation.

Dead loads are applied to the body in proportion to a single load (or displacement) parameter λ. On S_T prescribe surface tractions according to $T^i = \lambda T_S^i$ and on S_u prescribe displacements $u_i = \lambda u_i^S$, where T_S^i and u_i^S are independent of λ. Attention is directed to bifurcations which occur prior to any limit point of λ. All quantities associated with the fundamental solution whose uniqueness is in question are labeled by a subscript or superscript 0. It is to be understood that the fundamental solution is the solution starting at $\lambda = 0$ and is associated with monotonically increasing λ.

1. *Bifurcation Analysis for Solids with Smooth Yield Surfaces*

At any stage of deformation characterized by $u_i^0(\lambda)$, suppose that bifurcation is possible so that for a given increment in load $\dot{\lambda}$ (either positive or negative) there are at least two solutions $\dot{u}_i^a$ and $\dot{u}_i^b$. Introduce the following differences between the two solution increments:

$$\tilde{u}_i = \dot{u}_i^b - \dot{u}_i^a, \qquad \tilde{\eta}_{ij} = \dot{\eta}_{ij}^b - \dot{\eta}_{ij}^a, \qquad \tilde{\tau}^{ij} = \dot{\tau}_b^{ij} - \dot{\tau}_a^{ij},$$
$$\text{and} \quad \tilde{T}^i = \dot{T}_b^i - \dot{T}_a^i,$$

where from (3.7)

$$\tilde{\eta}_{ij} = \tfrac{1}{2}(\tilde{u}_{i,j} + \tilde{u}_{j,i}) + \tfrac{1}{2}(u_{,j}^{0k}\tilde{u}_{k,i} + u_{,i}^{0k}\tilde{u}_{k,j}). \tag{3.11}$$

Since $\tilde{T}^i$ vanishes on S_T and $\tilde{u}_i$ vanishes on S_u and since both solutions are assumed to satisfy the equilibrium equations, the usual construction in uniqueness proofs gives

$$0 = \int_S \tilde{T}^i \tilde{u}_i \, dS = \int_V \{\tilde{\tau}^{ij}\tilde{\eta}_{ij} + \tau_0^{ij}\tilde{u}_{,i}^k \tilde{u}_{k,j}\} \, dV \equiv H, \tag{3.12}$$

where H is defined by the last equality.

In the current state at load λ define the moduli $\mathbf{L}_c$ of an *elastic comparison solid* such that $\mathbf{L}_c$ equals $\mathbf{L}$ where the stress is currently on the yield surface, independent of the sign of $m^{ij}\dot{\eta}_{ij}$, and $\mathbf{L}_c$ equals $\mathscr{L}$ where the stress lies within the yield surface. To obtain Hill's (1958) sufficiency condition for uniqueness, introduce the following quadratic functional,

$$F(\lambda, \tilde{u}) = \int_V \{L_c^{ijkl}\tilde{\eta}_{ij}\tilde{\eta}_{kl} + \tau_0^{ij}\tilde{u}_{,i}^k \tilde{u}_{k,j}\} \, dV. \tag{3.13}$$

The difference between the integrands of F and H depends on $m^{ij}\dot{\eta}_{ij}^a$ and $m^{ij}\dot{\eta}_{ij}^b$ according to [from (3.8) to (3.10)]

† Later, the additional restriction $\mathscr{L}^{ijkl} = \mathscr{L}^{klij}$ will be needed.

$$\tilde{\tau}^{ij}\tilde{\eta}_{ij} - L_c^{ijkl}\tilde{\eta}_{ij}\tilde{\eta}_{kl} = 0 \begin{cases} \text{for} \quad m^{ij}\dot{\eta}^a_{ij} \geq 0 \quad \text{and} \quad m^{ij}\dot{\eta}^b_{ij} \geq 0, \\ \text{or stress within the yield surface,} \end{cases}$$

$$= g^{-1}[m^{ij}(\dot{\eta}_{ijSb} - \dot{\eta}^a_{ij})]^2$$

$$\text{for} \quad m^{ij}\dot{\eta}^a_{ij} \leq 0 \quad \text{and} \quad m^{ij}\dot{\eta}^b_{ij} \leq 0,$$

$$= g^{-1}m^{ij}(\dot{\eta}^b_{ij} - \dot{\eta}^a_{ij})m^{kl}\dot{\eta}^b_{kl}$$

$$\text{for} \quad m^{ij}\dot{\eta}^a_{ij} \geq 0 \quad \text{and} \quad m^{ij}\dot{\eta}^b_{ij} \leq 0,$$

$$= g^{-1}m^{ij}(\dot{\eta}^a_{ij} - \dot{\eta}^b_{ij})m^{kl}\dot{\eta}^a_{kl}$$

$$\text{for} \quad m^{ij}\dot{\eta}^a_{ij} \leq 0 \quad \text{and} \quad m^{ij}\dot{\eta}^b_{ij} \geq 0. \tag{3.14}$$

It is therefore apparent that for positive g the integrand of H is nowhere less than the integrand of F and $H \geq F$. Consequently, the condition

$$F(\lambda, \tilde{u}) > 0 \tag{3.15}$$

for all admissible nonvanishing $\tilde{u}_i$ (which vanish on S_u) is sufficient to ensure uniqueness of the solution increment.

Let λ_c be the lowest eigenvalue with an associated eigenmode $\overset{(1)}{u}_i$ such that $F(\lambda_c, \overset{(1)}{u}) = 0$. The mode is taken to be normalized in some definite way and for simplicity it is assumed to be unique. The variational statement of the eigenvalue problem, $\delta F = 0$, leads to the eigenvalue equations:

$$\overset{(1)}{\eta}_{ij} = \tfrac{1}{2}(\overset{(1)}{u}_{i,j} + \overset{(1)}{u}_{j,i}) + \tfrac{1}{2}(u^{0c}_{k,j}\overset{(1)}{u}{}^{k}_{,i} + u^{0c}_{k,i}\overset{(1)}{u}{}^{k}_{,j}), \tag{3.16}$$

$$\overset{(1)}{\tau}{}^{ij} = L_c^{ijkl}\overset{(1)}{\eta}_{kl}, \tag{3.17}$$

$$(\overset{(1)}{\tau}{}^{ij} + \overset{(1)}{\tau}{}^{kj}u^{0i}_{c,k} + \tau^{kj}_{0c}\overset{(1)}{u}{}^{i}_{,k})_{,j} = 0, \tag{3.18}$$

$$\overset{(1)}{T}{}^{i} = (\overset{(1)}{\tau}{}^{ij} + \overset{(1)}{\tau}{}^{kj}u^{0i}_{,k} + \tau^{kj}_{0c}\overset{(1)}{u}{}^{i}_{,k})n_j = 0 \quad \text{on} \quad S_T, \tag{3.19}$$

and

$$\overset{(1)}{u}_i = 0 \quad \text{on} \quad S_u. \tag{3.20}$$

For bifurcation to be possible at the lowest eigenvalue of F it is necessary that H vanish when F does. However from the inequalities in (3.14) it is seen that $H > F$ when $m^{ij}\dot{\eta}^a_{ij} < 0$ and/or $m^{ij}\dot{\eta}^b_{ij} < 0$ in a finite portion of V. In words, both solutions are possible when $F = 0$ if and only if *both* solutions share the property that no elastic unloading occurs.

The following condition on the fundamental solution ensures that bifurcation can take place at the lowest eigenvalue λ_c. It should be possible to relax

this condition in special cases but for many problems of interest it is clearly satisfied. Suppose there exists a $\Delta > 0$ such that the fundamental solution satisfies

$$m^{ij}(d\eta_{ij}^0/d\lambda) \geq \Delta \tag{3.21}$$

throughout the current yielded region. As already emphasized it is to be understood that the derivative in (3.21) is the one-sided derivative in the sense that the fundamental solution is associated with monotonically increasing λ.

Identify the fundamental solution increment with $\dot{u}_i^a$ and consider a bifurcation solution $\dot{u}_i^b$ in the form of a linear combination of $\dot{u}_i^0$ and $\overset{(1)}{u}_i$. Let $\xi \overset{(1)}{u}_i$ be the contribution of the eigenmode to the bifurcation solution. Define the amplitude ξ such that it is positive. To obtain the opposite-signed contribution of the eigenmode change the sign of $\overset{(1)}{u}_i$ but not ξ. Regarding ξ as the independent variable on the bifurcation branch, write

$$\lambda = \lambda_c + \lambda_1 \xi + \cdots \qquad \text{and} \qquad (du_i^b/d\xi)|_{\lambda_c} = \lambda_1 (du_i^0/d\lambda)|_{\lambda_c} + \overset{(1)}{u}_i, \tag{3.22}$$

so that at bifurcation

$$m^{ij}\, d\eta_{ij}^b/d\xi = m^{ij}[\lambda_1 (d\eta_{ij}^0/d\lambda) + \overset{(1)}{\eta}_{ij}] \geq 0. \tag{3.23}$$

By (3.21), the above inequality can clearly be satisfied if λ_1 is large enough.

Unless $m^{ij}\overset{(1)}{\eta}_{ij} > 0$ throughout the current yielded region, (3.23) implies that $\lambda_1 > 0$ and thus bifurcation takes place under increasing load in the sense of Shanley as generalized by Hill. One can conceive of rather extraordinary problems in which it would turn out that $m^{ij}\overset{(1)}{\eta}_{ij} > 0$ throughout the current yielded region. In such cases bifurcation may be possible under decreasing load in such a way that it is still true that no elastic unloading occurs.

2. *Bifurcation Analysis for Solids with Corners on Their Yield Surfaces*

Generalizations of the constitutive relation (3.8)–(3.10) which account for a singular yield surface with a pyramidal corner have been given by Koiter (1953), Sanders (1954), Mandel (1965), and Hill (1966). At any stage of deformation suppose there are N potentially active deformation systems such that, with $\dot{\gamma}_{(p)}$ denoting the plastic shear rate on the pth system, the plastic part of the strain rate is given by

$$\dot{\eta}_{ij}^{\text{plastic}} = \sum \dot{\gamma}_{(p)} \nu_{ij}^{(p)}.$$

The rate of change of the yield stress on the pth system is denoted by $\dot{\tau}_{(p)}$ and is assumed to be related to the shear rates by (Hill, 1966)

$$\dot{\tau}_{(p)} = \sum h_{(p)(q)} \dot{\gamma}_{(q)} ,$$

where we will take the hardening matrix $h_{(p)(q)}$ to be symmetric. We will formulate the constitutive relation using the convected rates of the contravariant components of the Kirchhoff stress since they arise naturally in the bifurcation analysis. Other choices may be preferable depending on the application (Hill and Rice, 1972), and the development may be altered to accommodate a different choice. The conditions for plastic loading or elastic unloading of the pth system are

$$\dot{\gamma}_{(p)} \geq 0 \qquad \text{if} \quad \dot{\tau}^{ij} v_{ij}^{(p)} = \dot{\tau}_{(p)} \tag{3.24a}$$

and

$$\dot{\gamma}_{(p)} = 0 \qquad \text{if} \quad \dot{\tau}^{ij} v_{ij}^{(p)} < \dot{\tau}_{(p)} . \tag{3.24b}$$

Hill (1966) has shown that a sufficient condition for uniqueness of the stress rate given a prescribed strain rate is that the elastic moduli $\mathscr{L}$ be positive definite and that the hardening matrix $h_{(p)(q)}$ be positive semidefinite.

Since

$$\dot{\tau}^{ij} = \mathscr{L}^{ijkl}(\dot{\eta}_{kl} - \sum \dot{\gamma}_{(p)} v_{kl}^{(p)}),$$

the conditions for loading and unloading can be rewritten in terms of the strain rate and the shear rates as

$$\dot{\gamma}_{(p)} \geq 0 \qquad \text{if} \quad m_{(p)}^{ij} \dot{\eta}_{ij} = \sum A_{(p)(q)} \dot{\gamma}_{(q)} \tag{3.25a}$$

and

$$\dot{\gamma}_{(p)} = 0 \qquad \text{if} \quad m_{(p)}^{ij} \dot{\eta}_{ij} < \sum A_{(p)(q)} \dot{\gamma}_{(q)} , \tag{3.25b}$$

where

$$A_{(p)(q)} = v_{ij}^{(p)} \mathscr{L}^{ijkl} v_{kl}^{(q)} + h_{(p)(q)}$$

and

$$m_{(p)}^{ij} = \mathscr{L}^{ijkl} v_{kl}^{(p)}.$$

Let $\dot{\eta}_{ij}$ be prescribed. Within a subdomain of strain-rate space containing $\dot{\eta}_{ij}$ any solution for the shear rates associated with the systems which do not unload can be written as

$$\dot{\gamma}_{(p)} = \sum B_{(p)(q)} m_{(q)}^{ij} \dot{\eta}_{ij} ,$$

where $B_{(p)(q)}$ is a symmetric $M \times M$ matrix and the sum extends over the M system satisfying (3.25a). In general, the shear rates and B are not unique. If a complete basis can be chosen within the subdomain of strain-rate space in

question, it follows from the fact that the stress rate is unique that the moduli must also be unique in this subdomain. Using the above expression in the equation for $\dot{\tau}^{ij}$, the moduli can be written as

$$L^{ijkl} = \mathscr{L}^{ijkl} - \sum\sum B_{(p)(q)} m^{ij}_{(p)} m^{kl}_{(q)}, \tag{3.26}$$

where again the sums involve only the systems satisfying (3.25a).

Suppose the hardening matrix is *positive definite*. If $\mathscr{L}$ is also positive definite it can be shown that the $N \times N$ matrix A will always be positive definite. Let B^c be the $N \times N$ matrix given by $B^c = A^{-1}$. Define comparison moduli $\mathbf{L}_c$ using B^c in (3.26) with the sums extending over all N systems. Sewell (1972, Section 3, iv) has shown that comparison moduli defined in this way ensure that the fundamental inequality,

$$\tilde{\tau}^{ij}\tilde{\eta}_{ij} - L_c^{ijkl}\tilde{\eta}_{ij}\tilde{\eta}_{kl} \geq 0, \tag{3.27}$$

holds for all strain rates $\dot{\eta}^a_{ij}$ and $\dot{\eta}^b_{ij}$, where $\tilde{\tau}^{ij} = \dot{\tau}^{ij}_b - \dot{\tau}^{ij}_a$ and $\tilde{\eta}_{ij} = \dot{\eta}^b_{ij} - \dot{\eta}^a_{ij}$.

A central concept to our subsequent discussion is *total loading*. Suppose there exists a subdomain of strain-rate space such that no elastic unloading occurs on any system [i.e., (3.25a) holds for all systems]—this is called the total loading subdomain. Within such a domain the comparison moduli $\mathbf{L}_c$ are the actual moduli, and it immediately follows that if $\dot{\eta}^a_{ij}$ and $\dot{\eta}^b_{ij}$ are both within the total loading subdomain then the equality holds in (3.27). It can be shown [from Sewell's construction of (3.27)] that, in general, the equality will not hold if no total loading domain exists or, if it does exist, if *both* $\dot{\eta}^a_{ij}$ and $\dot{\eta}^b_{ij}$ do not lie within it.

In the application of the comparison moduli $\mathbf{L}_c$ to the bifurcation analysis, suppose that the fundamental solution increment satisfies total loading at each point in the body. Then, by the same argument that was made in the analysis of the solid with a smooth yield surface, it is possible to construct a bifurcation solution as some linear combination of the fundamental solution increment and the eigenmode in such a way that the bifurcation solution also satisfies total loading at each point in the body. Consequently, H vanishes when F does as it must if bifurcation is to be possible. The initial slope λ_1 in (3.22) must be chosen to ensure that the bifurcation solution satisfies the total loading constraint.

The requirement that the hardening matrix be positive definite is more restrictive than one would generally wish since, for example, it excludes the case of perfectly plastic behavior. However, for the arguments to be made later in this article it does suffice to assume a positive definite hardening matrix.

Koiter (1953) showed that the slip theory of Batdorf and Budiansky (1949) is a special case of this class of theories in the limiting sense as $N \to \infty$. Sanders (1954) discussed a class of theories broader than slip theory

but also based on the present structure with linear loading functions which for strain-hardening materials has the property that the hardening matrix is positive definite. These theories are pertinent to the discussion of the use of deformation theories in bifurcation analyses to be given later since for total loading histories they coincide with deformation theories of plasticity.

B. General Bifurcation Criterion for the Donnell–Mushtari–Vlasov Theory of Plates and Shells

The Donnell–Mushtari–Vlasov (DMV) approximate strain measures for plates and shells apply when the strains are small and when the characteristic wavelength of deformation is large compared to the thickness of the shell yet small compared to the radii of curvatures of its middle surface. Their application is also restricted to relatively small rotations as discussed by Sanders (1963) and Koiter (1966). A modern treatment of elastic buckling using DMV theory has been given by Budiansky (1968).

Let the material points in a thin plate or shell be identified by convected coordinates x^α ($\alpha = 1, 2$) lying in the middle surface of the undeformed body and the coordinate x^3 normal to the undeformed middle surface. The DMV approximation to the Lagrangian strain tensor in this coordinate system is

$$\eta_{\alpha\beta} = E_{\alpha\beta} + x^3 K_{\alpha\beta}\,, \tag{3.28}$$

where $E_{\alpha\beta}$ and $K_{\alpha\beta}$ are called the stretching and bending strains. They are given in terms of the displacements of the middle surface U_α and W which are tangential and normal, respectively, to the undeformed middle surface by

$$E_{\alpha\beta} = \tfrac{1}{2}(U_{\alpha,\beta} + U_{\beta,\alpha}) + b_{\alpha\beta} W + \tfrac{1}{2} W_{,\alpha} W_{,\beta} \tag{3.29}$$

and

$$K_{\alpha\beta} = -W_{,\alpha\beta}\,, \tag{3.30}$$

where $b_{\alpha\beta}$ is the curvature tensor of the undeformed middle surface and the comma denotes covariant differentiation with respect to a surface coordinate. Greek indices range from 1 to 2.

The approximation to the three-dimensional expression for the internal virtual work in this theory is

$$\int_V \tau^{ij}\,\delta\eta_{ij}\,dV \cong \int_A \{M^{\alpha\beta}\,\delta K_{\alpha\beta} + N^{\alpha\beta}\,\delta E_{\alpha\beta}\}\,dA, \tag{3.31}$$

where dA is the undeformed element of area of the middle surface. The bending moment and resultant stress tensors are given by

$$M^{\alpha\beta} = \int_{-t/2}^{t/2} \tau^{\alpha\beta} x^3\,dx^3 \qquad \text{and} \qquad N^{\alpha\beta} = \int_{-t/2}^{t/2} \tau^{\alpha\beta}\,dx^3, \tag{3.32}$$

where t is the undeformed thickness. An exact principle of virtual work is postulated for the variables of DMV theory. Let $\mathbf{p}$ be the resultant force per unit original area with components p^α and p referred to the base vectors of the undeformed shell. The principle of virtual work is

$$\int_A \{M^{\alpha\beta}\,\delta K_{\alpha\beta} + N^{\alpha\beta}\,\delta E_{\alpha\beta}\}\,dA = \int_A \{p^\alpha\,\delta U_\alpha + p\,\delta W\}\,dA + \text{boundary terms.} \tag{3.33}$$

Equilibrium equations in terms of the stretching force and bending moment tensors are obtained without approximation from (3.33).

To obtain the rate-constitutive relations in terms of the DMV variables we invoke the same approximations as are used in the theory of linearly elastic thin plates and shells. The state of approximate plane stress at each point through the thickness is assumed to apply. The transverse shear-rate components $\dot\eta_{13}$ and $\dot\eta_{23}$ are taken to be zero, and it is assumed that $\tau^{33} = 0$ so that there is no contribution to the internal virtual work from the normal strain rate $\dot\eta_{33}$. For a given strain rate denote the three-dimensional moduli by $\mathbf{L}$ so that

$$\dot\tau^{ij} = L^{ijkl}\dot\eta_{kl}\,. \tag{3.34}$$

The assumption of approximate plane stress gives

$$\dot\tau^{\alpha\beta} = \bar L^{\alpha\beta\kappa\gamma}\dot\eta_{\kappa\gamma}\,, \tag{3.35}$$

where again the Greek indices range from 1 to 2 and the plane-stress moduli are given by

$$\bar L^{\alpha\beta\kappa\gamma} = L^{\alpha\beta\kappa\gamma} - L^{\alpha\beta 33}L^{33\kappa\gamma}/L^{3333}. \tag{3.36}$$

For the special case of the relation (3.8)–(3.10) for solids with a smooth yield surface the plane-stress elastic moduli are given in terms of the three-dimensional quantities by

$$\bar{\mathscr{L}}^{\alpha\beta\kappa\gamma} = \mathscr{L}^{\alpha\beta\kappa\gamma} - \mathscr{L}^{\alpha\beta 33}\mathscr{L}^{33\kappa\gamma}/\mathscr{L}^{3333}. \tag{3.37}$$

One can also show after some manipulation that the assumption of approximate plane stress leads to

$$\dot\tau^{\alpha\beta} = (\bar{\mathscr{L}}^{\alpha\beta\kappa\gamma} - \alpha\bar g^{-1}\bar m^{\alpha\beta}\bar m^{\kappa\gamma})\dot\eta_{\kappa\gamma}\,, \tag{3.38}$$

where $\alpha = 1$ for $\bar m^{\alpha\beta}\dot\eta_{\alpha\beta} \geq 0$ and $\alpha = 0$ otherwise, and where

$$\bar m^{\alpha\beta} = m^{\alpha\beta} - m^{33}\mathscr{L}^{\alpha\beta 33}/\mathscr{L}^{3333} \qquad \text{and} \qquad \bar g^{-1} = g^{-1}\mathscr{L}^{3333}/L^{3333}. \tag{3.39}$$

Using (3.32) and (3.35) the rate-constitutive relations involving the DMV

variables are

$$\dot{N}^{\alpha\beta} = H_{(1)}^{\alpha\beta\kappa\gamma}\dot{E}_{\kappa\gamma} + H_{(2)}^{\alpha\beta\kappa\gamma}\dot{K}_{\kappa\gamma},$$
$$\dot{M}^{\alpha\beta} = H_{(2)}^{\alpha\beta\kappa\gamma}\dot{E}_{\kappa\gamma} + H_{(3)}^{\alpha\beta\kappa\gamma}\dot{K}_{\kappa\gamma}, \tag{3.40}$$

where

$$H_{(i)}^{\alpha\beta\kappa\gamma} = \int_{-t/2}^{t/2} \bar{L}^{\alpha\beta\kappa\gamma}(x^3)^{i-1}\, dx^3. \tag{3.41}$$

In the linear elastic theory of shells the integrations in (3.41) can be performed once and for all. In the elastic-plastic version of the theory the moduli are stress dependent and the active branch of the moduli depends on the strain rate. Thus an essential part of a general elastic-plastic calculation using this theory is the computation of the local stress distribution using the incremental relation (3.35) and evaluation of the integrals in (3.41) by one means or another at each stage of the loading process.

Now we turn to the question of uniqueness within the context of the DMV theory. At a given stage of deformation suppose there are two possible solution rates associated with the same rate of applied (dead) load. Denote these by $\dot{U}_\alpha^a$, $\dot{W}^a$, $\dot{U}_\alpha^b$, $\dot{W}^b$, etc. Following the uniqueness construction of Section III.A introduce the differences $\tilde{U}_\alpha = \dot{U}_\alpha^b - \dot{U}_\alpha^a$, $\tilde{\tau}^{\alpha\beta} = \dot{\tau}_b^{\alpha\beta} - \dot{\tau}_a^{\alpha\beta}$, etc. Then if both solution rates are indeed possible solutions it must follow that

$$H \equiv \int_A \{\tilde{M}^{\alpha\beta}\tilde{K}_{\alpha\beta} + \tilde{N}^{\alpha\beta}\tilde{E}_{\alpha\beta} + N_0^{\alpha\beta}\tilde{W}_{,\alpha}\tilde{W}_{,\beta}\}\, dA = 0, \tag{3.42}$$

where $N_0^{\alpha\beta}$ is the current resultant stress tensor and

$$\tilde{E}_{\alpha\beta} = \tfrac{1}{2}(\tilde{u}_{\alpha,\beta} + \tilde{u}_{\beta,\alpha}) + b_{\alpha\beta}\tilde{W} + \tfrac{1}{2}(W_{,\alpha}^0\tilde{W}_{,\beta} + W_{,\beta}^0\tilde{W}_{,\alpha}),$$
$$\tilde{K}_{\alpha\beta} = -\tilde{W}_{,\alpha\beta}. \tag{3.43}$$

Define three-dimensional comparison moduli in the same way as in Section III.A and use them in (3.36) to obtain the plane-stress comparison moduli $\bar{\mathbf{L}}_c$. Denote the integrals in (3.41) evaluated using $\bar{\mathbf{L}}_c$ by $\overset{c}{\mathbf{H}}_{(i)}$. If the three-dimensional constitutive relation satisfies the fundamental inequality (3.27), then one can show that the DMV quantities as they have been defined satisfy

$$\tilde{M}^{\alpha\beta}\tilde{K}_{\alpha\beta} + \tilde{N}^{\alpha\beta}\tilde{E}_{\alpha\beta} \geq \overset{c}{\mathrm{H}}_{(3)}^{\alpha\beta\kappa\gamma}\tilde{K}_{\alpha\beta}\tilde{K}_{\kappa\gamma} + 2\overset{c}{\mathrm{H}}_{(2)}^{\alpha\beta\kappa\gamma}\tilde{E}_{\alpha\beta}\tilde{K}_{\kappa\gamma} + \overset{c}{H}_{(1)}^{\alpha\beta\kappa\gamma}\tilde{E}_{\alpha\beta}\tilde{E}_{\kappa\gamma}. \tag{3.44}$$

The equality holds if and only if both the solution rates satisfy total loading (i.e., no elastic unloading if $N = 1$) through the shell thickness.

The quadratic functional for testing for bifurcation in the DMV theory is therefore

$$F = \int_A \{\overset{c}{H}{}^{\alpha\beta\kappa\gamma}_{(3)} \tilde{K}_{\alpha\beta} \tilde{K}_{\kappa\gamma} + 2\overset{c}{H}{}^{\alpha\beta\kappa\gamma}_{(2)} \tilde{E}_{\alpha\beta} \tilde{K}_{\kappa\gamma} + \overset{c}{H}{}^{\alpha\beta\kappa\gamma}_{(1)} \tilde{E}_{\alpha\beta} \tilde{E}_{\kappa\gamma} + N_0^{\alpha\beta} \tilde{W}_{,\alpha} \tilde{W}_{,\beta}\}\, dA. \tag{3.45}$$

For any three-dimensional relation which satisfies the inequality (3.27) the condition that $F > 0$ for all admissible, nonvanishing fields $\tilde{U}_\alpha$, $\tilde{W}$ ensures uniqueness. Furthermore by the same argument given in Section III,A, if the fundamental solution rate satisfies total loading, then bifurcation is possible when F first vanishes with the bifurcation mode composed of a linear combination of the fundamental solution rate and the eigenmode. The eigenvalue equations associated with $\delta F = 0$ are listed in Section IV,A.

The Kirchhoff stress tensor arises naturally in the above formulation by virtue of the fact that the theory employs an approximation to the Lagrangian strain tensor and the undeformed configuration as reference. Since the difference between two stress-rate measures involves terms like $\tau\dot{\eta}$, such differences will be small if the stress is small compared to the instantaneous moduli. In the compressive buckling of columns, plates, and shells the stress level is usually a small fraction of the instantaneous moduli at buckling. For example, the compressive bifurcation stress of a column is given by the tangent-modulus formula $CE_t(t/L)^2$, where C is a constant of order unity determined by the cross section and end conditions, and t and L are the characteristic thickness and length of the column. For a practical analysis of a slender column one can therefore use a "small strain" theory of strain-hardening plasticity in which no care is paid to the specification of the stress-rate measure. On the other hand, when the stress at bifurcation is comparable in magnitude to the instantaneous moduli it is necessary to correctly identify $\dot{\tau}^{\alpha\beta}$ as the convected rate of change of the contravariant components of the Kirchhoff stress. The moduli in (3.34) must also be chosen consistent with this interpretation. A recent discussion of the extent to which the stress-rate choice influences bifurcation predictions is illustrated in a number of examples examined by Bazant (1971).

As it stands, (3.45) is referred to the original configuration as has been discussed. If it is desired to use the deformed configuration at bifurcation as the reference then (3.45) remains unchanged in form except that now the comma denotes covariant differentiation base vectors of the deformed middle surface, $\tilde{W}$ represents a deflection normal to the current middle surface, etc., and the components $N^{0\alpha\beta}$ are referred to the current base vectors. Also, W^0 must be set to zero in (3.43), t represents the current

thickness, and dA the current element of area of the middle surface. Since the theory is restricted to small strains it is usually unnecessary to draw a distinction between the area and thickness of the shell at bifurcation and in the undeformed state.

C. Discussion of Bifurcation Predictions Based on the Simplest Incremental and Deformation Theories of Plasticity

In the examples to be discussed below the stress levels at bifurcation are a small fraction of the instantaneous moduli so that a discussion within the context of small strain theories of strain-hardening plasticity is justified. The most widely used incremental strain-hardening theory is J_2 flow theory. In Cartesian coordinates the stress deviator is $s_{ij} = \tau_{ij} - \frac{1}{3}\tau_{kk}\delta_{ij}$ and $J_2 = \frac{1}{2}s_{ij}s_{ij}$. The instantaneous moduli are given by

$$L_{ijkl} = \frac{E}{1+\nu}\left(\frac{1}{2}(\delta_{ik}\delta_{jl} + \delta_{il}\delta_{jk}) + \frac{\nu}{1-2\nu}\delta_{ij}\delta_{kl} - \frac{\alpha h_1 s_{ij}s_{kl}}{1+\nu+2h_1 J_2}\right), \tag{3.46}$$

where E is Young's modulus and ν is Poisson's ratio. For $J_2 = (J_2)_{\max}$, $\alpha = 1$ if $\dot{J}_2 \geq 0$, $\alpha = 0$ if $\dot{J}_2 < 0$, and $\alpha = 0$ if $J_2 < (J_2)_{\max}$. The function $h_1(J_2)$ is determined from the tensile stress–strain curve in terms of the tangent modulus E_t (i.e., $\dot{\sigma} = E_t\dot{\varepsilon}$) as

$$h_1 = 3[E/E_t - 1]/(4J_2). \tag{3.47}$$

The comparison moduli are given by (3.46) with $\alpha = 1$ where $J_2 = (J_2)_{\max}$.

Since J_2 flow theory satisfies the inequality (3.27) the functional F defined in (3.45) does form the basis of the sufficiency condition for uniqueness. Furthermore when the fundamental solution has the property that $\dot{J}_2 > 0$ everywhere the yield condition is currently satisfied, then bifurcation is possible at the lowest eigenvalue of F.

The simplest total strain theory of plasticity is usually referred to as J_2 deformation theory. It is a small-strain nonlinear elasticity relation in which the total strain can be expressed as a function of the stress according to

$$\varepsilon_{ij} = (1/E)\{(1+\nu)\sigma_{ij} - \nu\sigma_{kk}\delta_{ij} + h_2(J_2)s_{ij}\}, \tag{3.48}$$

where

$$h_2(J_2) = \tfrac{3}{2}(E/E_s - 1), \tag{3.49}$$

and where $E_s = \sigma/\varepsilon$ is the secant modulus in a tension test. The instantaneous moduli are

$$L_{ijkl} = \frac{E}{1+\nu+h_2}\left(\frac{1}{2}(\delta_{ik}\delta_{jl}+\delta_{il}\delta_{jk})+\frac{3\nu+h_2}{3(1-2\nu)}\delta_{ij}\delta_{kl}\right.$$
$$\left. - \frac{h_2' s_{ij}s_{kl}}{1+\nu+h_2+2h_2'J_2}\right), \tag{3.50}$$

where $h_2' \equiv dh_2/dJ_2$.

Bifurcation predictions based on F in (3.45) with either (3.46) or (3.50) reduce to results obtained by many authors. Most problems which have been worked out in detail have a fundamental pre-bifurcation solution which is a trivial uniform state of stress. Many solutions (some involving additional approximations) are presented in the well-known references by Bijlaard (1949), Stowell (1948), and Gerard and Becker (1957). More recent work includes Lee's (1961, 1962) cylindrical shell studies, Batterman's (1964) equations for axisymmetric shells, and Jones' (1967) results for eccentrically stiffened shells. Sewell's (1972) bibliography includes many more references to problems in this class.

Sanders (1954) has shown that incremental theories of plasticity based on linear loading functions such as those alluded to in Section III,A are integrable for total loading histories on which no activated loading function unloads. In particular, he has shown that there exists an incremental theory with infinitely many loading functions which coincides exactly with J_2 deformation theory for total loading. Put another way, for a restricted range of deformations J_2 deformation theory coincides with a physically acceptable incremental theory which develops a corner on its yield surface.

Slip theory of Batdorf and Budiansky (1949) is also integrable for total loading deformations but it coincides with a deformation theory involving both J_2 and the third invariant of the stress. We have already remarked that theories based on multiple loading functions satisfy the fundamental inequality required to establish the validity of the bifurcation criterion based on F.

It follows from Sanders' observation that most of the results which have been obtained using J_2 deformation theory are *rigorously* valid bifurcation predictions based on the incremental theory mentioned above which coincides with J_2 deformation for total loading. This is contrary to statements made repeatedly in the literature to the effect that bifurcation predictions based on deformation theory are physically unacceptable. To be more specific, suppose the fundamental solution satisfies proportional loading everywhere, as is the case for almost all the examples which have been worked out in detail in the literature. The bifurcation solution is a linear sum of the fundamental solution increment and the eigenmode. We can always include a sufficiently large amount of the fundamental solution increment relative to the eigenmode such that the bifurcation mode satisfies the total loading restriction. It seems to be widely appreciated that J_2 deformation

theory cannot be labeled physically unacceptable for total loading histories (Budiansky, 1959). The confusion in bifurcation applications apparently stems from the misconception that when bifurcation occurs total loading will be violated. On the contrary, it is the total-loading condition itself which supplies the constraint on the combination of fundamental solution increment and eigenmode which must pertain—just as it is the condition $m^{ij}\dot{\eta}^b_{ij} \geq 0$ which provides the constraint in (3.23) for the case of a smooth yield surface. The above line of reasoning is due to Batdorf (1949) who used slip theory, which was developed for this purpose, as the basis for his argument.

As long as the fundamental solution satisfies total loading there are no grounds that we have yet mentioned which favor the bifurcation-load predictions based on J_2 flow theory over those based on J_2 deformation theory or vice versa.

Perhaps the best example which brings out the essence of the difference between the two simple theories in bifurcation applications is the buckling of a cruciform column under axial compression shown in Fig. 9 and studied

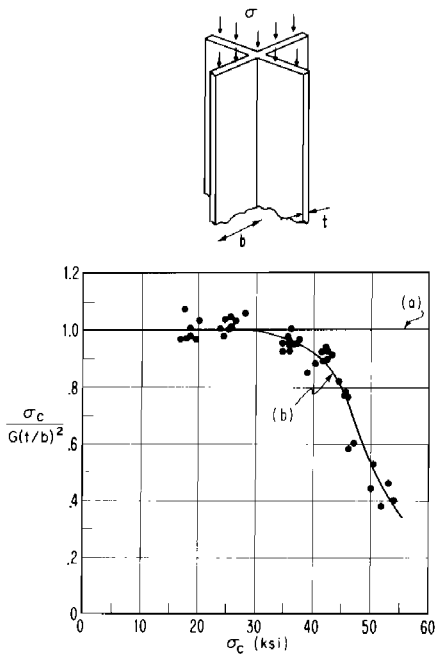

FIG. 9. Theoretical and experimental results for the plastic buckling of a cruciform column. Curve a, prediction of incremental theory with smooth yield surface; curve b, prediction of any deformation theory with $\nu = \frac{1}{2}$; test data from 2024-T4 cruciform sections. From Gerard and Becker, (1957).

originally by Stowell (1948). If the column is not too long, it undergoes torsional buckling in which the specimen twists about its axis. Only the effective shear modulus enters into the formula for the bifurcation stress. In the elastic range the compressive stress at bifurcation is

$$\sigma_c = G(t/b)^2, \tag{3.51}$$

where G is the elastic shear modulus, t is the thickness, and b is the width of the flange plates. This result can be obtained in several ways; but, in particular, it can be obtained from the DMV theory as a limiting case for a long plate which is simply supported along one of the long edges and free on the other (Timoshenko and Gere, 1961).†

In the plastic range (3.51) still holds according to J_2 flow theory. Because this plasticity theory has a smooth yield surface, the increments in the relevant components of shear stress and shear strain following uniaxial compression are related by the elastic shear modulus. On the other hand, for *any* deformation theory for an initially isotropic material it can be shown that the relevant instantaneous shear modulus $\bar{G}$ following uniaxial compression is given by

$$\bar{G} = \frac{G}{1 + 3G(1/E_s - 1/E)}, \tag{3.52}$$

where $E_s \equiv \sigma/\varepsilon$ is the secant modulus. The deformation-theory prediction (and consequently that of slip theory too) is

$$\sigma_c = \bar{G}(t/b)^2. \tag{3.53}$$

Thus the ratio of the deformation-theory result to the simple flow-theory result is $\bar{G}/G$ and for Poisson's ratio equal to $\frac{1}{2}$ so $G = \frac{1}{3}E$ in (3.52) this ratio equals E_s/E.

Experimental results in the form of the buckling stress normalized by $G(t/b)^2$ are plotted as a function of σ_c in Fig. 9. These experiments were performed on specimens of 2024-T4 aluminum and the figure was taken from Gerard and Becker (1957). The discrepancy between the two theories for the cruciform column is more dramatic than occurs in most problems. Nevertheless, it is generally agreed that bifurcation-load predictions for plates based on J_2 deformation theory give reasonably good agreement with experimental buckling loads while predictions based on J_2 flow theory are consistently high.‡

The cruciform column was discussed extensively in the literature by

† For flat plates the DMV equations reduce to the von Kármán plate equations.

‡ A strong assertion to the contrary made by J. B. Newman [Inelastic column buckling of internally pressurized tubes, *Exp. Mech.* **13**, 265–273 (1973)], stems from the use of an incorrect formula for the bifurcation load according to deformation theory.

Drucker (1949), Cicala (1950), Bijlaard (1950), and Onat and Drucker (1953). In part, this discussion centered on whether or not imperfections could account for the discrepancy between the predictions of simple flow theory and deformation theory. Based on a rather approximate analysis Cicala (1950) concluded that small imperfections, which would inevitably be present in any actual specimen, would reduce the maximum support load calculated using J_2 flow theory to the level of the deformation-theory bifurcation load. Bijlaard (1950) refuted Cicala's claim on the grounds that the imperfection levels Cicala was considering would by no means inevitably be present. Onat and Drucker (1953) carried out a more detailed, but still approximate, calculation of the maximum support load based on J_2 flow theory and found that extremely small imperfections did reduce the maximum load to essentially the level of the deformation-theory bifurcation load. The imperfections required to bring about this reduction were so small that they suggested that no significant scatter in the buckling loads should be expected (as is usually the case when imperfection sensitivity is involved), as the test data seems to indicate. If they are correct in asserting that the yield surface should be taken to be smooth and if their conclusion regarding the effect of small imperfections is also correct, the prospect of having to take into account initial imperfections in this manner just to calculate an effective buckling load is hardly a happy one. In any case, this example does lend further credibility to the use of bifurcation-load predictions of deformation theory for engineering purposes.

As discussed above the essential difference between the two sets of predictions revolves around the question of whether the description of the yield surface should allow for corners. Theoretical models based on single-crystal slip (such as slip theory or the more elaborate models which followed it) definitely indicate that corners should develop (Hill, 1967b; Hutchinson, 1970; Lin, 1971). However, experimental evidence on this question is contradictory. Adequate direct evidence in the form of measured yield surfaces is extremely difficult to obtain for these purposes since experimental probing of the yield surface tends to obliterate any potential corner. Nevertheless, many tests do show that a region of high curvature does develop at the loading point on the yield surface. Biaxial tests or tension–torsion tests which directly measure incremental stiffnesses are more likely to shed light on this matter. But here too, the experimental evidence is contradictory with some investigators finding evidence which suggests corners and others finding none. A recent survey of the history of yield surface experimentation is given by Michno and Findley (1972).

So far the evidence from basic stress–strain tests must be regarded as inconclusive with regard to whether or not adequate models of the elastic-plastic behavior of common metals should incorporate yield surfaces with

corners. Fortunately, experimental work in this area is continuing and the accuracy of the tests is improving so that there may be clearer evidence available in the future. In the meantime there seems to be little doubt that for engineering purposes bifurcation prediction based on deformation theory should be favored over those based on incremental theories with smooth yield surfaces. This should not be construed as an argument for the universal application of deformation theory. In fact where deformation histories do depart from total loading, as may be the case in the post-bifurcation regime, for example, deformation-theory predictions must obviously be regarded with suspicion.

We conclude this section with two additional examples which more typically illustrate the discrepancy between the bifurcation predictions of these two theories. Bifurcation results for these two examples will serve as the starting point for post-bifurcation and imperfection-sensitivity studies presented in Sections IV and V.

Consider a clamped circular plate of radius R and thickness t subject to a uniform radial stress σ. The elastic bifurcation stress for compressive loading obtained from the DMV criterion is

$$\sigma_c = -k^2 Et^2/12(1 - \nu^2)R^2, \tag{3.54}$$

where $k \cong 3.832$ is the first zero of the Bessel function of the first kind of first order (Timoshenko and Gere, 1961).

In the plastic range the fundamental solution continues to be the uniform state of equal biaxial compression. The plane-stress comparison moduli relating the inplane stress rates and strain rates must be isotropic at bifurcation. Without any approximation we can introduce an instantaneous modulus $\bar{E}$ and contraction ratio $\bar{\nu}$ so that

$$\bar{E}\dot{\eta}_{\alpha\beta} = (1 + \bar{\nu})\dot{\tau}_{\alpha\beta} - \bar{\nu}\dot{\tau}_{\gamma\gamma}\delta_{\alpha\beta}\,. \tag{3.55}$$

Also without approximation the lowest bifurcation stress according to DMV theory is given (3.54) using $\bar{E}$ and $\bar{\nu}$ instead of E and ν, i.e.,

$$\sigma_c = -k^2 \bar{E}t^2/12(1 - \bar{\nu}^2)R^2. \tag{3.56}$$

For J_2 flow theory $\bar{E}$ and $\bar{\nu}$ are given by

$$\begin{aligned} E/\bar{E} &= [1 + (E/E_t - 1)/4], \\ \bar{\nu} &= (\bar{E}/E)[\nu - (E/E_t - 1)/4], \end{aligned} \tag{3.57}$$

where E_t is the tangent modulus in simple tension which is regarded as a function of J_2 as in (3.47). For J_2 deformation theory,

$$\begin{aligned} \bar{E}^{-1} &= (E_t^{-1} + 3E_s^{-1})/4, \\ \bar{\nu}\bar{E}^{-1} &= -[2(1 - 2\nu)E^{-1} + E_t^{-1} - 3E_s^{-1}]/4, \end{aligned} \tag{3.58}$$

where E_s is the secant modulus in simple tension and is also taken to be a function of J_2.

An example studied by Needleman (1973) to be discussed further in Section V uses a uniaxial tensile stress–strain curve which has a definite yield stress σ_y and yield strain $\varepsilon_y = \sigma_y/E$ and a continuous tangent modulus where

$$\varepsilon/\varepsilon_y = \begin{cases} \sigma/\sigma_y & \text{for} \quad \sigma \leq \sigma_y\,, \\ n^{-1}(\sigma/\sigma_y)^n + 1 - n^{-1}, & \text{for} \quad \sigma > \sigma_y\,. \end{cases} \tag{3.59}$$

This curve is shown in Fig. 10 with a strain-hardening exponent of $n = 12$.

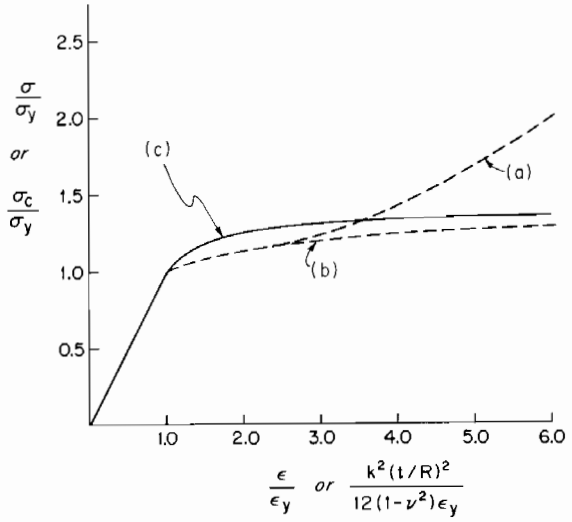

FIG. 10. Stress–strain curve and bifurcation predictions for a clamped circular plate under radial compression. Curve a, J_2 flow-theory predictions; curve b, J_2 deformation-theory predictions; curve c, σ/σ_y vs $\varepsilon/\varepsilon_y$: Eq. (3.59), $n = 12$; for (a) and (b) σ_c/σ_y vs $k^2(t/R)^2/12(1-\nu^2)\varepsilon_y$; $\nu = \frac{1}{3}$.

Also shown in Fig. 10 are the predictions for the bifurcation stress from (3.56) using (3.57) and (3.58) derived from this tensile stress–strain curve. The bifurcation results are conveniently plotted as σ_c/σ_y against $k^2(t/R)^2/[12\varepsilon_y(1-\nu^2)]$ so that in the elastic range the bifurcation curves plot on top of the stress–strain curve. For bifurcation stresses which are not more than about 20% in excess of the yield stress (and thus bifurcation strains not exceeding about $2\frac{1}{2}$ times the yield strain) the difference between the two theories is very small. For larger values of the abscissa the difference is no longer insignificant.

A second example which can be analyzed in an equally simple manner is

the thin spherical shell under uniform external pressure. The pre-bifurcation solution is again the uniform state of equal biaxial compression. In terms of $\bar{E}$ and $\bar{\nu}$ in (3.55) the stress in the spherical shell at bifurcation is

$$\sigma_c = -\bar{E}t/[3(1-\bar{\nu}^2)]^{1/2}R, \tag{3.60}$$

where now t and R are the thickness and radius of the shell. This result also comes from DMV theory as discussed by Hutchinson (1972); with $\bar{E}$ and $\bar{\nu}$ assuming their elastic values, (3.60) is the elastic formula. Figure 11 has been

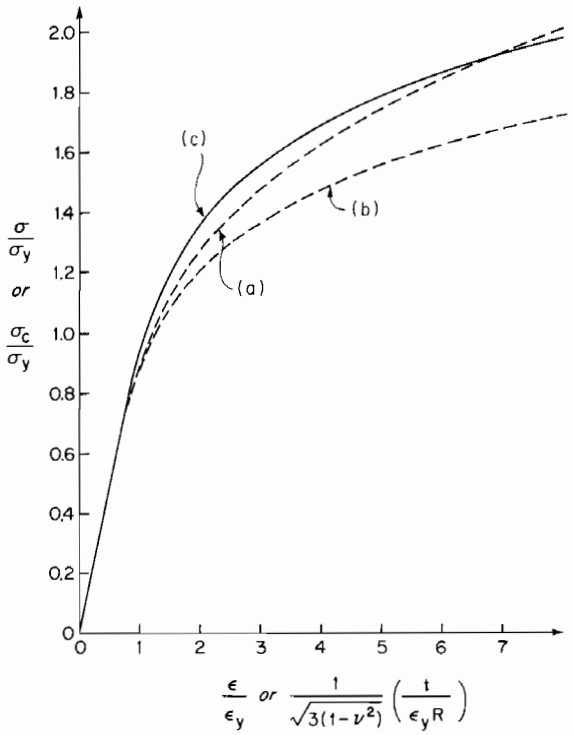

FIG. 11. Stress strain curve and bifurcation predictions for a complete spherical shell under external pressure. Curve a, flow-theory predictions; curve b, deformation-theory predictions; curve c, $\varepsilon/\varepsilon_y = \sigma/\sigma_y + 0.1(\sigma/\sigma_y)^6$; for (a) and (b): σ_c/σ_y vs $[3(1-\nu^2)]^{-1/2}(t/\varepsilon_y R)$; $\nu = \frac{1}{3}$.

plotted in the same way as was done for the corresponding plate curves. Here, however, a Ramberg–Osgood-type tensile relation has been used where ε_y and $\sigma_y \equiv E\varepsilon_y$ are now an effective yield strain and yield stress, and $n = 6$ was chosen as illustrative of relatively high strain hardening.

Bijlaard (1949) recognized that the elastic results for the above sphere and

circular plate problems could be simply converted to give bifurcation loads in the plastic range. His paper includes predictions based on the two simple theories used above. A rederivation of Bijlaard's result for the sphere has been given by Batterman (1969) for J_2 flow theory.

Sewell (1963, 1964) studied the extent to which the orientation of the normal to the smooth yield surface influenced the lowest bifurcation load. In his study of rectangular plates under uniaxial compression which are simply supported on all four sides he found that by allowing the normal to differ from that of J_2 flow theory somewhat lower bifurcation loads could be obtained. Justification for the different choice of normal requires an appeal to initial plastic anisotropy. In a more recent study Sewell (1973) reexamined this same plate problem using a plasticity theory based on the two loading functions associated with the corner of the Tresca yield surface. Appreciable reductions below the predictions of J_2 flow theory were found. However it does not follow from these findings that the Tresca yield surface is generally suitable for bifurcation calculations. If the Tresca yield surface is used in the analysis of the cruciform column one still obtains the elastic prediction (3.51) since the corner associated with the Tresca surface does not lower the effective shear modulus in question below its elastic value.

IV. Initial Post-Bifurcation Behavior for Donnell–Mushtari–Vlasov Theory

In this section behavior immediately following bifurcation is studied within the context of DMV theory. Attention is focused on bifurcations emanating from the lowest possible bifurcation point. Growth of the region of elastic unloading is involved in an essential way in the determination of the initial post-bifurcation behavior as has been previously brought out by the continuous model of Section II,B. The analysis will parallel that given for the continuous model as well as a treatment of three-dimensional solids given by Hutchinson (1973a).

One difficulty which must be faced immediately in the initial post-bifurcation analysis is the choice of constitutive relation. A deformation theory which incorporates elastic unloading is generally unsatisfactory in that it violates continuity requirements, as is well known. This is in addition to the loss of its justification once total loading can no longer be claimed, which will often be the case in the post-bifurcation regime. On the other hand, we have seen that where deformation theory predictions for the bifurcation load fall significantly below those of a simple incremental theory the deformation-theory predictions are in better accord with experimental data. We strike a compromise here by using the incremental theory based on a smooth yield surface and by restricting consideration to specific examples

where the bifurcation load is only slightly greater than the J_2 deformation-theory prediction. In two column problems which will be looked at in some detail this question does not even arise since the stress–strain behavior is essentially unidirectional. However in the general situation this predicament underlines the lack of a reasonably simple yet adequate constitutive relation for common structural metals even for the restricted class of deformation histories involved in plastic buckling problems.

The general constitutive relation (3.8)–(3.10) will be used; under the assumption of approximate plane stress this relation has been rewritten in terms of the in-plane stress and strain components in (3.37) to (3.39). Although it is not crucial to the analysis we will make the simplifying assumption that the body becomes fully plastic prior to bifurcation.

Let λ be the single load parameter and let dead loads (and/or displacements) be applied proportional to λ. Let the fundamental solution be associated with monotonically increasing λ prior to the occurrence of any limit point of λ and label the fundamental solution with a superscript or subscript 0. Attention is restricted to bifurcations which occur prior to a limit point of λ. With ξ denoting the (positive) amplitude of the eigenmode associated with the lowest bifurcation load λ_c, we will show that the initial post-bifurcation expansion is of the form

$$\lambda = \lambda_c + \lambda_1 \xi + \lambda_2 \xi^{1+\beta} + \cdots, \tag{4.1}$$

where $0 < \beta \leq 1$. Generally, $\lambda_1 > 0$; in the examples examined below, $\beta = \frac{1}{3}$ or $\frac{2}{5}$ and $\lambda_2 < 0$.

A. General Theory

1. *Equations for the Eigenvalue Problem and Determination of* λ_1

Denote the eigenmodal quantities associated with the lowest value λ_c for which F vanishes by

$$\{\overset{(1)}{U}_\alpha, \overset{(1)}{W}, \overset{(1)}{E}_{\alpha\beta}, \overset{(1)}{K}_{\alpha\beta}, \overset{(1)}{\eta}_{\alpha\beta}, \overset{(1)}{N}^{\alpha\beta}, \overset{(1)}{M}^{\alpha\beta}, \overset{(1)}{\tau}^{\alpha\beta}\}, \tag{4.2}$$

where the local quantities which vary through the thickness are listed along with the quantities which are functions of just the two middle surface coordinates x^α. The first variation of F also vanishes at λ_c, i.e.,

$$\int_A \{\overset{(1)}{M}^{\alpha\beta}\delta K_{\alpha\beta} + \overset{(1)}{N}^{\alpha\beta}\delta^c E_{\alpha\beta} + \overset{(1)}{N}^{\alpha\beta}_{0c} W_{,\alpha}\delta W_{,\beta}\}\, dA = 0, \tag{4.3a}$$

with

$$\delta^c E_{\alpha\beta} \equiv \tfrac{1}{2}(\delta U_{\alpha,\beta} + \delta U_{\beta,\alpha}) + b_{\alpha\beta}\delta W + \tfrac{1}{2}(W^{0c}_{,\alpha}\delta W_{,\beta} + W^{0c}_{,\beta}\delta W_{,\alpha}), \tag{4.3b}$$

which generates the equilibrium equations and homogeneous boundary conditions for the eigenvalue problem. In addition, the eigenmodal quantities satisfy:

$$\overset{(1)}{N}{}^{\alpha\beta} = \overset{c}{H}{}^{\alpha\beta\kappa\gamma}_{(1)} \overset{(1)}{E}_{\kappa\gamma} + \overset{c}{H}{}^{\alpha\beta\kappa\gamma}_{(2)} \overset{(1)}{K}_{\kappa\gamma},$$

$$\overset{(1)}{M}{}^{\alpha\beta} = \overset{c}{H}{}^{\alpha\beta\kappa\gamma}_{(2)} \overset{(1)}{E}_{\kappa\gamma} + \overset{c}{H}{}^{\alpha\beta\kappa\gamma}_{(3)} \overset{(1)}{K}_{\kappa\gamma}, \tag{4.3c}$$

$$\overset{(1)}{K}_{\alpha\beta} = -\overset{(1)}{W}_{,\alpha\beta},$$

$$\overset{(1)}{E}_{\alpha\beta} = \tfrac{1}{2}(\overset{(1)}{U}_{\alpha,\beta} + \overset{(1)}{U}_{\beta,\alpha}) + b_{\alpha\beta}\overset{(1)}{W} + \tfrac{1}{2}(W^{0c}_{,\alpha}\overset{(1)}{W}_{,\beta} + W^{0c}_{,\beta}\overset{(1)}{W}_{,\alpha}), \tag{4.3d}$$

$$\overset{(1)}{\tau}{}^{\alpha\beta} = \bar{L}^{\alpha\beta\kappa\gamma}_{c}\overset{(1)}{\eta}_{\kappa\gamma}, \tag{4.3e}$$

and

$$\overset{(1)}{\eta}_{\alpha\beta} = \overset{(1)}{E}_{\alpha\beta} + x^3\overset{(1)}{K}_{\alpha\beta}. \tag{4.3f}$$

A superscript or subscript c denotes quantities evaluated at λ_c. The quantities $\bar{\mathbf{L}}_c$ and $\overset{c}{\mathbf{H}}_{(i)}$ were defined in Section III.B and, in general, $\bar{\mathbf{L}}_c$ may vary through the thickness as well as over the middle surface. Equations (4.3e) and (4.3f) are auxiliary to the eigenvalue problem but nonetheless are important to the initial post-bifurcation analysis.

Attention is restricted to problems in which the eigenmode associated with λ_c is unique. The mode is normalized in some definite way. As defined previously, ξ is the amplitude of the eigenmodal contribution to the bifurcated solution. It is used as the expansion variable; ξ is defined to be positive and is increased monotonically in the initial post-bifurcation regime. To analyze the opposite-signed deflection in the eigenmode we will change the sign of the eigenmodal quantities (4.2).

It is assumed that the fundamental solution satisfies

$$\bar{m}^{\alpha\beta}_{c}\overset{0}{\eta}{}'_{\alpha\beta} \geq \Delta > 0, \tag{4.4}$$

where for the remainder of the paper

$$(\,)' \equiv [d(\quad)/d\lambda]_c. \tag{4.5}$$

As already discussed, the bifurcated solution is of the form,

$$\begin{Bmatrix} U_\alpha \\ W \end{Bmatrix} = \begin{Bmatrix} U^{0c}_\alpha \\ W^{0}_{c} \end{Bmatrix} + \xi \begin{Bmatrix} \lambda_1 \overset{0}{U}{}'_\alpha + \overset{(1)}{U}_\alpha \\ \lambda_1 \overset{0}{W}{}' + \overset{(1)}{W} \end{Bmatrix} + \cdots, \tag{4.6}$$

with similar expressions for the other variables and where λ_1 was introduced in (4.1). An equivalent form for the expansion is

$$\begin{Bmatrix} \dot{U}_\alpha \\ \dot{W} \end{Bmatrix} = \begin{Bmatrix} \dot{U}^0_\alpha \\ \dot{W}^0 \end{Bmatrix} + \begin{Bmatrix} \overset{(1)}{U}_\alpha \\ \overset{(1)}{W} \end{Bmatrix} + \cdots, \tag{4.7}$$

where

$$(\dot{\ }) \equiv d(\quad)/d\xi \tag{4.8}$$

and, for example, $\dot{W}^0$ is shorthand for $(dW^0/d\lambda)(d\lambda/d\xi)$. The Shanley condition for no elastic unloading at bifurcation requires

$$\bar{m}^{\alpha\beta}_c(\lambda_1 \overset{\prime}{\eta}{}^0_{\alpha\beta} + \overset{(1)}{\eta}_{\alpha\beta}) \geq 0 \tag{4.9}$$

at every point in the body which provides a constraint on λ_1 which clearly can be met if (4.4) holds.

Recall that two possibilities were encountered in the analysis of the models of Section II. Either no elastic unloading occurred on the bifurcated solution branch in some finite neighborhood of λ_c or neutral loading occurred at one point in the body at bifurcation and elastic unloading spread from this point as the amplitude of the bifurcation deflection increased. The same is true here. In the unlikely event that the structure possesses a sufficiently large stabilizing geometric nonlinearity such that λ_1 is greater than the smallest value needed to ensure (4.9), then no elastic unloading will occur for some range of *positive* ξ. The criterion for identifying this possibility will be given later, along with the associated formula for λ_1. The second possibility is more typical and by far the more important. Then λ_1 assumes the smallest value consistent with (4.9). This is the case which is analyzed below.

2. *Lowest-Order Boundary-Layer Terms*

The instantaneous neutral loading surface separating the regions of elastic unloading and plastic loading spreads from a point x^i_c as ξ increases from zero as depicted in Fig. 12. The initial neutral loading point is denoted by x^i_c and is the point where the equality in (4.9) is attained. In some problems neutral loading at bifurcation may occur at more than one isolated point or along a line of points, as for example in an axisymmetric bifurcation of a shell of revolution. We will carry out all the details of the analysis for the case where x^i_c is an isolated point. In most problems x^i_c will lie on one of the

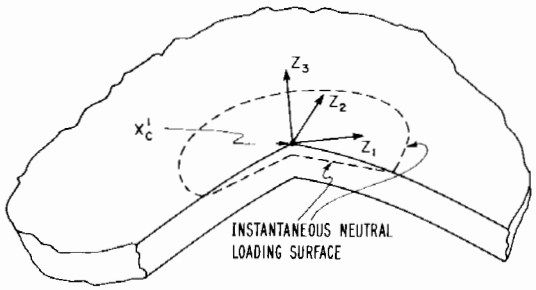

FIG. 12. Sketch of the initial neutral loading point, the subsequent instantaneous neutral-loading surface and the local Cartesian triad.

two surfaces of the shell as in Fig. 12 and this will be assumed to be the case here. Other variants can be analyzed with the same approach.

With λ_1 chosen such that the equality holds at x_c^i in (4.9), the function on the left-hand side of this inequality is greater than zero elsewhere in the body. It enters into the initial post-bifurcation analysis in an essential way. To display the behavior of this function in the neighborhood of x_c^i introduce a set of local Cartesian coordinates z_i centered at x_c^i as shown in Fig. 12 such that z_3 is directed along the outward normal to the surface on which x_c^i lies. Using a Taylor series expansion about x_c^i, write

$$\bar{m}_c^{\alpha\beta}(\lambda_1 \overset{\prime}{\eta}{}^0_{\alpha\beta} + \overset{(1)}{\eta}_{\alpha\beta}) = C_3 z_3 + C_{\alpha\beta} z_\alpha z_\beta + \cdots, \tag{4.10}$$

where

$$C_3 = \frac{\partial}{\partial z_3}[\bar{m}_c^{\alpha\beta}(\lambda_1 \overset{\prime}{\eta}{}^0_{\alpha\beta} + \overset{(1)}{\eta}_{\alpha\beta})]\Big|_{x_c^i},$$
$$C_{\kappa\gamma} = \frac{1}{2}\frac{\partial}{\partial z_\kappa}\frac{\partial}{\partial z_\gamma}[\bar{m}_c^{\alpha\beta}(\lambda_1 \overset{\prime}{\eta}{}^0_{\alpha\beta} + \overset{(1)}{\eta}_{\alpha\beta})]\Big|_{x_c^i}. \tag{4.11}$$

Since (4.10) attains its minimum in the body at x_c^i, $C_1 = C_2 = 0$ and $C_3 \leq 0$. In the subsequent analysis it is crucial to distinguish between instances where $C_3 < 0$ and where $C_3 = 0$. It will almost always be the case that $C_3 \neq 0$ if the eigenmode involves bending. For example, suppose the fundamental state is a uniform state of stress; then from (4.11) and (4.3f)

$$C_3 = -|\bar{m}_c^{\alpha\beta} \overset{(1)}{K}_{\alpha\beta}|_{x_c^i},$$

which will vanish only under exceptional circumstances. We will carry out the analysis under the assumption that $C_3 < 0$ and later comment on the case where $C_3 = 0$.

Motivated by the simple model results, an expansion is attempted in the form (4.1) so that

$$\dot{\lambda} = \lambda_1 + (1 + \beta)\lambda_2 \xi^{\beta} + \tilde{\lambda}, \tag{4.12}$$

where the remainder satisfies $(\xi^{-\beta}\tilde{\lambda}) = 0$ as $\xi \to 0$. Using this relation to expand the fundamental solution about λ_c gives for a typical quantity such as the stress

$$\dot{\tau}_0^{ij} \equiv \frac{d\tau_0^{ij}}{d\lambda}\frac{d\lambda}{d\xi} = \lambda_1 \overset{\prime}{\tau}{}_0^{ij} + (1 + \beta)\lambda_2 \xi^{\beta} \overset{\prime}{\tau}{}_0^{ij} + \cdots. \tag{4.13}$$

As the region of elastic unloading spreads from x_c^i and engulfs a point, the relation between the stress rate and strain rate changes from being determined by the plastic moduli $\mathbf{L}$ to the elastic moduli $\mathscr{L}$. A set of stretched boundary-layer coordinates z_i^* will be introduced such that the equation of the neutral loading surface will be independent of ξ to lowest order when written in terms of these coordinates. These same coordinates are the natural choice for use in the description of behavior in the vicinity of the growing elastic unloading region.

Anticipating that the lowest-order correction to the bifurcation mode (4.7) are of order ξ^{β} we can write quite generally that

$$\begin{Bmatrix} \dot{\eta}_{\alpha\rho} \\ \dot{\tau}^{\alpha\rho} \end{Bmatrix} = \begin{Bmatrix} \dot{\eta}_{\alpha\rho}^{0} \\ \dot{\tau}_0^{\alpha\rho} \end{Bmatrix} + \begin{Bmatrix} \overset{(1)}{\eta}{}_{\alpha\rho} \\ \overset{(1)}{\tau}{}^{\alpha\rho} \end{Bmatrix} + \xi^{\beta} \begin{Bmatrix} \overset{a}{\eta}{}_{\alpha\rho}(\xi, x^i) \\ \overset{a}{\tau}{}^{\alpha\rho}(\xi, x^i) \end{Bmatrix}. \tag{4.14}^{\dagger}$$

To introduce the boundary-layer description two distinct limits of the last terms in (4.14) are considered. In the first the point x^i $(x^i \neq x_c^i)$ is held fixed so that the elastic-unloading region leaves x^i behind as it shrinks to the point x_c^i as $\xi \to 0$, i.e.,

$$\lim_{\xi \to 0,\, x^i \text{fixed}} \begin{Bmatrix} \overset{a}{\eta}{}_{\alpha\beta}(\xi, x^i) \\ \overset{a}{\tau}{}^{\alpha\beta}(\xi, x^i) \end{Bmatrix} = \begin{Bmatrix} \bar{\eta}_{\alpha\beta}(x^i) \\ \bar{\tau}^{\alpha\beta}(x^i) \end{Bmatrix}. \tag{4.15}$$

Next, take the limit with z_i^* fixed so that the point in question stays at the same position relative to the shrinking boundary-layer region as $\xi \to 0$. Define the boundary-layer quantities by

† The quantities $\overset{a}{\boldsymbol{\eta}}$ and $\overset{a}{\tau}$ have no connection with quantities identified by an a in the uniqueness construction.

$$\lim_{\substack{\xi\to 0,\ z_i \text{ fixed}}} \begin{Bmatrix} \overset{a}{\eta}_{\alpha\beta}(\xi, x^i) \\ \overset{a}{\tau}{}^{\alpha\beta}(\xi, x^i) \end{Bmatrix} = \begin{Bmatrix} \overset{*}{\eta}_{\alpha\beta}(z_i) \\ \overset{*}{\tau}{}^{\alpha\beta}(z_i) \end{Bmatrix}. \tag{4.16}$$

Having defined these limits we now proceed to obtain the lowest-order equation for the instantaneous neutral-loading surface. The normal to the yield surface in strain-rate space is regarded as a function of stress, and for plastic loading

$$\bar{m}^{\alpha\beta} = \bar{m}_c^{\alpha\beta} + (\tau^{\kappa\gamma} - \tau_c^{\kappa\gamma}) \frac{\partial \bar{m}^{\alpha\beta}}{\partial \tau^{\kappa\gamma}}\bigg|_c + \cdots = \bar{m}_c^{\alpha\beta} + \xi(\lambda_1 \overset{'}{\tau}{}_0^{\kappa\gamma} + \overset{(1)}{\tau}{}^{\kappa\gamma}) \frac{\partial \bar{m}^{\alpha\beta}}{\partial \tau^{\kappa\gamma}}\bigg|_c + \cdots. \tag{4.17}$$

Thus the equation for the neutral-loading surface can be written as

$$0 = \bar{m}^{\alpha\rho}\dot{\eta}_{\alpha\rho} = \bar{m}_c^{\alpha\rho}(\lambda_1 \overset{'}{\eta}{}^0_{\alpha\rho} + \overset{(1)}{\eta}{}_{\alpha\rho}) + \xi^\beta[(1+\beta)\lambda_2 \bar{m}_c^{\alpha\rho}\overset{'}{\eta}{}^0_{\alpha\rho} + \bar{m}_c^{\alpha\rho}\overset{a}{\eta}_{\alpha\rho}] + \cdots. \tag{4.18}$$

Noting the expansion (4.10) for the zeroth-order term in the above equation, define the stretched coordinates according to

$$\overset{*}{z}_3 = \xi^{-\beta} z_3 / -(1+\beta)\lambda_2 \quad \text{and} \quad \overset{*}{z}_\alpha = \xi^{-\beta/2} z_\alpha / \{-(1+\beta)\lambda_2\}^{1/2}, \tag{4.19}$$

where it has been anticipated that λ_2 is negative. Introduce the stretched coordinates into (4.18) and take the limit as $\xi \to 0$ with $\overset{*}{z}_i$ fixed with the result

$$0 = \bar{m}^{\alpha\rho}\dot{\eta}_{\alpha\rho} = \xi^\beta[(1+\beta)\lambda_2 f(\overset{*}{z}_i) + \bar{m}_c^{\alpha\rho}(x_c^i)\overset{*}{\eta}_{\alpha\rho}] + \cdots, \tag{4.20}$$

where

$$f(\overset{*}{z}_i) \equiv \bar{m}_c^{\alpha\beta}\overset{'}{\eta}{}^0_{\alpha\beta}\,|_{x_c{}^i} - C_3\overset{*}{z}_3 - C_{\alpha\beta}\overset{*}{z}_\alpha\overset{*}{z}_\beta. \tag{4.21}$$

The boundary-layer strain-rate quantities $\overset{*}{\eta}_{\alpha\beta}$ are zero as a consequence of the kinematic assumptions which have been adopted. With $\overset{a}{E}_{\alpha\beta}$ and $\overset{a}{K}_{\alpha\beta}$ defined analogous to the definitions in (4.14), (3.28) gives

$$\overset{a}{\eta}_{\alpha\beta}(x^i) = \overset{a}{E}_{\alpha\beta}(x^\alpha) + x^3\overset{a}{K}_{\alpha\beta}(x^\alpha). \tag{4.22}$$

Since the strains are constrained to vary linearly through the thickness, the

existence of boundary-layer terms $\overset{*}{E}_{\alpha\beta}(z_\alpha)$ and $\overset{*}{K}_{\alpha\beta}(z_\alpha)$ would result in the quantities $\overset{*}{\eta}_{\alpha\beta}$ varying linearly through the entire thickness. This possibility is excluded by the situation envisioned in Fig. 12 where the region of elastic unloading spreads into the shell in the z_3 direction as well as in the two tangential directions. To proceed we must take

$$\overset{*}{E}_{\alpha\beta} = \overset{*}{K}_{\alpha\beta} = \overset{*}{\eta}_{\alpha\beta} = 0. \tag{4.23}$$

At this point one might want to question the retention of the assumption that the strains vary linearly through the thickness according to (3.28) once elastic unloading sets in. We will take this matter up again in the discussion of some specific examples. Here, however, it is possible to instill some confidence in this assumption by noting that the full boundary-layer treatment for a three-dimensional solid also gives $\overset{*}{\eta}_{\alpha\beta} = 0$ (Hutchinson, 1973a, Section 6.2). Consequently, the lowest-order equation for the neutral-loading surface (4.20) reduces to

$$\overset{*}{f}(z_i) = 0 \tag{4.24a}$$

or, in terms of the unstretched local coordinates,

$$C_3 z_3 + C_{\alpha\beta} z_\alpha z_\beta = -(1 + \beta)\lambda_2 \xi^\beta \bar{m}_c^{\alpha\rho} \overset{\prime}{\eta}{}^0_{\alpha\rho} \big|_{x_c^i}. \tag{4.24b}$$

Because of (4.4) and $C_3 < 0$, (4.24b) implies that $\lambda_2 < 0$ if the neutral-loading surface is to spread into the body as previously anticipated.

Within the region of elastic unloading,

$$\dot{\tau}^{\alpha\rho} = \bar{\mathscr{L}}^{\alpha\rho\kappa\gamma}[\lambda_1 \overset{\prime}{\eta}{}^0_{\kappa\gamma} + \overset{(1)}{\eta}_{\kappa\gamma} + (1 + \beta)\lambda_2 \xi^\beta \overset{\prime}{\eta}{}^0_{\kappa\gamma} + \xi^\beta \overset{a}{\eta}_{\kappa\gamma} + \cdots]. \tag{4.25}$$

Using (4.14), (4.3e), together with

$$\overset{\prime}{\tau}{}^{0\alpha\beta} = \bar{L}_c^{\alpha\beta\kappa\gamma} \overset{\prime}{\eta}{}^0_{\kappa\gamma} \quad \text{and} \quad \bar{\mathscr{L}}^{\alpha\beta\kappa\gamma} - \bar{L}_c^{\alpha\beta\kappa\gamma} = \bar{g}_c^{-1} \bar{m}_c^{\alpha\beta} \bar{m}_c^{\kappa\gamma},$$

(4.25) can be rewritten as

$$\xi^\beta \overset{a}{\tau}{}^{\alpha\rho} = \bar{g}_c^{-1} \bar{m}_c^{\alpha\rho}[\bar{m}_c^{\kappa\gamma}(\lambda_1 \overset{\prime}{\eta}{}^0_{\kappa\gamma} + \overset{(1)}{\eta}_{\kappa\gamma})] + \xi^\beta \bar{\mathscr{L}}^{\alpha\rho\kappa\gamma} \overset{a}{\eta}_{\kappa\gamma}$$
$$+ \xi^\beta (1 + \beta)\lambda_2 \bar{g}_c^{-1} \bar{m}_c^{\alpha\rho} \bar{m}_c^{\kappa\gamma} \overset{\prime}{\eta}{}^0_{\kappa\gamma} + \cdots.$$

Now divide by ξ^β and take the limit as $\xi \to 0$ with $\overset{*}{z}_i$ fixed (thus remaining

within the elastic unloading region as $\xi \to 0$). In this limiting process make use of (4.10), (4.19), (4.21), and (4.23). The result is the lowest-order correction to the bifurcation mode for the stress rate within the elastic unloading region:

$$\overset{*}{\tau}{}^{\alpha\rho} = (1 + \beta)\lambda_2[\bar{g}_c^{-1}\bar{m}_c^{\alpha\rho}]_{x_c^i} f(\overset{*}{z}_i). \tag{4.26}$$

A similar analysis gives $\overset{*}{\tau}{}^{\alpha\beta} = 0$ outside the region of elastic unloading. Note that the boundary-layer stress rate is continuous across the neutral-loading surface $f = 0$.

Let $\overset{*}{N}{}^{\alpha\beta}$ and $\overset{*}{M}{}^{\alpha\beta}$ be the contributions of boundary-layer stress rate to the resultant inplane stress and bending moment tensors defined in accord with (3.32) by

$$\overset{*}{N}{}^{\alpha\beta} = \int_{-t/2}^{t/2} \overset{*}{\tau}{}^{\alpha\beta}\, dx^3 \quad \text{and} \quad \overset{*}{M}{}^{\alpha\beta} = \int_{-t/2}^{t/2} \overset{*}{\tau}{}^{\alpha\beta} x^3\, dx^3. \tag{4.27}$$

Changing to the stretched coordinate for the integration variable,

$$\begin{aligned} \overset{*}{N}{}^{\alpha\rho} &= -(1 + \beta)\lambda_2 \xi^\beta \int \overset{*}{\tau}{}^{\alpha\rho}\, d\overset{*}{z}_3 + \cdots \\ &= -(1 + \beta)^2 \lambda_2^2 \xi^\beta [\bar{g}_c^{-1}\bar{m}_c^{\alpha\rho}]_{x_c^i} \int f(\overset{*}{z}_i)\, d\overset{*}{z}_3 + \cdots, \end{aligned} \tag{4.28a}$$

and similarly,

$$\overset{*}{M}{}^{\alpha\rho} = -(1 + \beta)^2 \lambda_2^2 \xi^\beta [\bar{g}_c^{-1}\bar{m}_c^{\alpha\rho}]_{x_c^i} (\pm t/2) \int f(\overset{*}{z}_i)\, d\overset{*}{z}_3 + \cdots, \tag{4.28b}$$

where the integration extends from the edge of the elastic unloading region to the shell surface in a sense consistent with that which $z_3 = \pm(x^3 \mp t/2)$ holds. Also, $+t/2$ pertains when $x_c^3 = t/2$ and $-t/2$ when $x_c^3 = -t/2$.

3. *Determination of β and λ_2*

To evaluate β and λ_2 the lowest-order boundary-layer terms are displayed explicitly in the initial post-bifurcation expansion, and in this form the expansion is substituted into the principle of virtual work. Following some further manipulation of the virtual work equation, an examination of the lowest-order nonvanishing terms in this equation permits us to identify β by inspection and provides a general equation for λ_2.

The bifurcated solution rate is written as

$$\begin{Bmatrix} \dot{U}_{\alpha,\rho} \\ \dot{\eta}_{\alpha\rho} \\ \dot{\tau}^{\alpha\rho} \\ \dot{N}^{\alpha\rho} \end{Bmatrix} = \begin{Bmatrix} \dot{U}^0_{\alpha,\rho} \\ \dot{\eta}^0_{\alpha\rho} \\ \dot{\tau}^{\alpha\rho}_0 \\ \dot{N}^{\alpha\rho}_0 \end{Bmatrix} + \begin{Bmatrix} \overset{(1)}{U}_{\alpha,\rho} \\ \overset{(1)}{\eta}_{\alpha\rho} \\ \overset{(1)}{\tau}{}^{\alpha\rho} \\ \overset{(1)}{N}{}^{\alpha\rho} \end{Bmatrix} + \xi^{\beta} \begin{Bmatrix} 0 \\ 0 \\ \overset{*}{\tau}{}^{\alpha\rho} \\ \overset{*}{N}{}^{\alpha\rho} \end{Bmatrix} + \begin{Bmatrix} \overset{b}{U}_{\alpha,\rho}(\xi, x^{\gamma}) \\ \overset{b}{\eta}_{\alpha\rho}(\xi, x^{i}) \\ \overset{b}{\tau}{}^{\alpha\rho}(\xi, x^{i}) \\ \overset{b}{N}{}^{\alpha\rho}(\xi, x^{\gamma}) \end{Bmatrix}, \tag{4.29}$$

with similar definitions for the other quantities. Since the lowest order boundary-layer terms have been separated out it can be asserted that

$$\lim_{\substack{\xi \to 0,\ z_i \text{ fixed} \\ * \\ \xi \to 0,\ z_i \text{ fixed}}} \xi^{-\beta} \{ \overset{b}{U}_{\alpha,\rho}; \overset{b}{\eta}_{\alpha\rho}; \overset{b}{\tau}{}^{\alpha\rho}; \xi^{-\beta} \overset{b}{N}{}^{\alpha\rho} \} = 0. \tag{4.30}$$

The incremental form of the principle of virtual work (3.33) is

$$\int_A \{ \dot{M}^{\alpha\beta} \delta K_{\alpha\beta} + \dot{N}^{\alpha\beta} \delta E_{\alpha\beta} + N^{\alpha\beta} \dot{W}_{,\alpha} \delta W_{,\beta} \} \, dA = EVW, \tag{4.31}$$

which is satisfied by both the fundamental solution and the bifurcated solution. Eliminate the right-hand side of (4.31) using the equation satisfied by the fundamental solution and rearrange the resulting equation to the following form:

$$\begin{aligned} \int_A \{ & (\dot{M}^{\alpha\beta} - \dot{M}^{\alpha\beta}_0) \delta K_{\alpha\beta} + (\dot{N}^{\alpha\beta} - \dot{N}^{\alpha\beta}_0)(\delta U_{\alpha,\beta} + W^0_{,\alpha} \delta W_{,\beta}) + \dot{N}^{\alpha\beta}(W_{,\alpha} - W^0_{,\alpha}) \delta W_{,\beta} \\ & + N^{\alpha\beta}_0 (\dot{W}_{,\alpha} - \dot{W}^0_{,\alpha}) \delta W_{,\beta} + (N^{\alpha\beta} - N^{\alpha\beta}_0) \dot{W}_{,\alpha} \delta W_{,\beta} \} \, dA = 0. \end{aligned} \tag{4.32}$$

Substitute (4.29) into (4.32) using (4.3a), (4.12), and expansions such as (4.13) to obtain

$$\begin{aligned} & \int_A \{ \overset{b}{M}{}^{\alpha\beta} \delta K_{\alpha\beta} + \overset{b}{N}{}^{\alpha\beta} \delta^c E_{\alpha\beta} + N^{\alpha\beta}_{0c} \overset{b}{W}_{,\alpha} \delta W_{,\beta} \} \, dA + \xi^{\beta} \int_A \{ \overset{*}{M}{}^{\alpha\rho} \delta K_{\alpha\rho} + \overset{*}{N}{}^{\alpha\rho} \delta^c E_{\alpha\rho} \} \, dA \\ & + \xi \int_A \{ 2\lambda_1 \overset{(1)}{N}{}^{\alpha\beta} W^{0\prime}_{,\alpha} \delta W_{,\beta} + 2(\lambda_1 \dot{N}^{\alpha\beta}_0 + \overset{(1)}{N}{}^{\alpha\beta}) W_{,\alpha} \delta W_{,\beta} \} \, dA + \cdots = 0, \end{aligned} \tag{4.33}$$

where $\delta^c \mathbf{E}$ is defined by (4.3b).

Equation (4.33) can be regarded as the variational equation of equilibrium for the quantities with the superscript b. We will argue that all three terms shown in (4.33) must be of order ξ and this will enable us to identify β.

In preparation for this argument we first digress to consider the initial post-bifurcation behavior of a nonlinear hypoelastic comparison problem in which the unloading branch of the constitutive relation is suppressed. That

is $\dot{\tau}^{\alpha\beta} = \bar{L}^{\alpha\beta\kappa\gamma}\dot{\eta}_{\kappa\gamma}$ for *all* strain rates where $\bar{\mathbf{L}}$ will be taken as a function of the stress. For the comparison problem the initial slope λ_1 is not constrained by (4.9) but will be determined below. Since the boundary-layer region does not develop the associated term in (4.33) must be deleted and the superscripted b quantities are of order ξ. Introduce the limit

$$\lim_{\xi \to 0,\ x \text{ fixed}} \xi^{-1}\{\overset{b}{U}_\alpha;\ \overset{b}{\eta}_{\alpha\beta};\ \overset{b}{\tau}^{\alpha\beta};\ \overset{b}{N}^{\alpha\beta}\} = 2\{\overset{(2)}{U}_\alpha;\ \overset{(2)}{\eta}_{\alpha\beta};\ \overset{(2)}{\tau}^{\alpha\beta};\ \overset{(2)}{N}^{\alpha\beta}\}, \tag{4.34}$$

where the multiplicative factor of 2 brings the notation into line with previous work on elastic post-buckling expansions to be cited later. The variational equation for the second-order quantities is

$$2\int_A \{\overset{(2)}{M}^{\alpha\beta}\delta K_{\alpha\beta} + \overset{(2)}{N}^{\alpha\beta}\delta^c E_{\alpha\beta} + N_{0c}^{\alpha\beta}\overset{(2)}{W}_{,\alpha}\delta W_{,\beta}\}\, dA + 2\int_A \{\lambda_1 \overset{(1)}{N}^{\alpha\beta}W'^0_{,\alpha}\delta W_{,\beta} + (\lambda_1 N_0'^{\alpha\beta} + \overset{(1)}{N}^{\alpha\beta})\overset{(1)}{W}_{,\alpha}\delta W_{,\beta}\}\, dA = 0. \tag{4.35}$$

One can also establish the connections

$$\overset{(2)}{K}_{\alpha\beta} = -\overset{(2)}{W}_{,\alpha\beta}$$

and

$$\overset{(2)}{E}_{\alpha\beta} = \tfrac{1}{2}(\overset{(2)}{U}_{\alpha,\beta} + \overset{(2)}{U}_{\beta,\alpha}) + b_{\alpha\beta}\overset{(2)}{W} + \tfrac{1}{2}(W^{0c}_{,\alpha}\overset{(2)}{W}_{,\beta} + W^{0c}_{,\beta}\overset{(2)}{W}_{,\alpha}) + \tfrac{1}{2}\overset{(1)}{W}_{,\alpha}\overset{(1)}{W}_{,\beta}. \tag{4.36}$$

Writing

$$\bar{L}^{\alpha\beta\kappa\gamma} = \bar{L}_c^{\alpha\beta\kappa\gamma} + (\tau^{\mu\nu} - \tau_c^{\mu\nu})(\partial\bar{L}^{\alpha\beta\kappa\gamma}/\partial\tau^{\mu\nu})\big|_c + \cdots, \tag{4.37}$$

one can show

$$\overset{(2)}{\tau}^{\alpha\beta} = \bar{L}_c^{\alpha\beta\kappa\gamma}\overset{(2)}{\eta}_{\kappa\gamma} + D^{\alpha\beta}, \tag{4.38}$$

where

$$D^{\alpha\beta} \equiv \frac{1}{2}\lambda_1 \tau_0'^{\mu\nu}\frac{\partial\bar{L}^{\alpha\beta\kappa\gamma}}{\partial\tau^{\mu\nu}}\bigg|_c \overset{(1)}{\eta}_{\kappa\gamma} + \frac{1}{2}\overset{(1)}{\tau}^{\mu\nu}\frac{\partial\bar{L}^{\alpha\beta\kappa\gamma}}{\partial\tau^{\mu\nu}}\bigg|_c (\lambda_1 \eta_{\kappa\gamma}'^0 + \overset{(1)}{\eta}_{\kappa\gamma}). \tag{4.39}$$

In addition, it follows that

$$\overset{(2)}{N}{}^{\alpha\beta} = \overset{c}{H}{}^{\alpha\beta\kappa\gamma}_{(1)} \overset{(2)}{E}_{\kappa\gamma} + \overset{c}{H}{}^{\alpha\beta\kappa\gamma}_{(2)} \overset{(2)}{K}_{\kappa\gamma} + \int_{-t/2}^{t/2} D^{\alpha\beta}\, dx^3,$$

$$\overset{(2)}{M}{}^{\alpha\beta} = \overset{c}{H}{}^{\alpha\beta\kappa\gamma}_{(2)} \overset{(2)}{E}_{\kappa\gamma} + \overset{c}{H}{}^{\alpha\beta\kappa\gamma}_{(3)} \overset{(2)}{K}_{\kappa\gamma} + \int_{-t/2}^{t/2} D^{\alpha\beta} x^3\, dx^3. \tag{4.40}$$

Now set $\delta U_\alpha = \overset{(1)}{U}_\alpha$ and $\delta W = \overset{(1)}{W}$ in (4.35) to get

$$2\int_A \{\overset{(2)}{M}{}^{\alpha\beta} \overset{(1)}{K}_{\alpha\beta} + \overset{(2)}{N}{}^{\alpha\beta} \overset{(1)}{E}_{\alpha\beta} + N^{\alpha\beta}_{0c} \overset{(1)}{W}_{,\alpha} \overset{(2)}{W}_{,\beta}\}\, dA$$

$$+ 2\int_A \{\lambda_1 \overset{(1)}{N}{}^{\alpha\beta} \overset{\prime}{W}{}^0_{,\alpha} \overset{(1)}{W}_{,\beta} + (\lambda_1 \overset{\prime}{N}{}^{\alpha\beta}_0 + \overset{(1)}{N}{}^{\alpha\beta}) \overset{(1)}{W}_{,\alpha} \overset{(1)}{W}_{,\beta}\}\, dA = 0. \tag{4.41}$$

An identity for the first term of (4.41) is

$$\int_A \{\overset{(2)}{M}{}^{\alpha\beta} \overset{(1)}{K}_{\alpha\beta} + \overset{(2)}{N}{}^{\alpha\beta} \overset{(1)}{E}_{\alpha\beta} + N^{\alpha\beta}_{0c} \overset{(1)}{W}_{,\alpha} \overset{(2)}{W}_{,\beta}\}\, dA$$

$$= \int_A \{\tfrac{1}{2} \overset{(1)}{N}{}^{\alpha\beta} \overset{(1)}{W}_{,\alpha} \overset{(1)}{W}_{,\beta} + \lambda_1 \overset{(1)}{N}{}^{\alpha\beta} \overset{\prime}{W}{}^0_{,\alpha} \overset{(1)}{W}_{,\beta}\}\, dA + \int_V D^{\alpha\beta} \overset{(1)}{\eta}_{\alpha\beta}\, dV, \tag{4.42}$$

where dV represents the volume element in the undeformed shell. This identity is obtained by setting $\delta U_\alpha = \overset{(2)}{U}_\alpha$ and $\delta W = \overset{(2)}{W}$ in the variational equation for the eigenmode (4.3a) and then by making use of (4.3b), (4.3c), (4.36), (4.40), and the property $\bar{L}^{\alpha\beta\kappa\gamma}_c = \bar{L}^{\kappa\gamma\alpha\beta}_c$. Eliminate the common term in (4.41) and (4.42) to obtain the following equation for λ_1:

$$\mathscr{A} + \lambda_1 \mathscr{B} = 0, \tag{4.43}$$

where

$$\mathscr{A} = \int_A 3 \overset{(1)}{N}{}^{\alpha\beta} \overset{(1)}{W}_{,\alpha} \overset{(1)}{W}_{,\beta}\, dA + \int_V \overset{(1)}{\tau}{}^{\mu\nu} \frac{\partial \bar{L}^{\alpha\beta\kappa\gamma}}{\partial \tau^{\mu\nu}}\bigg|_c \overset{(1)}{\eta}_{\alpha\beta} \overset{(1)}{\eta}_{\kappa\gamma}\, dV, \tag{4.44a}$$

$$\mathscr{B} = \int_A \{2 \overset{\prime}{N}{}^{\alpha\beta}_0 \overset{(1)}{W}_{,\alpha} \overset{(1)}{W}_{,\beta} + 4 \overset{(1)}{N}{}^{\alpha\beta} \overset{\prime}{W}{}^0_{,\alpha} \overset{(1)}{W}_{,\beta}\}\, dA$$

$$+ \int_V \left\{ \overset{\prime}{\tau}{}^{\mu\nu}_0 \frac{\partial \bar{L}^{\alpha\beta\kappa\gamma}}{\partial \tau^{\mu\nu}}\bigg|_c \overset{(1)}{\eta}_{\alpha\beta} \overset{(1)}{\eta}_{\kappa\gamma} + \overset{(1)}{\tau}{}^{\mu\nu} \frac{\partial \bar{L}^{\alpha\beta\kappa\gamma}}{\partial \tau^{\mu\nu}}\bigg|_c \overset{\prime}{\eta}{}^0_{\alpha\beta} \overset{(1)}{\eta}_{\kappa\gamma}\, dV \right\}. \tag{4.44b}$$

The expression (4.43) for λ_1 in terms of the eigenmode specializes to formulas given by Budiansky and Hutchinson (1964), Budiansky (1969), Cohen (1968), and Fitch (1968) for constant elastic moduli. When the variable moduli are derivable from a strain energy density the result can be

regarded as deriving from Koiter's (1945, 1963a) general approach to conservative elastic systems. The formula is more general, however, in that it applies to the nonlinear hypoelastic comparison problem for which the moduli are given by the loading branch of the elastic-plastic constitutive relation and are not, in general, derivable from a strain-energy-density function. The initial slope of the comparison problem is denoted by λ_1^{he} to distinguish it from the slope of the elastic-plastic problem λ_1 and in this notation (4.43) is replaced by

$$\mathscr{A} + \lambda_1^{\mathrm{he}}\mathscr{B} = 0.$$

The symmetry of the eigenmode in many problems implies that $\mathscr{A} = 0$ and thus $\lambda_1^{\mathrm{he}} = 0$. But if λ_1^{he} as given above is sufficiently large such that

$$\bar{m}_c^{\alpha\beta}(\lambda_1^{\mathrm{he}}\overset{\prime}{\eta}{}^{0}_{\alpha\beta} + \overset{(1)}{\eta}_{\alpha\beta}) > 0 \tag{4.45}$$

throughout the body, then no reversal in sign of the strain rate will occur in some finite range of positive ξ. The behavior of the comparison problem will coincide with that of the elastic-plastic problem in this range and, in particular, $\lambda_1 = \lambda_1^{\mathrm{he}}$. However as has been indicated, the typical and more interesting situation occurs when strain-rate reversal occurs at bifurcation in the comparison problem. In this case λ_1 is the minimum value consistent with (4.9) and $\lambda_1 > \lambda_1^{\mathrm{he}}$.

We return to the analysis of the elastic-plastic problem in which elastic unloading must be taken into account. The contribution of the boundary-layer terms in (4.33) can be rewritten using the stretched coordinates and (4.28) as

$$\xi^{\beta}\int_{\mathrm{A}}\{\overset{*}{M}{}^{\alpha\rho}\delta K_{\alpha\rho} + \overset{*}{N}{}^{\alpha\rho}\delta^{c}E_{\alpha\rho}\}\,dA$$

$$= \xi^{3\beta}(1+\beta)^3\lambda_2^3[\bar{g}_c^{-1}\bar{m}_c^{\alpha\rho}\delta\eta_{\alpha\rho}]_{x_c^i}\int_{\overset{*}{V}} f(\overset{*}{z}_i)\,d\overset{*}{V} + \cdots. \tag{4.46}$$

The volume $\overset{*}{V}$ is the region of elastic unloading expressed in terms of the stretched coordinates. It is enclosed between the two surfaces

$$f(\overset{*}{z}_i) = 0 \quad \text{and} \quad \pm 2\overset{*}{z}_3 + b_{\alpha\beta}|_{x_c}\overset{*}{z}_{\alpha}\overset{*}{z}_{\beta} = 0, \tag{4.47}$$

where the plus $(+)$ holds if $x_c^3 = t/2$ and the minus $(-)$ if $x_c^3 = -t/2$.

By considering the three possibilities, $\beta > \frac{1}{3}$, $\beta < \frac{1}{3}$, and $\beta = \frac{1}{3}$, we will show that $\beta = \frac{1}{3}$ must hold implying a balance between the three terms listed in (4.33). First, suppose $\beta > \frac{1}{3}$. Then by (4.46) the boundary-layer contribution to (4.33) would be of order larger than ξ. A balance between the first and third terms in (4.33) would require the first term to be of order ξ. With the limit *for fixed* x^i defined as in (4.34), the subsequent analysis leading to (4.43)

would pertain. That is, with $\beta > \frac{1}{3}$ the effect of elastic unloading would drop out to this order requiring λ_1 to satisfy (4.43). But this is not possible because $\lambda_1 > \lambda_1^{he}$ by assumption.

If it is supposed that $\beta < \frac{1}{3}$ then there must be a balance between the first and second terms in (4.33), and in the limit $\xi \to 0$ for fixed x^i the quantities $\overset{b}{W}$ and $\overset{b}{U}_\alpha$ must be of order $\xi^{3\beta}$. Proceeding in a manner similar to that outlined in Eqs. (3.34)–(4.43), one can show that the only solution for these limit quantities is some multiple of the eigenmode. Furthermore, $\beta < \frac{1}{3}$ requires the boundary-layer contribution (4.46) to be identically zero.

As already suggested, the proper choice is $\beta = \frac{1}{3}$. Then all three terms in (4.33) are of order ξ and (4.34) still pertains.† The boundary-layer contribution [(4.46) with $\delta\boldsymbol{\eta} = \overset{(1)}{\boldsymbol{\eta}}$] must be added to the left-hand side of (4.35) as well as to (4.41). Equations (4.36)–(4.40) and (4.42) remain unchanged. Equation (4.43) is replaced by

$$(\tfrac{4}{3}\lambda_2)^3[\bar{g}_c^{-1}\bar{m}_c^{\alpha\beta}\overset{(1)}{\eta}_{\alpha\beta}]_{x_c^3}\int_{\overset{*}{V}} \overset{*}{f}(z_i)\, d\overset{*}{V} = -(\mathscr{A} + \lambda_1\mathscr{B}), \tag{4.48}$$

where $\mathscr{A}$ and $\mathscr{B}$ are still given by (4.44). This equation is the general equation for λ_2. Note that it involves the eigenmode, the initial slope λ_1, and the derivatives of the instantaneous moduli evaluated at bifurcation.

The integral $\int \overset{*}{f}\, d\overset{*}{V}$ can be evaluated in closed form for most cases of interest. With $C_{12} = 0$ and $b_{12} = 0$ the general expression is

$$\int_{\overset{*}{V}} \overset{*}{f}(z_i)\, d\overset{*}{V} = \frac{\pi c_1 c_2}{(-2C_3)}\left[1 - \tfrac{1}{2}(a_1 + a_2 + b_1 + b_2) + \tfrac{1}{8}(a_1^2 + a_2^2 + b_1^2 + b_2^2)\right.$$
$$\left. + \tfrac{1}{12}(a_1a_2 + b_1b_2 + a_1b_2 + a_2b_1 + 3a_1b_1 + 3a_2b_2)\right]\cdot[(\bar{m}_c^{\alpha\beta}\overset{0}{\eta}_{\alpha\beta})_{x_c^3}]^3. \tag{4.49}$$

In this formula

$$c_\alpha = (C_{\alpha\alpha} \pm C_3 b_{\alpha\alpha}/2)^{-1/2}, \qquad a_\alpha = c_\alpha^2 C_{\alpha\alpha}, \qquad b_\alpha = \pm c_\alpha^2 b_{\alpha\alpha} C_3/2$$

($\alpha = 1, 2$; no summation implied), where the minus ($-$) holds if $x_c^3 = t/2$ and the plus ($+$) if $x_c^3 = -t/2$.

The analog of (4.48) for three-dimensional solids derived by Hutchinson (1973a) can be specialized directly to (4.48) when the assumptions of DMV

†Eigenmodal contributions to $(\overset{b}{U}_\alpha, \overset{b}{W})$ of order lower than ξ are possible; however, it is readily shown that such contributions do not influence the term $\lambda_2\xi^{1+\beta}$ in (4.1). To carry the expansion beyond this term it does become necessary to require the higher-order terms in (4.29) to be orthogonal to the eigenmode in some specific way.

theory are invoked. An example will be given in the next subsection in which neutral loading at bifurcation occurs along a line of points. In such cases two coordinates rather than three are stretched and one finds an expression similar to (4.48) but with $\beta = \frac{2}{5}$.

When $C_3 \neq 0$, the unloading region is a thin sliver whose penetration in the z_3 direction normal to the shell surface is $O(\xi^{\beta})$ and whose extent along the surface is $O(\xi^{\beta/2})$. Thus, as will be seen more clearly in examples which follow, the lateral extent of the unloading region will in general be on the order of the lateral dimensions of the plate or shell before the normal penetration is more than a small fraction of the thickness. It is therefore not unreasonable to retain the assumption of approximate plane stress even after elastic unloading sets in. For an unusual problem in which $C_3 = 0$ one cannot necessarily still make this claim since a different choice of stretched coordinates will have to be made. Such cases must be examined individually.

B. Two Column Problems

1. *Simply Supported Column with a Solid Circular Cross Section*

Although the theory given above was derived for plates and shells it can be converted by inspection to apply to one-dimensional column theory. Tensor quantities become their counterpart scalars. For a column under axial compression $\mathscr{L} \equiv E$, $\bar{m} \equiv -1$, $\bar{g}^{-1} \equiv E - E_t$, and $dL/d\tau \equiv dE_t/d\tau$. It is well known that the approximate strain-displacement relations of DMV theory are not adequate for an accurate analysis of the post-buckling behavior of linearly elastic columns. In the plastic range, however, the nonlinearity associated with the material behavior dominates the initial post-bifurcation behavior and more accurate strain-displacement relations are not needed.

The tangent-modulus load for a solid cylindrical column of radius R and length L is

$$P_c = \pi^2 E_t^c I/L^2, \tag{4.50}$$

where $I = \frac{1}{4}\pi R^4$. The eigenmode and its associated stress and strain fields are

$$\overset{(1)}{U}_x = 0, \qquad \overset{(1)}{W} = R\cos(\pi x_1/L),$$

$$\overset{(1)}{\eta} = (\pi^2 R x_3/L^2)\cos(\pi x_1/L), \qquad \text{and} \qquad \overset{(1)}{\tau} = E_t^c \overset{(1)}{\eta}, \tag{4.51}$$

where the Cartesian coordinates x_i are orientated as shown in Fig. 13a. With

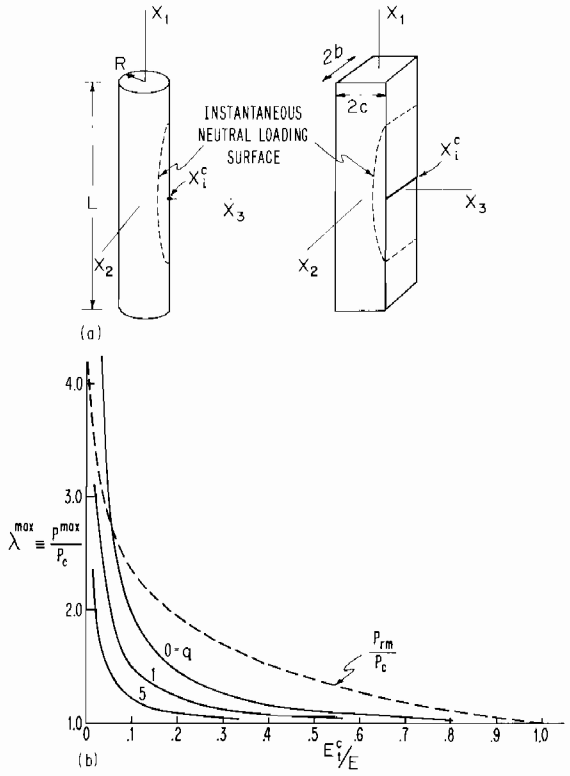

FIG. 13. (a) Conventions for analysis of columns of circular and rectangular cross sections. (b) Approximate maximum support load from (4.61) for the column with a circular cross section and comparison with the reduced-modulus load for a column with a constant tangent modulus equal to E_t^c; $q = (\pi R/2L)^2(dE_t/d\tau)_c$.

this normalization an eigenmodal contribution $\xi W^{(1)}$ corresponds to a one-radius lateral deflection when $\xi = 1$.

Let

$$\lambda = P/P_c\,. \tag{4.52}$$

Then $\eta'^0 = -(\pi R/2L)^2$ and, with $\bar{m}_c = -1$,

$$\bar{m}_c(\lambda_1 \eta'^0 + \eta^{(1)}) = (\pi R/L)^2[\tfrac{1}{4}\lambda_1 - (x_3/R)\cos(\pi x_1/L)]. \tag{4.53}$$

The requirement that λ_1 be the smallest value such that (4.53) is non-negative gives

$$\lambda_1 = 4 \tag{4.54}$$

and $x_i^c = (0, 0, R)$. From (4.11)

$$C_3 = -(\pi R/L)^2 R^{-1}, \qquad C_{11} = \tfrac{1}{2}(\pi R/L)^2(\pi/L)^2, \qquad C_{22} = C_{12} = 0,$$

so that from (4.21)

$$\overset{*}{f}(\overset{*}{z}_i) = (\pi R/L)^2[\tfrac{1}{4} + (\overset{*}{z}_3/R) - \tfrac{1}{2}(\pi \overset{*}{z}_1/L)^2]. \tag{4.55}$$

The term $\mathscr{A}$ of (4.44) is zero by symmetry as can easily be verified; and for the one-dimensional column theory

$$\lambda_1 \mathscr{B} = \lambda_1 \int_V \{2\tau^0 \overset{(1)}{W}{}^2 + (dE_t/d\tau)_c(\tau^0 \overset{(1)}{\eta}{}^2 + \overset{(1)}{\tau}\eta^0 \overset{(1)}{\eta})\}\, dV \tag{4.56a}$$

$$= -E_t^c(\pi R/L)^4 \pi R^2 L(1 + q), \tag{4.56b}$$

where $q = (\pi R/2L)^2(dE_t/d\tau)_c$. In the stretched coordinates the lowest-order equation for the surface of the column is $2\overset{*}{z}_3 + \overset{*}{z}_2^2/R = 0$; and using the general formula (4.49) one obtains

$$(4\lambda_2/3)^3[\bar{g}_c^{-1}\bar{m}_c \overset{(1)}{\eta}]_{x_c^i} \int_{\overset{*}{V}} \overset{*}{f}(\overset{*}{z}_i)\, d\overset{*}{V} = -(\tfrac{4}{3}\lambda_2)^3(E - E_t^c)(\pi R/L)^4 R^2 L/192. \tag{4.57}$$

Combining (4.56) and (4.57) according to (4.48) gives

$$\lambda_2 = -3[3\pi E_t^c(1 + q)/(E - E_t^c)]^{1/3}. \tag{4.58}$$

Thus the initial post-bifurcation expansion is

$$\lambda \equiv P/P_c = 1 + 4\xi + \lambda_2 \xi^{4/3} + \cdots, \tag{4.59}$$

where $\xi = 1$ corresponds to a lateral deflection of one radius at the center of the column. From (4.24b) the lowest-order equation for the instantaneous neutral-loading surface is

$$(x_3 - R)/R - \tfrac{1}{2}(\pi x_1/L)^2 = \tfrac{1}{3}\lambda_2 \xi^{1/3}. \tag{4.60}$$

An alternative expression for λ_2 was obtained by Hutchinson (1973a) within the context of the full three-dimensional theory by using the Euler–Bernoulli approximations to obtain approximate eigenmode fields. That expression agrees exactly with (4.58) when Poisson's ratio is $\frac{1}{2}$.

If the truncated three-term expansion (4.59) is used to estimate the maximum support load one finds

$$d\lambda/d\xi = 0 \Rightarrow \xi^{1/3} = -3/\lambda_2$$

and

$$\lambda^{\max} = 1 + (E - E_t^c)/3\pi E_t^c(1 + q) = 1 + 0.106[(E - E_t^c)/E_t^c(1 + q)]. \tag{4.61}$$

From (4.60) the elastic unloading region has penetrated to the middle of the column and along the length of the column to $x_1 = \pm\sqrt{2}\,L/\pi$. Figure 13b shows the approximate support load (4.61) as a function of E_t^c/E for several values of q. Included in this figure is the von Kármán (1910) reduced-modulus load calculated for a circular cross-sectional column with constant tangent modulus E_t^c. If the tangent modulus is constant the load should approach the reduced-modulus load (neglecting nonlinear geometry effects) and (4.61) is not accurate for this case. However, q is typically of order unity or larger for relatively slender columns with a stress–strain curve representative of common structural metals and thus enters into (4.61) in a significant way.

A further comparison of these approximate results with predictions based on full numerical calculations will be made in Section V,A. The main point to be made here is that the initial slope in (4.59) is reduced after extremely small lateral deflections due to the term $\lambda_2 \xi^{4/3}$ which gives rise to an infinite curvature to the λ–ξ relation at bifurcation.

2. *Simply Supported Column with a Solid Rectangular Cross Section*

Let b and c be the half widths of the cross section of the column as in Fig. 13a. The tangent-modulus load (4.50) still applies with $I = \frac{4}{3}c^3 b$. Now we choose the following normalization for the eigenmode:

$$\overset{(1)}{W} = c\cos(\pi x_1/L). \tag{4.62}$$

Proceeding as in the previous example one finds:

$$\lambda_1 = 3, \tag{4.63}$$

$$f(\overset{*}{z}_i) = (\pi c/L)^2[\tfrac{1}{3} + (\overset{*}{z}_3/c) - \tfrac{1}{2}(\pi \overset{*}{z}_1/L)^2], \tag{4.64}$$

and

$$\lambda_1 \mathscr{B} = -4E_t^c(\pi c/L)^4 cbL(1 + q), \tag{4.65}$$

where here

$$q = \tfrac{1}{3}(\pi c/L)^2(dE_t/d\tau)_c\,. \tag{4.66}$$

The main difference between this example and the previous one is that neutral loading occurs along a line (*viz* $x_1 = 0$, $x_3 = c$ as depicted in Fig. 13a) rather than at an isolated point. To evaluate the lowest-order boundary-layer contribution to the principle of virtual work one now introduces only two stretched coordinates $\overset{*}{z}_1$ and $\overset{*}{z}_3$ defined as before in (4.19).

Instead of (4.46) one obtains

$$\xi^{\beta} \int \{\overset{*}{M}^{\alpha\rho}\, \delta K_{\alpha\rho} + \overset{*}{N}^{\alpha\rho}\, \delta^{c} E_{\alpha\rho}\}\, dA$$
$$= -\xi^{5\beta/2}[-(1+\beta)\lambda_2]^{5/2}[\bar{g}_c^{-1}\bar{m}_c^{\alpha\rho}\, \delta\eta_{\alpha\rho}]_{x_c^i} \int_{\overset{*}{V}} f(\overset{*}{z}_i)\, d\overset{*}{z}_1\, dz_2\, d\overset{*}{z}_3 .$$

By the same argument made when the neutral-loading surface is isolated, it follows that $\beta = \frac{2}{5}$. The equation for λ_2 becomes

$$(-\tfrac{7}{5}\lambda_2)^{5/2}[\bar{g}_c^{-1}\bar{m}_c^{\alpha\beta}\overset{(1)}{\eta}_{\alpha\beta}]_{x_c^i} \int_{\overset{*}{V}} f(\overset{*}{z}_i)\, d\overset{*}{z}_1\, dz_2\, d\overset{*}{z}_3 = \mathscr{A} + \lambda_1 \mathscr{B}. \quad (4.67)$$

Evaluating the left-hand side for the present case gives

$$-(-\tfrac{7}{5}\lambda_2)^{5/2}[16\sqrt{2}/(135\pi\sqrt{3})](E - E_t^c)(\pi c/L)^4 bcL.$$

Combining the above and (4.65) according to (4.67) gives

$$\lambda_2 = -(15/7)[15\pi E_t^c(1+q)/4\sqrt{2}(E - E_t^c)]^{2/5}.$$

Thus the initial post-bifurcation expansion for the column with the rectangular cross section is

$$\lambda = 1 + 3\xi + \lambda_2 \xi^{7/5} + \cdots. \quad (4.68)$$

The maximum value of λ as predicted by the truncated series is

$$\lambda^{\max} = 1 + 8\sqrt{2}(E - E_t^c)/35\pi E_t^c(1+q) = 1 + 0.103[(E - E_t^c)/E_t^c(1+q)], \quad (4.69)$$

which is almost identical to the cylindrical column result (4.61) except that q is defined by (4.66).

C. Circular Plate under Radial Compression

Bifurcation of a clamped circular plate of thickness t and radius R and subject to compressive loading by a uniform radial stress σ was discussed in Section III,C. The formula (3.56) for the lowest bifurcation stress σ_c involves the instantaneous modulus $\bar{E}_c$ and contraction ratio $\bar{\nu}_c$ in (3.55); i.e.,

$$\sigma_c = -k^2 \bar{E}_c t^2/[12(1 - \bar{\nu}_c^2)R^2]. \quad (4.70)$$

The difference between the predictions of J_2 flow theory and J_2 deformation theory is illustrated by Fig. 10. In this section the coefficients in the initial post-bifurcation expansion will be evaluated using J_2 flow theory which, of course, is a special case of the plasticity theory employed in the general

development of Section IV,A. We have already remarked that numerical results will be presented only for the range of parameters where the flow-theory predictions for the bifurcation load are very close to the deformation-theory predictions.

The fundamental solution is characterized by the uniform state of stress and strain (in Cartesian coordinates x_i with x_3 normal to the undeformed plate):

$$\tau^0_{\alpha\beta} = \sigma\delta_{\alpha\beta} \quad \text{and} \quad \eta^0_{\alpha\beta} = \varepsilon\delta_{\alpha\beta}\,. \tag{4.71}$$

It is convenient to introduce the moduli T and T_t for equal biaxial compression where $\dot{\sigma} = T\dot{\varepsilon}$ for an elastic response and $\dot{\sigma} = T_t\dot{\varepsilon}$ for a plastic response where from (3.55)

$$T = E/(1 - \nu) \quad \text{and} \quad T_t = \bar{E}/(1 - \bar{\nu}). \tag{4.72}$$

In the notation of Section IV,A

$$\bar{m}^c_{\alpha\beta} = -\delta_{\alpha\beta} \quad \text{and} \quad \bar{g}_c^{-1} = \tfrac{1}{2}(T - T^c_t). \tag{4.73}$$

The eigenmode associated with the lowest bifurcation stress is

$$\overset{(1)}{U}_\alpha = 0 \quad \text{and} \quad \overset{(1)}{W} = at[J_0(kr/R) - J_0(k)], \tag{4.74}$$

where

$$a^{-1} = 1 - J_0(k) \cong 1.4027, \tag{4.75}$$

and $r^2 = x_1^2 + x_2^2$. Here J_n is the Bessel function of the first kind of nth order and $k \cong 3.8317$ is the first root of $J_1(k) = 0$. The normalization in (4.74) implies that the maximum eigenmodal deflection occurs at $r = 0$ and is equal to the thickness t. Define the load parameter according to

$$\lambda = \sigma/\sigma_c\,. \tag{4.76}$$

The function for determining λ_1 is found to be

$$\bar{m}^c_{\alpha\beta}(\lambda_1\overset{\prime}{\eta}{}^0_{\alpha\beta} + \overset{(1)}{\eta}_{\alpha\beta}) = -2\lambda_1\overset{\prime}{\varepsilon} - ak^2(x_3 t/R^2)J_0(kr/R),$$

where $(\,)' \equiv [d(\,)/d\lambda]_c$ as previously defined and $\overset{\prime}{\varepsilon} = \sigma_c/T^c_t$. The minimum of this function occurs at $x^c_i = (0, 0, t/2)$ and choosing λ_1 such that its value is zero at this point gives

$$\lambda_1 = 3(1 + \bar{\nu}_c)a, \tag{4.77}$$

and thus

$$\bar{m}^c_{\alpha\beta}(\lambda_1\overset{\prime}{\eta}{}^0_{\alpha\beta} + \overset{(1)}{\eta}_{\alpha\beta}) = (-2\sigma_c\lambda_1/T^c_t)[1 - 2(x_3/t)J_0(kr/R)]. \tag{4.78}$$

Using the definitions (4.11) and (4.21) one obtains

$$\overset{*}{f}(z_i) = -\frac{2\sigma_c}{T_t^c}\left[1 + 2\lambda_1\left(\frac{\overset{*}{z}_3}{t}\right) - \frac{k^2\lambda_1}{4}\left(\frac{\overset{*}{r}}{R}\right)^2\right], \tag{4.79}$$

where $\overset{*}{r} = (\overset{*}{x}_1^2 + \overset{*}{x}_2^2)^{1/2} = \xi^{-\beta/2} r/\{-(1+\beta)\lambda_2\}^{1/2}$. The boundary-layer contribution to (4.48) can be evaluated using the general formula (4.49) for $\int \overset{*}{f}\, d\overset{*}{V}$ and is found to be

$$\left(\frac{4\lambda_2}{3}\right)^3 [\bar{g}_c^{-1}\bar{m}^c_{\alpha\beta}\overset{(1)}{\eta}_{\alpha\beta}]_{x_i^c} \int_{\overset{*}{V}} \overset{*}{f}\, d\overset{*}{V}$$

$$= -\frac{2}{27}\left(\frac{4\lambda_2}{3}\right)^3 \left(\frac{T - T_t^c}{\lambda_1 k^2}\right)\left[\frac{(1+\nu)\sigma_c^2}{(1-\nu)T_t^c}\right]^2 \pi R^2 t. \tag{4.80}$$

The term $\mathscr{A}$ in (4.48) is zero as a consequence of the symmetry properties of the eigenmode. Using the facts $\overset{(1)}{\eta}_{\alpha\beta} = x_3 \overset{(1)}{K}_{\alpha\beta}$ and $\overset{(1)}{\tau}_{\alpha\beta} = (12x_3/t^3)\overset{(1)}{M}_{\alpha\beta}$, $\mathscr{B}$ defined by (4.44b) can be written as

$$\mathscr{B} = \int_A \left\{ 2t\tau^0_{\alpha\beta}\overset{(1)}{W}_{,\alpha}\overset{(1)}{W}_{,\beta} + \frac{t^3}{12}\tau^0_{\mu\nu}\left.\frac{\partial \bar{L}_{\alpha\beta\kappa\gamma}}{\partial\tau_{\mu\nu}}\right|_c \overset{(1)}{K}_{\alpha\beta}\overset{(1)}{K}_{\kappa\gamma} + \overset{(1)}{M}_{\mu\nu}\left.\frac{\partial \bar{L}_{\alpha\beta\kappa\gamma}}{\partial\tau_{\mu\nu}}\right|_c \overset{'}{\eta}{}^0_{\alpha\beta}\overset{(1)}{K}_{\kappa\gamma}\right\} dA. \tag{4.81}$$

A fairly lengthy calculation using J_2 flow theory gives the derivatives of the instantaneous moduli evaluated at the state of stress $\tau_{\alpha\beta} = \sigma_c \delta_{\alpha\beta}$:

$$\left.\frac{\partial \bar{L}_{\alpha\beta\kappa\gamma}}{\partial\tau_{\mu\nu}}\right|_c = \psi_1\, \delta_{\alpha\beta}\, \delta_{\kappa\gamma}\, \delta_{\mu\nu} + \tfrac{1}{4}\psi_2 \cdot (\delta_{\alpha\mu}\, \delta_{\beta\nu}\, \delta_{\kappa\gamma} + \delta_{\alpha\nu}\, \delta_{\beta\mu}\, \delta_{\kappa\gamma} + \delta_{\alpha\beta}\, \delta_{\kappa\mu}\, \delta_{\gamma\nu} + \delta_{\alpha\beta}\, \delta_{\kappa\nu}\, \delta_{\gamma\mu}), \tag{4.82}$$

where

$$\psi_1 = -\psi_2\left[\frac{1}{2} + \frac{1}{12}\left(\frac{1+\nu}{1-\nu}\right)\left(\frac{\sigma_c}{T - T_t^c}\right)\left.\frac{dT_t}{d\sigma}\right|_c\right]$$

and

$$\psi_2 = -3(T - T_t^c)(1-\nu)/[(1+\nu)\sigma_c].$$

Here $dT_t/d\sigma$ denotes the derivative of the biaxial tangent modulus (4.72) with respect to the biaxial stress σ introduced in (4.71).

Using standard identities for Bessel functions, $\mathscr{B}$ can be evaluated without

approximation. The result is

$$\mathscr{B} = -\frac{T_t^c[ak^2J_0(k)]^2(t/R)^4\pi R^2 t}{6(1+\bar{v}_c)} \cdot \left\{1 + \frac{3(1-\nu)(1-\bar{v}_c)}{4(1+\nu)}\left(\frac{T-T_t^c}{T_t^c}\right) + \frac{k^2}{24}\left(\frac{t}{R}\right)^2 \frac{dT_t}{d\sigma}\bigg|_c\right\}. \tag{4.83}$$

Thus (4.48) gives

$$\lambda_2 = -\text{const}(1+\bar{v}_c)\left\{\left(\frac{T_t^c}{T-T_t^c}\right)\left[1 + \frac{k^2}{24}\left(\frac{t}{R}\right)^2 \frac{dT_t}{d\sigma}\bigg|_c + \frac{3(1-\nu)(1-\bar{v}_c)}{4(1+\nu)}\left(\frac{T-T_t^c}{T_t^c}\right)\right]\right\}^{1/3}, \tag{4.84}$$

where

$$\text{const} = \tfrac{9}{4}\{12[a^2kJ_0(k)]^2\}^{1/3} \cong 4.3808. \tag{4.85}$$†

The initial post-bifurcation expansion for the clamped circular plate is

$$\lambda = 1 + \lambda_1\xi + \lambda_2\xi^{4/3} + \cdots, \tag{4.86}$$

where λ_1 is given by (4.77) and recall that $\xi = 1$ corresponds to a deflection at the center of the plate of one thickness. As an illustration, Fig. 14 shows a plot of λ as a function of ξ as given by (4.86) for an example for which a full

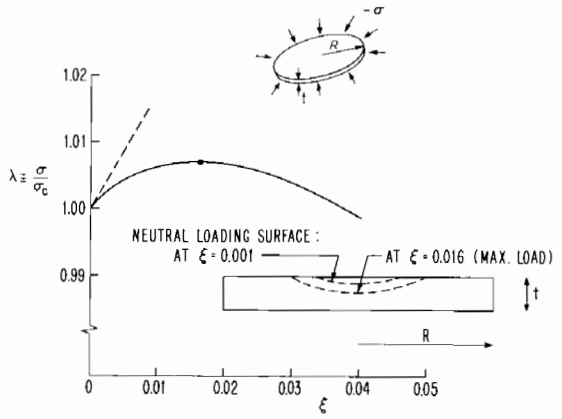

FIG. 14. Initial post-bifurcation behavior of a clamped circular plate under radial compression [see (4.87) for a specification of parameters]. The thickness is exaggerated in the insert. Dashed line: $\lambda = 1 + 1.730\xi$; solid line with dot: $\lambda = 1 + 1.730\xi - 5.143\xi^{4/3}$.

† I am indebted to A. Needleman of MIT who independently derived these results and made them available to me to provide a check on my own analysis.

numerical analysis will be reported in Section V,B. The stress–strain curve (3.59) for uniaxial tension† is used in this analysis with a strain-hardening exponent $n = 12$ so that the bifurcation results of Fig. 10 for J_2 flow theory apply. The abscissa in Fig. 10 was chosen to have the value $k^2(t/R)^2/[12\varepsilon_y(1 - \nu^2)] = 2$ and Poisson's ratio ν was taken to be $\frac{1}{3}$. The associated values of the quantities which enter into the evaluation of λ_1 and λ_2 are

$$\sigma_c/\sigma_y = 1.12, \qquad \bar{\nu}_c = -0.191, \qquad \bar{E}_c/E = 0.607,$$
$$T_t^c/E = 0.510, \qquad \text{and} \qquad \varepsilon_y(dT_t/d\sigma)_c = 4.58. \tag{4.87}$$

All the terms in λ_1 and λ_2 can be expressed in terms of these nondimensional values and one finds

$$\lambda_1 = 1.730 \quad \text{and} \quad \lambda_2 = -5.14, \tag{4.88}$$

and these were the values used in (4.86) to plot Fig. 14. Also shown there is the neutral-loading surface at two values of ξ, where the larger value corresponds to the maximum load point. According to these results the slope has been reduced substantially from its initial value at $\xi = 0.01$ corresponding to a normal deflection at the center of the plate of only one-hundredth of its thickness. The three term asymptotic expansion indicates the maximum load is less than 1% higher than the bifurcation load and is attained when the normal deflection is approximately 1/50 the plate thickness. We will see in Section V,B that these values are underestimated by the truncated initial post-bifurcation expansion, although not by much. The rapid transition from stable to unstable behavior under dead load (i.e., the transition from increasing to decreasing load) in the plastic range as typified by this example can be contrasted with the highly stable post-bifurcation of the plate in the elastic range.

D. Effect of Initial Imperfections

No general treatment, analogous to Koiter's (1945, 1963a) theory for conservative elastic systems, is available for the effect of initial imperfections on the maximum support load of a structure compressed into the plastic range. The importance of accounting for the interaction of imperfections and plastic deformation has long been recognized in the design of columns against buckling where approximate ways for estimating the effect of imperfections, such as the Perry first-yield formula, are used [see, for example, the

† In (3.59) σ denotes a uniaxial stress while in this section σ has been reserved for the applied radial stress and the pre-bifurcation biaxial stress (4.71).

monograph by Johnson (1966) and the recent paper by Calladine (1973)]. In addition to the results already presented for the models of Section II, some selected numerical results for columns, plates, and shells will be given in the next section. In this section two theoretical points will be made which have a bearing on imperfection sensitivity in the plastic range.

1. *Effect of an Imperfection on the Behavior in the Plastic Range Prior to the Onset of Elastic Unloading*

Assume the imperfection is an initial stress-free deflection of the middle surface from the perfect configuration in the form $\bar{\xi}\bar{W}(x^\alpha)$, where $\bar{\xi}$ is the amplitude of the imperfection. For simplicity we will restrict consideration to problems in which the stress histories are proportional at every point (as in the column problem) or in which a deformation theory is used. In either case the constitutive relation can be regarded as being nonlinear elastic prior to elastic unloading and Koiter's general theory for elastic systems can be applied. The general case where the loading is not proportional is somewhat more complicated than that which will be presented below but may still be worked out along the lines given by Hutchinson (1973b) for the three-dimensional theory.

The result of applying the Koiter approach is an asymptotically exact relation involving the load parameter λ, the amplitude ξ of the eigenmodal contribution to the deflection, and the lowest-order contribution of the imperfection $\bar{\xi}$:

$$(\lambda_c - \lambda)\xi + \lambda_1^e \xi^2 + \lambda_2^e \xi^3 + \cdots = \lambda\rho\bar{\xi}, \tag{4.89}$$

where

$$\rho = (\tfrac{1}{2}\lambda_c \mathscr{B})^{-1} \int_A \{N_{0c}^{\alpha\beta} \overset{(1)}{W}_{,\alpha} \bar{W}_{,\beta} + \overset{(1)}{N}^{\alpha\beta} W_{,\alpha}^{0c} \bar{W}_{,\beta}\}\, dA. \tag{4.90}$$

The superscript e is used to emphasize that this result holds for nonlinear elastic solids but not for hypoelastic solids; $\lambda_1^e = -\mathscr{A}/\mathscr{B}$, where $\mathscr{A}$ and $\mathscr{B}$ are still given by (4.44). Associated expansions for other quantities such as the strains are of the form

$$\eta_{\alpha\beta} = \eta_{\alpha\beta}^0(\lambda) + \xi \overset{(1)}{\eta}_{\alpha\beta} + \xi^2 \overset{(2)}{\eta}_{\alpha\beta} + \cdots \tag{4.91}$$

$$= \eta_{\alpha\beta}^{0c} + (\lambda - \lambda_c)\eta_{\alpha\beta}^{0\prime} + \xi \overset{(1)}{\eta}_{\alpha\beta} + \xi^2 \overset{(2)}{\eta}_{\alpha\beta} + \cdots, \tag{4.92}$$

where terms of order $(\lambda - \lambda_c)^2$ and higher-order terms involving $\bar{\xi}$ are not needed in the subsequent analysis and are not shown.

The above results apply to the elastic-plastic structure (under the restrictions mentioned) prior to the onset of elastic unloading. Reversal in sign of

the strain rate occurs for the first time when $\bar{m}^{\alpha\beta}\dot{\eta}_{\alpha\beta} = 0$. Using (4.17), (4.92), and $(\dot{\ }) \equiv d(\ )/d\xi$ we find

$$\bar{m}^{\alpha\beta}\dot{\eta}_{\alpha\beta} = \bar{m}_c^{\alpha\beta}\left(\frac{d\lambda}{d\xi}\,\overset{0}{\eta}{}'_{\alpha\beta} + \overset{(1)}{\eta}{}_{\alpha\beta}\right) + O(\lambda - \lambda_c, \xi, \bar{\xi}). \tag{4.93}$$

The initial slope λ_1 of the perfect structure, required for bifurcation to occur at λ_c, is the smallest value consistent with (4.9). From (4.93) it follows that in the slightly imperfect structure the onset of elastic unloading occurs when $d\lambda/d\xi$ is reduced to the value λ_1, i.e.,

$$\frac{d\hat{\lambda}}{d\xi} = \lambda_1 + O(\hat{\lambda} - \lambda_c, \hat{\xi}, \bar{\xi}), \tag{4.94}$$

where $(\hat{\ })$ identifies quantities evaluated at the onset of strain-rate reversal. Using (4.89) and the condition (4.94) one finds

$$\hat{\xi} = [\lambda_c \rho \bar{\xi}/(\lambda_1 - \lambda_1^e)]^{1/2} + \cdots, \tag{4.95}$$

$$\hat{\lambda}/\lambda_c = 1 - [(\lambda_1 - 2\lambda_1^e)/\lambda_c][\lambda_c \rho \bar{\xi}/(\lambda_1 - \lambda_1^e)]^{1/2} + \cdots, \tag{4.96}$$

generalizing the simple-model results (2.54) and (2.55).

The maximum load occurs following the onset of elastic unloading when $d\lambda/d\xi = 0$. If the destabilizing nonlinearities are large the maximum load will be attained shortly after the onset of elastic unloading; and (4.96) is suggestive of the effect of very small imperfections on the maximum load, as discussed in conjunction with the simple model. In general, however, it is not possible to predict the effect of an imperfection on the maximum support load by developing a perturbation expansion about the bifurcation point, as in the elastic range. For the discrete model of Section II,A it was possible to obtain a closed-form formula, (2.19) or (2.20), for the effect of an imperfection. The reduction in the maximum load was proportional to the square root of the imperfection. Although no explicit formula could be obtained for the continuous model, the expansion (2.57) as well as the approximate formula (2.58) suggests that the imperfection enters through the square root of its amplitude in this case too.

2. *Effect of an Imperfection on First Yielding When Bifurcation of the Perfect Structure Occurs in the Elastic Range*

We turn now to the complementary situation where the bifurcation load of the perfect plate or shell occurs in the elastic range at stress levels only slightly below the initial yield stress. Using the asymptotic initial post-bifurcation expansions for the response prior to plastic yielding, we examine the condition for the first occurrence of plastic yielding when imperfections are present. It is assumed that there is a smooth initial yield surface

$\mathscr{F}(\tau^{\alpha\beta}) = 0$ such that for stresses within the surface (i.e., $\mathscr{F} < 0$) the material response is linearly elastic. If at any point the bifurcation stress of the perfect structure is just within or on the yield surface then the first-yield condition can be approximated by

$$\mathscr{F}_c + (\tau^{\alpha\beta} - \tau_c^{\alpha\beta})(\partial\mathscr{F}/\partial\tau^{\alpha\beta})_c = 0, \tag{4.97}$$

where $\mathscr{F}_c \equiv \mathscr{F}(\tau_c^{\alpha\beta}) \leq 0$.

Prior to first yielding the expansion (4.89) to (4.92) applies with the moduli taken to be the constant elastic moduli. The solid-line curves in

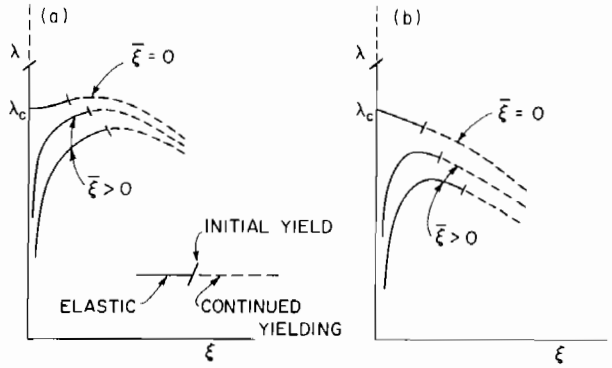

FIG. 15. Sketches of the initial post-bifurcation behavior and imperfection sensitivity where the bifurcation stress of the perfect structure falls just below the initial yield stress. (a) Symmetric bifurcation point. (b) Asymmetric bifurcation point.

Fig.15 depict the elastic load-deflection response; the slash indicates first yield and thereafter the curve is dashed to indicate further yielding. Using the expansion for the stresses which is similar to (4.92) the first-yield condition can be rewritten as

$$\mathscr{F}_c + [(\lambda - \lambda_c)\overset{\prime}{\tau}{}_0^{\alpha\beta} + \xi\overset{(1)}{\tau}{}^{\alpha\beta} + \xi^2\overset{(2)}{\tau}{}^{\alpha\beta} + \cdots](\partial\mathscr{F}/\partial\tau^{\alpha\beta})_c = 0. \tag{4.98}$$

Multiply (4.98) by ξ and use (4.89) to eliminate $(\lambda - \lambda_c)$ thereby obtaining the first-yield condition in terms of ξ and $\bar{\xi}$:

$$\xi\mathscr{F}_c + \xi^2(\overset{(1)}{\mathscr{F}} + \lambda_1^e\overset{\prime}{\mathscr{F}}_0) - \bar{\xi}\rho\lambda\overset{\prime}{\mathscr{F}}_0 + \cdots = 0, \tag{4.99}$$

where

$$\overset{(1)}{\mathscr{F}} \equiv \overset{(1)}{\tau}{}^{\alpha\beta}(\partial\mathscr{F}/\partial\tau^{\alpha\beta})_c \quad \text{and} \quad \overset{\prime}{\mathscr{F}}_0 \equiv \overset{\prime}{\tau}{}_0^{\alpha\beta}(\partial\mathscr{F}/\partial\tau^{\alpha\beta})_c\,. \tag{4.100}$$

Equation (4.99), together with (4.89), provides a set of equations for obtaining the values of λ and ξ at which yielding will first occur.

To simplify the discussion assume that the fundamental solution is a uniform state of stress and that for $\bar{\xi} = 0$ bifurcation occurs on the verge of yield so that $\mathscr{F}_c = 0$. Thus the fundamental solution has the property that $\overset{\prime}{\mathscr{F}}_0$ is a positive constant; in general, $\overset{(1)}{\mathscr{F}}$ will be positive over part of the structure and negative over the rest. Let

$$\omega = \text{maximum value of } (\overset{(1)}{\mathscr{F}} + \lambda_1^e \overset{\prime}{\mathscr{F}}_0). \tag{4.101}$$

If $\omega > 0$, then from (4.99) first yield occurs at the point (or points) in the structure where the maximum in (4.101) is attained and

$$\xi_{\text{first yield}} = (\bar{\xi}\rho\lambda_c \overset{\prime}{\mathscr{F}}_0/\omega)^{1/2} + \cdots. \tag{4.102}$$

Here λ_c has been substituted for λ by neglecting terms of order $\sqrt{\bar{\xi}}(\lambda - \lambda_c)$. Note also from (4.89) that $\bar{\xi}\rho > 0$ implies $\xi > 0$; the opposite-signed deflection in the eigenmode corresponding to $\bar{\xi}\rho < 0$ can be treated similarly. Equation (4.102) is asymptotically exact for small imperfections. If the bifurcation point is symmetric so that $\lambda_1^e = 0$, it is readily verified from (4.89) that a maximum load for the *elastic* structure occurs in the neighborhood of λ_c only if $\lambda_2^e < 0$. It is attained at a value of $\xi = O(\bar{\xi}^{1/3})$, which is inherently larger than (4.102) for sufficiently small imperfections. Thus if a perfect structure has a symmetric bifurcation point and undergoes bifurcation just on the verge of yield, the maximum load of a slightly imperfect version of the structure will always be attained *after* plastic yielding has occurred, whether or not the bifurcation point of the elastic structure is stable or unstable. Using (4.89) and (4.102), the asymptotic equation for the effect of small imperfections on the first yield of a structure with a symmetric bifurcation point is

$$\lambda_{\text{first yield}} = \lambda_c - (\rho\bar{\xi}\lambda_c\omega/\overset{\prime}{\mathscr{F}}_0)^{1/2} + \cdots. \tag{4.103}$$

Thus when $\mathscr{F}_c = 0$ the imperfection reduces the first-yield load in proportion to the square root of the imperfection as has been noted for columns on the basis of the Perry first-yield formula by Thompson and Hunt (1973) and Calladine (1973).

If the bifurcation point is asymmetric it can be possible for the maximum load to be attained *before* first yielding occurs in the imperfect structure even when the perfect structure buckles just at initial yield. If $\lambda_1^e < 0$ the maximum load of the elastic structure calculated from (4.89) occurs when $\xi^2 = \lambda\rho\bar{\xi}/(-\lambda_1^e)$. Substituting this value into (4.99) (still with $\mathscr{F}_c = 0$) gives $\rho\bar{\xi}\lambda[\omega + \lambda_1^e \overset{\prime}{\mathscr{F}}_0]$ for the point where the stress is nearest the yield surface. If this quantity decreases with increasing $\bar{\xi}$, then the maximum load will occur

before first yield for sufficiently small imperfections. The significance of this, of course, is that the maximum load can be obtained from the elastic analysis. Using (4.101), the condition that yielding occur following attainment of the maximum load in the slightly imperfect structure, when the perfect structure bifurcates just at the yield stress, is that λ_1^e be sufficiently negative such that

$$\text{maximum value of } (\overset{(1)}{\mathscr{F}} + 2\lambda_1^e \mathscr{F}_0') \leq 0. \tag{4.104}$$

The long cylindrical shell under axial compression is one of the best known examples of a structure with a highly asymmetric bifurcation point. This problem has a multiplicity of eigenmodes associated with its bifurcation stress and is not described by the one-mode expansion (4.89). However the generalization of (4.104) for the multiple-mode case can easily be obtained. Using Koiter's (1945, 1963a) solution to this problem we have found that for the case of an axisymmetric imperfection in the shape of the axisymmetric eigenmode the condition analogous to (4.104) is *not* satisfied. In other words, if the perfect shell buckles just at the initial yield stress, the buckling load of the slightly imperfect shell will *not* be given by the elastic analysis but undoubtedly will be somewhat lower. Further results on this problem will be given in Section V,C. There it will be shown that, if the yield stress is just 5% above the bifurcation stress of the perfect cylinder, buckling of the imperfect shell will be elastic over the entire range of imperfection levels of interest, at least for this particular imperfection.

V. Numerical Examples

A. Column under Axial Compression

Consider a simply supported column of length L with a solid circular cross section of radius R. The elastic-plastic material comprising the column is taken to have a Ramberg–Osgood uniaxial stress–strain curve, as in Section IV,B, i.e.,

$$\varepsilon/\varepsilon_y = \sigma/\sigma_y + \tfrac{3}{7}(\sigma/\sigma_y)^n, \tag{5.1}$$

where ε_y is the effective yield strain and $\sigma_y \equiv E\varepsilon_y$ is the effective yield stress. The tangent-modulus load P_c is given by (4.50) and the bifurcation stress σ_c is given in terms of the single geometric parameter $(\pi R/2L)^2\varepsilon_y^{-1}$, by

$$(\pi R/2L)^2\varepsilon_y^{-1} = (\sigma_c/\sigma_y) + \tfrac{3}{7}n(\sigma_c/\sigma_y)^n. \tag{5.2}$$

This relation is plotted in the form most often used for displaying column-

buckling results as a solid-line curve in Fig. 16 for $n = 10$, where $P_c = \pi R^2 \sigma_c$ and $P_y = \pi R^2 \sigma_y$.

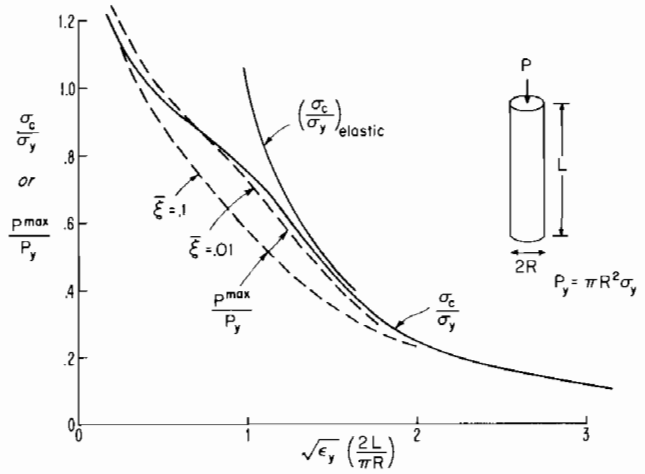

FIG. 16. Bifurcation stress of perfect column and maximum support load for two imperfection levels for a circular cylindrical column under axial compression. $W^{IMP} = \bar{\xi} R \cos(\pi X/L)$. (Ramberg–Osgood stress–strain curve with $n = 10$.)

Included in Fig. 16 are the results of an accurate numerical analysis for the maximum support load (normalized by P_y) of the column with two levels of imperfection, where the imperfection is in the shape of the buckling mode

$$W^{imp} = \bar{\xi} R \cos(\pi x/L). \tag{5.3}$$

The results are based on a column theory which is a one-dimensional version of the plate and shell theory used in Sections III and IV; details of the numerical calculations are similar to those reported for the axisymmetric deformation of shells by Hutchinson (1972) and to those employed in a recent paper on column buckling by Huang (1973). The influence of imperfections is most marked in the region where the elastic predictions break down. Results such as these are well known and have been incorporated into column design procedures. The monograph by Johnson (1966) reviews many of the column-buckling studies, both theoretical and experimental, and discusses design criteria. A recent contribution by Calladine (1973) considers the application of a Perry first-yield-type formula for imperfect columns comprised of strain-hardening metals. The papers by Malvick and Lee (1965) and Huang (1973) discuss additional aspects of plastic column buckling.

Figure 17 displays these same results replotted in the manner of Duberg

(1962) and the simple-model results of Fig. 8. Here the maximum support load is normalized by the tangent-modulus load P_c of the perfect column and is plotted as a function of the bifurcation stress of perfect column σ_c normalized by σ_y. These curves bring out the fact that even when the bifurcation stress is substantially below the effective yield stress the effect of a small imperfection can be appreciable due to plastic deformation. These

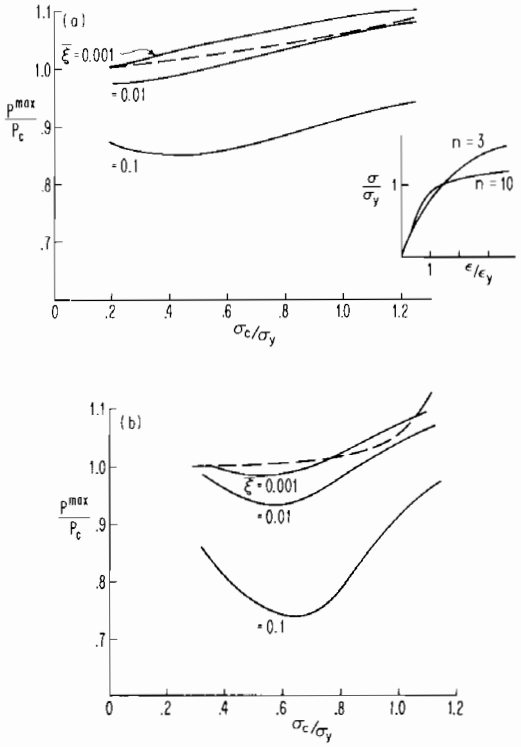

FIG. 17. Effect of imperfections on the maximum support load as a function of the bifurcation stress of the perfect column σ_c normalized by the effective yield stress σ_y. Dashed curve is the approximate maximum load (P^{max}/P_c) for the perfect column as predicted by the initial post-bifurcation analysis [Eq. (4.61)]. (a) $n = 3$; (b) $n = 10$, $W^{IMP} = \bar{\xi}R\cos(\pi X/L)$.

curves are quantitatively similar to Duberg's (1962) curves for a two-flanged column model, as well as to those for the continuous model of Fig. 8. Also shown in Fig. 17 are the predictions of P^{max}/P_c for the perfect column calculated using the approximate formula (4.61) of the initial post-bifurcation analysis. The values of E_t^c/E and q needed in this evaluation can be expressed in terms of the tangent modulus and its derivative evaluated at σ_c together with the geometric parameter of (5.2). The approximate predictions appear

to underestimate the maximum support of the perfect column slightly as would be expected from the discussion given previously in connection with Fig. 13. Recall that the asymptotic equation (4.60) for the neutral-loading surface predicts that the elastic unloading region penetrates to the middle of the column at its midpoint at maximum load and along the column to a distance $\sqrt{2}\,L/\pi$ on either side of its midpoint. The numerical analysis indicates that asymptotic results at maximum load somewhat overestimate the penetration on the midplane and underestimate the distance attained along the column.

B. Circular Plate under Radial Compression

Bifurcation results for a clamped circular plate under radial compression were discussed in Section III,C and the initial post-bifurcation expansion was given in Section IV,C. Needleman (1973) has carried out a full numerical analysis of the post-bifurcation behavior and imperfection sensitivity of clamped and simply supported circular plates using a finite element method. A few of his examples will be presented here.

Needleman (1973) used J_2 flow theory together with the tensile stress–strain relation (3.59) which has a distinct yield stress and a continuous tangent modulus. The first example is the one considered in Section IV,C. The strain-hardening exponent is taken to be $n = 12$ with $\nu = \frac{1}{3}$, and the bifurcation curves of Fig. 10 apply. The geometric parameter is chosen to be

$$k^2(t/R)^2/[12(1 - \nu^2)\varepsilon_y] = 2, \tag{5.4}$$

At this value the flow-theory and deformation-theory predictions are essentially identical; $\sigma_c/\sigma_y = 1.12$ and other parameters are given in (4.87). In Fig.18 curves of the applied edge stress σ normalized by the bifurcation stress of the perfect plate σ_c are plotted as a function of $\xi \equiv W(0)/t$, where $W(0)$ is the additional deflection at the center of the plate. The imperfection is taken as an initial stress-free normal deflection in the shape of the buckling mode and its amplitude at the center of the plate is denoted by $\bar{W}(0)$. Responses for two slightly imperfect plates are shown; the curve for the "perfect" plate was calculated for a plate with an extremely small imperfection, $\bar{\xi} = \bar{W}(0)/t = 10^{-4}$.

The maximum support load of the "perfect" plate is only about 1.5% higher than the bifurcation load and the maximum load is attained at a lateral deflection of about $0.065t$. Comparing these values with the corresponding values from the initial post-bifurcation analysis shown in Fig. 14

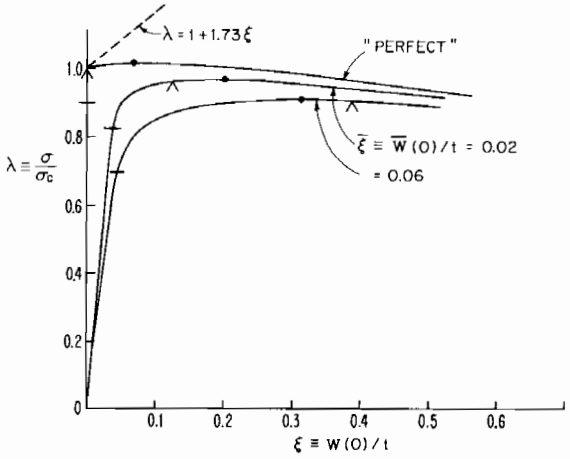

FIG. 18. Post-bifurcation behavior and imperfection sensitivity of a circular plate radially compressed into the plastic range. Solid line ↔ initial yield; • ↔ maximum load: ∧ ↔ onset of strain-rate reversal. (From Needleman, 1973.)

indicates that the initial post-bifurcation analysis in this case underestimates both the increase above the bifurcation load and the value of the deflection at which the maximum load is attained. At deflections beyond the maximum load the initial post-bifurcation curve turns down rapidly while the actual curve remains quite flat. This is characteristic of the behavior of a truncated (asymptotic) series beyond its range of validity. The importance of the initial post-bifurcation expansion is that it explains how the stable region (for dead loading) can be as extremely small as it is in spite of the substantial initial slope of the load-deflection curve. Coupled with this is a definite imperfection sensitivity which is completely absent in the elastic range. The size of the elastic unloading region at maximum load predicted by the asymptotic analysis of Section IV,C is in reasonably good agreement with the numerical predictions (Needleman, 1973), although the penetration of the region into the plate at its center falls slightly short of the asymptotic prediction.

Figure 19a shows load-deflection curves for a simply supported plate which bifurcates just outside the elastic range [$\sigma_c/\sigma_y = 1.02$, $n = 12$; the stress–strain curve (3.59) is still used]. As the first-yield analysis of Section IV,D would suggest, the imperfection sensitivity is about as pronounced as for a compressed column. The significant difference between the column and the plate shows up when the bifurcation stress of the perfect plate is somewhat below the yield stress. Then, as can be seen from the curves of Fig. 19b, the imperfection has relatively less effect in reducing the maximum load below the bifurcation load. This is related to the fact that in the elastic range

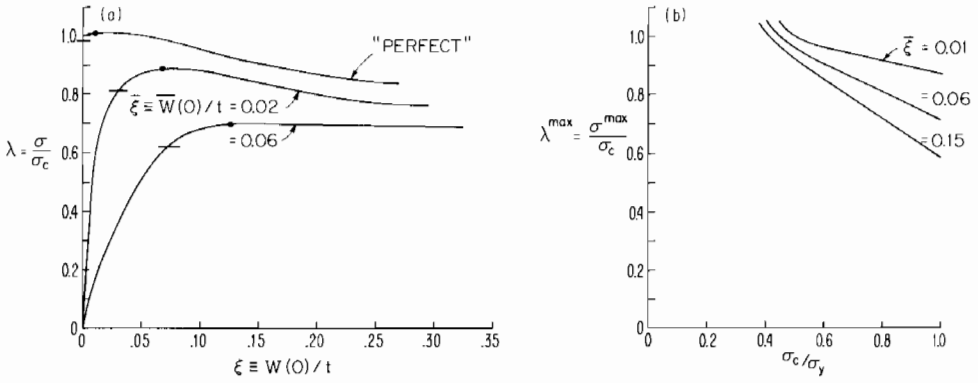

FIG. 19. (a) Post-bifurcation behavior and imperfection sensitivity of a circular plate under radial compression where the bifurcation stress of the perfect plate is nearly equal to the yield stress. Solid line ↔ initial yield; • ↔ maximum load. (b) Maximum support stress for several levels of imperfection as a function of σ_c/σ_y. (From Needleman, 1973.)

the plate has a highly stable post-bifurcation behavior and undergoes much smaller lateral deflections at loads above the bifurcation load than does the column. Consequently it is subject to far smaller bending stresses.

Graves Smith (1971) has studied the effect of imperfections on the buckling of thin-walled box columns which are built up of flat plates. He also has shown that the effect of imperfections on plate buckling can be significant when the yield stress is not sufficiently in excess of the bifurcation stress. Tests and calculations of Dwight and Moxham (1969) and Dwight (1971) definitely show that imperfections of various kinds can have an important influence on the buckling of flat plates in the plastic range.

C. Spherical and Cylindrical Shells

The two-shell structures discussed below are characterized by highly imperfection-sensitive behavior in the elastic range as opposed to the columns and plates discussed above which are relatively insensitive to small imperfections in the elastic range.

The bifurcation stress for a thin, perfect spherical shell under external pressure is given by (3.60), and predictions for a shell whose material is characterized by a Ramberg–Osgood-type tensile stress–strain relation (2.50) with $\alpha = \frac{1}{10}$ and $n = 6$ are shown in Fig. 11. Full numerical calculations for the axisymmetric post-buckling behavior of the sphere were reported by Hutchinson (1972) for J_2 flow theory and a J_2 deformation theory with elastic unloading incorporated. In Fig. 20a curves of applied

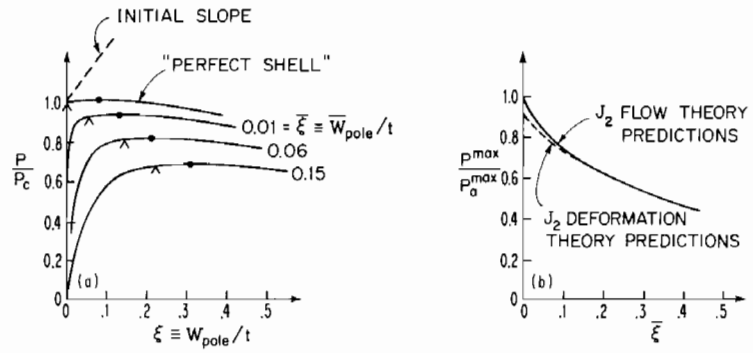

FIG. 20. (a) Plastic post-bifurcation behavior and imperfection sensitivity of a spherical shell under external pressure. (b) Imperfection sensitivity of spherical shell. From Hutchinson (1972) *J. Appl. Mech.* **39**, 155–162, with permission.

pressure are shown as a function of the amplitude of the buckling deflection ξ (corresponding to the inward dimpling at the poles of the sphere normalized by the shell thickness t). The geometric parameter of the sphere is

$$[3(1 - \nu^2)]^{-1/2} t/\varepsilon_y R = 3, \tag{5.5}$$

and J_2 flow theory was used for the calculations of Fig. 20a. From Fig. 11 it is seen that the bifurcation stress of the perfect shell is 1.5 times the effective yield stress σ_y and is about 7% above the prediction of J_2 deformation theory. The imperfection was taken in the shape of the eigenmode and its amplitude is denoted by $\bar{\xi}$, corresponding to the inward initial deflection of the dimples at the poles of the sphere normalized by t. Additional details are given in the above-mentioned reference.

Imperfection-sensitivity curves are shown in Fig. 20b in the form of the maximum pressure normalized by the maximum pressure of the perfect sphere. Results for flow theory and deformation theory are shown; the maximum load of perfect shell calculated using J_2 flow theory was used for the normalization in both cases. Significant imperfection sensitivity is indicated. Very small imperfections reduce the discrepancy between the two sets of predictions. Similar behavior has been noted for the cruciform column by Cicala (1950) and Onat and Drucker (1953) where, as discussed in Section III,C, the disparity between simple flow and deformation theories for the perfect structure is considerably larger.

Highly unstable post-buckling behavior in the plastic range was observed by Leckie (1969) in a series of tests on hemispherical shells subject to concentrated loads applied through rigid bosses of various diameters. A large variation in the maximum support load as a function of the boss size was found and was correlated approximately with a rigid-plastic post-bifurcation analysis.

The thin monocoque cylindrical shell under axial compression provides an interesting illustration of the phenomena brought out by the simple model in Fig. 4 where, due to high imperfection sensitivity, the buckling of an imperfect version of a structure may be less influenced by plasticity than is the perfect structure. Recall from Section IV,D,2 that when the perfect cylindrical shell bifurcates just at initial yield, the asymptotic analysis indicates that a slightly imperfect shell will start to yield plastically before the maximum load is attained. A closer look at this problem shows that for even larger imperfections the opposite will happen. We make use of Koiter's (1963b) special solution for the effect of an axisymmetric imperfection on the *elastic* buckling of a long cylindrical shell under axial compression. The imperfection is in the shape of the axisymmetric eigenmode associated with the bifurcation stress, and an exact, relatively simple nonlinear solution for the axisymmetric pre-buckling deformation is available. Koiter's (1963b) upper bound to the buckling load of the imperfect shell P^* is plotted in Fig.21a as P^*/P_c as a function of $\bar{\xi}$, where $\bar{\xi}t$ is the amplitude of the imperfection and t is the shell thickness.†

Using the axisymmetric pre-buckling solution for the elastic shell the maximum value of the effective stress, $\sigma_{\text{eff}} = (\frac{3}{2}s_{ij}s_{ij})^{1/2}$, occurring in the shell can be calculated. With P denoting the axial load and $\lambda \equiv P/P_c$, this value is given by

$$(\sigma_{\text{eff}}/\sigma_c)^2 = \lambda^2 + \bar{\xi}\lambda^2(1-\lambda)^{-1}(6 + c - 3\nu) + \bar{\xi}^2\lambda^2(1-\lambda)^{-2}[9(1 - \nu + \nu^2) + c^2 + 3c - 6c\nu], \quad (5.6)$$

where $c = [3(1-\nu^2)]^{1/2}$ and σ_c is the bifurcation stress of the perfect cylinder. Furthermore, the maximum value of (5.6) to be attained prior to buckling does occur at P^*. Figure 21b shows a plot of $(\sigma_{\text{eff}}/\sigma_c)^*$ as a function of $\bar{\xi}$ calculated using $\lambda^* = P^*/P_c$ from Koiter's upper bound with $\nu = \frac{1}{3}$. For small $\bar{\xi}$ one can use the asymptotically exact result $\lambda^* = 1 - (\frac{3}{2}c\bar{\xi})^{1/2} + \cdots$ in (5.6) to obtain (with $\nu = \frac{1}{3}$)

$$(\sigma_{\text{eff}}/\sigma_c)^* = 1 + 0.55\bar{\xi}^{1/2} + \cdots, \quad (5.7)$$

consistent with the result mentioned in Section IV,D,2. However (5.7) holds only for very small $\bar{\xi}$; and in an intermediate range of $\bar{\xi}$, $(\sigma_{\text{eff}}/\sigma_c)^*$ drops below unity as seen in Fig. 21b.

If the perfect shell bifurcates just at yield (i.e., $\sigma_y/\sigma_c = 1$), then for P^*/P_c greater than about 0.5 the maximum load is attained after plastic yield

†The buckling load P^* in this context is defined to be the load at which bifurcation from the axisymmetric state occurs. Budiansky and Hutchinson (1972) have shown that this bifurcation load is actually the maximum support load of the elastic shell for all values of P^*/P_c greater than about $\frac{1}{4}$.

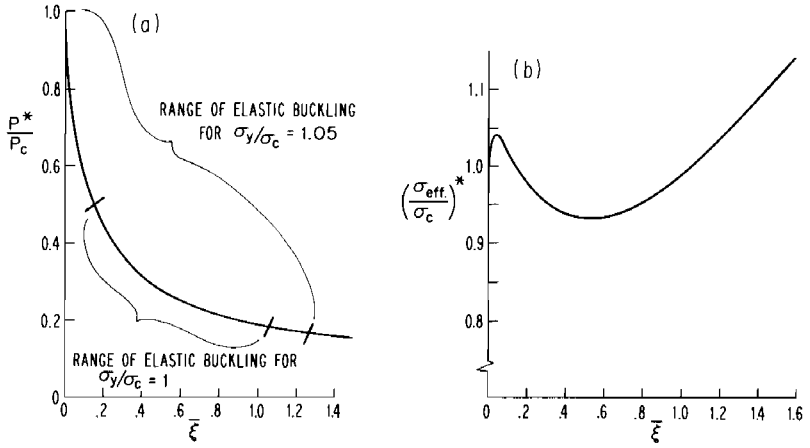

FIG. 21. (a) Imperfection-sensitivity curve for the elastic buckling of a long circular cylindrical shell with an axisymmetric imperfection and subject to axial compression. From Koiter (1963b). Also shown is the range of validity of the elastic results for two values of σ_y/σ_c. (b) Maximum effective stress occurring prior to buckling as predicted by the elastic analysis of the imperfect shell.

occurs, assuming the Mises yield condition applies. But in the intermediate range $0.2 < P^*/P_c < 0.5$ the buckling load is attained *before* plastic yielding sets in and thus the elastic analysis is strictly valid in this range. For thin cylindrical shells with typical imperfection levels this is the range in which many shells buckle. Since the elastic analysis is valid for the perfect shell and in the intermediate range, presumably it cannot be far off for $0.5 < P^*/P_c < 1$. In fact if $\sigma_y/\sigma_c \geq 1.05$, the elastic analysis holds over essentially the entire range of interest as indicated in Fig. 21a.

Although some experimentalists have drawn attention to the possibility of interaction of plastic deformation and imperfections in their buckling tests on thin cylindrical shells, most thin monocoque cylinders of structural metals are reported as having buckled elastically. The present observations suggest that this is not to be unexpected as long as the yield stress is somewhat above the bifurcation stress of the perfect shell, but other imperfection shapes and boundary effects may alter this conclusion to a certain extent. Mayers and Wesenberg (1969) and Wesenberg and Mayers (1969), have carried out detailed numerical calculations for the interaction of imperfections and plastic deformation in stiffened and unstiffened cylindrical shells under axial compression. They have delineated the range of thickness to radius in which this interaction will be important for several stress–strain curves of metals used in cylindrical shell construction which have rather ill-defined yield stresses.

ACKNOWLEDGMENTS

This work was supported in part by the Air Force Office of Scientific Research under Grant No. AFOSR-73-2476, in part by the National Aeronautics and Space Administration under Grant No. NGL 22-007-012, and by the Division of Engineering and Applied Physics, Harvard University.

REFERENCES

AUGUSTI, G. (1968). Buckling of inelastic arches: a simple model. *Meccanica* **2**, 102–105.

BATDORF, S. B. (1949). Theories of plastic buckling. *J. Aeronaut. Sci.* **16**, 405–408.

BATDORF, S. B., and BUDIANSKY, B. (1949). A mathematical theory of plasticity based on the concept of slip. *NACA TN* No. 1871.

BATTERMAN, S. C. (1964). Load-deformation behavior of shells of revolution. *J. Eng. Mech. Div., A.S.C.E.* **90**, No. EM6, 1–19.

BATTERMAN, S. C. (1969). Plastic stability of spherical shells, *J. Eng. Mech. Div., A.S.C.E.* **95**, EM2, 433–446.

BATTERMAN, S. C. (1971). Plastic stability of arches: reconsideration of a model. *Isr. J. Technol.* **9**, 467–476.

BAZANT, Z. P. (1971). A correlation study of formulations of incremental deformation and stability of continuous bodies. *J. Appl. Mech.* **38**, 919–928.

BIJLAARD, P. P. (1949). Theory and tests on the plastic stability of plates and shells. *J. Aeronaut. Sci.* **16**, 529–541.

BIJLAARD, P. P. (1950). On the plastic buckling of plates. *J. Aeronaut. Sci.* **17**, 742–743.

BOLOTIN, V. V. (1963). "Nonconservative Problems of the Theory of Elastic Stability" (G. Herrmann, ed.). (English transl.) Macmillan, New York.

BUDIANSKY, B. (1959). A reassessment of deformation theories of plasticity. *J. Appl. Mech.* **26**, 259–264.

BUDIANSKY, B. (1968). Postbuckling behavior of cylinders in torsion. *Proc. IUTAM Symp. Theory Thin Shells, 2nd Copenhagen, 1967*, pp. 212–233.

BUDIANSKY, B. (1969). Remarks on theories of solid and structural mechanics. *In* "Problems of Hydrodynamics and Continuum Mechanics," pp. 77–83. Soc. Ind. Appl. Math., Philadelphia, Pennsylvania.

BUDIANSKY, B., and HUTCHINSON, J. W. (1964). Dynamic buckling of imperfection-sensitive structures. *Proc. Int. Cong. Appl. Mech., 12th, Munich*, pp. 636–651.

BUDIANSKY, B., and HUTCHINSON, J. W. (1972). Buckling of circular cylindrical shells under axial compression. *In* "Contributions to the Theory of Aircraft Structures," pp. 239–259. Delft Univ. Press, Holland.

CALLADINE, C. R. (1973). Inelastic buckling of columns: the effect of imperfections. *Int. J. Mech. Sci.* **15**, 593–604.

CICALA, P. (1950). On the plastic buckling of a compressed strip. *J. Aeronaut. Sci.* **17**, 378–379.

COHEN, G. A. (1968). Effect of a noulinear prebuckling state on the postbuckling behavior and imperfection sensitivity of elastic structures. *AIAA J.* **6**, 1616–1620; see also **7**, 1407–1408.

CONSIDÈRE, A. (1891). Resistance des pieces comprimes. *Congr. Int. Proc. Construction*, p. 371.

DRUCKER, D. C. (1949). A discussion of theories of plasticity. *J. Aeronaut. Sci.* **16**, 567–568.

DUBERG, J. E. (1962). Inelastic buckling. *In* "Handbook of Engineering Mechanics" (W. Flugge, ed.), Chapter 52. McGraw-Hill, New York.

DUBERG, J. E., and WILDER, T. W. (1952). Inelastic column behavior. *Nat. Adv. Comm. Aeronaut. Rep.* 1072.

DWIGHT, J. B. (1971). Collapse of steel compression panels. *Proc. Conf. Devel. Bridge Design Construction, (1971)*. Cardiff University, Crosby Lockwood, London.

DWIGHT, J. B., and MOXHAM, K. E. (1969). Welded steel plates in compression. *Struct. Eng.* **47**, 49–66.

ENGESSER, F. (1889). Ueber die knickfestigkeit geradu sträbe. *Z. Architek. Ing.* **35**, 455.

FITCH, J. (1968). The buckling and postbuckling of spherical caps under concentrated load. *Int. J. Solids Struct.* **4**, 421–446.

GERARD, G., and BECKER, H. (1957). "Handbook of Structural Stability: Part I—Buckling of Flat Plates," *Nat. Adv. Comm. Aeronaut. Tech. Note* 3781.

GRAVES SMITH, T. R. (1971). The effect of initial imperfections on the strength of thin-walled box columns. *Int. J. Mech. Sci.* **13**, 911–925.

GREEN, A. E., and ZERNA, W. (1968). "Theoretical Elasticity," 2nd Ed. Oxford Univ. Press, London and New York.

HILL, R. (1956). On the problem of uniqueness in the theory of a rigid/plastic solid. *J. Mech. Phys. Solids* **4**, 247–255.

HILL, R. (1958). A general theory of uniqueness and stability in elastic/plastic solids. *J. Mech. Phys. Solids* **6**, 236–249.

HILL, R. (1959). Some basic principles in the mechanics of solids without a natural time. *J. Mech. Phys. Solids* **7**, 209–225.

HILL, R. (1961). Bifurcation and uniqueness in nonlinear mechanics of continua, pp. 155–164 (Muskhelishvili Volume). Soc. Ind. Appl. Math., Philadelphia, Pennsylvania.

HILL, R. (1966). Generalized constitutive relations for incremental deformation of metal crystals by multislip. *J. Mech. Phys. Solids* **14**, 95–102.

HILL, R. (1967a). On the classical constitutive relations for elastic/plastic solids. *In* "Recent Progress in Applied Mechanics," the Folke Odqvist Volume, pp. 241–249. Almqvist and Wiksell, Stockholm.

HILL, R. (1967b). The essential structure of constitutive laws for metal composites and polycrystals. *J. Mech. Phys. Solids* **15**, 79–95.

HILL, R., and RICE, J. R. (1972). Constitutive analysis of elastic-plastic crystals at arbitrary strain. *J. Mech. Phys. Solids* **20**, 401–413.

HUANG, N. C. (1973). Inelastic buckling of eccentrically loaded columns. *AIAA J.* **11**, 974–979.

HUTCHINSON, J. W. (1970). Elastic/plastic behavior of polycrystalline metals and composites. *Proc. Roy. Soc. London A* **319**, 247–272.

HUTCHINSON, J. W. (1972). On the postbuckling behavior of imperfection-sensitive structures in the plastic range. *J. Appl. Mech.* **39**, 155–162.

HUTCHINSON, J. W. (1973a). Post-bifurcation behavior in the plastic range. *J. Mech. Phys. Solids* **21**, 163–190.

HUTCHINSON, J. W. (1973b). Imperfection sensitivity in the plastic range. *J. Mech. Phys. Solids* **21**, 191–204.

JOHNSON, B. G. (1966). "Guide to Design Criteria for Metal Compression Members," 2nd Ed. Wiley, New York.

JONES, R. M. (1967). Plastic buckling of eccentrically stiffened circular cylindrical shells. *AIAA J.* **5**, 1147–1152.

KOITER, W. T. (1945). Over de stabiliteit van het elastisch evenwicht. Delft thesis, H. J. Paris, Amsterdam; (English transl.) Nat. Aeronaut. Space Admin. Rep. TTF-10, 1967.

KOITER, W. T. (1953). Stress–strain relations, uniqueness, and variational theorems for elastic-plastic materials with a singular yield surface. *Quart. Appl. Math.* **11**, 350–354.

KOITER, W. T. (1963a). Elastic stability and postbuckling behavior. *Proc. Symp. Nonlinear Problems*, pp. 257–275. University of Wisconsin, Madison.

KOITER, W. T. (1963b). The effect of axisymmetric imperfections on the buckling of cylindrical shells under axial compression. *Proc. Kon. Ned. Akad. Wetensch. Ser. B* **66**, 265–279.

KOITER, W. T. (1966). On the nonlinear theory of thin elastic shells. *Proc. Kon. Ned. Akad. Wetensch. Ser. B* **69**, 1–54.

LECKIE, F. A. (1969). Plastic instability of a spherical shell. *In* "Theory of Thin Shells" (F. I. Niordson, ed.). Springer-Verlag, Berlin and New York.

LEE, L. H. N. (1961). Inelastic buckling of cylindrical shells under axial compression and internal pressure. *Devel. Mech.* **1**, 190–202.

LEE, L. H. N. (1962). Inelastic buckling of initially imperfect cylindrical shells subject to axial compression. *J. Aeronaut. Sci.* **29**, 87–95.

LIN, T. H. (1971). Physical theory of plasticity. *Advan. Appl. Mech.* **11**, 255–311.

MALVICK, A. J., and LEE, L. H. N. (1965). Buckling behavior of an inelastic column. *J. Eng. Mech. Div., A.S.C.E.* **91**, EM3, 113–127.

MANDEL, J. (1965). Generalisation de la theorie de plasticite de W. T. Koiter. *Int. J. Solids Struct.* **1**, 273–295.

MAYERS, J., and WESENBERG, D. L. (1969). The maximum strength of initially imperfect axially compressed circular cylindrical shells. Dept. Aeronaut, Atronaut. Rep., Stanford University, Stanford, California.

MICHNO, M. J., and FINDLEY, W. N. (1972). An historical perspective of yield surface investigations for metals. Brown University Report. *Int. J. Nonlinear Mech.* (to be published).

NEEDLEMAN, A. (1973). Post-bifurcation behavior and imperfection sensitivity of elastic-plastic circular plates. *Int. J. Mech. Sci.* To be published.

ONAT, E. T., and DRUCKER, D. C. (1953). Inelastic instability and incremental theories of plasticity. *J. Aeronaut. Sci.* **20**, 181–186.

SANDERS, J. L. (1954). Plastic stress–strain relations based on linear loading functions. *Proc. U.S. Nat. Congr. Appl. Mech., 2nd, (1954)* pp. 455–460. University of Michigan, Ann Arbor.

SANDERS, J. L. (1963). Nonlinear theories for thin shells. *Quart. Appl. Math.* **21**, 21–36.

SEWELL, M. J. (1963). A general theory of elastic and inelastic plate failure: Part I. *J. Mech. Phys. Solids* **11**, 377–393.

SEWELL, M. J. (1964). A general theory of elastic and inelastic plate failure: Part II. *J. Mech. Phys. Solids* **12**, 279–297.

SEWELL, M. J. (1965). The static perturbation technique in buckling problems. *J. Mech. Phys. Solids* **13**, 247–264.

SEWELL, M. J. (1972). A survey of plastic buckling. *In* "Stability," (H. Leipholz, ed.), Chapter 5, pp. 85–197. Univ. of Waterloo Press, Ontario.

SEWELL, M. J. (1973). A yield surface corner lowers the buckling stress of an elastic-plastic plate under compression. *J. Mech. Phys. Solids* **21**, 19–45.

SHANLEY, F. R. (1947). Inelastic column theory. *J. Aeronaut. Sci.* **14**, 261–267.

STOWELL, E. Z. (1948). Critical shear stress of an infinitely long plate in the plastic region. *Nat. Adv. Comm. Aeronaut. Tech. Note*; See also: A unified theory of plastic buckling of columns and plates. *Nat. Adv. Comm. Aeronaut.* Rep. 898.

THOMPSON, J. M. T., and HUNT, G. W. (1973). "A General Theory of Elastic Stability," Wiley, London.

TIMOSHENKO, S. P., and GERE, J. M. (1961). "Theory of Elastic Stability," 2nd Ed. McGraw-Hill, New York.

VON KÁRMÁN, Th. (1910). Untensuchungen üder knickfestigkeit, mitteilungen üder forschungsarbeiten. *VDI (Ver. Deut. Ing.) Forschungsh.* **81**.

VON KÁRMÁN, Th. (1947). Discussion of "Inelastic column theory." *J. Aeronaut. Sci.* **14**, 267–268.

VON KÁRMÁN, Th., DUNN, L. G., and TSIEN, H. S. (1940). The influence of curvature on the buckling characteristics of structures. *J. Aeronaut. Sci.* **7**, 276.

WESENBERG, D. L., and MAYERS, J. (1969). Failure analysis of initially imperfect, axially compressed, orthotropic, sandwich, and eccentrically stiffened, circular cylindrical shells. Stanford Univ. Rep., Stanford, California.